Australian Government

Wine Australia

NSW GOVERNMENT Department of Primary Industries

UNSW SYDNEY Australia's Global University

Improved yield estimation for the Australian wine industry



FINAL REPORT to

WINE AUSTRALIA

Project Number: **DPI 1401**

Principal Investigators: **Dr Gregory Dunn (DPI NSW)**
Dr Mark Whitty (UNSW)

[redacted]

Research Organisations: **Department of Primary Industries NSW &**
University of NSW

Date: **November 2017**

[redacted]

Project Title:	**Improved yield estimation for the Australian wine industry**
Project Number:	**DPI 1401**
Authors:	Mark Whitty, Scarlett Liu, Stephen Cossell, Hiranya Jayakody, Michael Woods, Julie Tang, Sudeep Singh, Phillip van Kerk Oerle, Drew Wiseham, Steven Liu, Angus Davidson, Tina Stocco, Justin Jarrett, Pip Jarrett, Catherine Wotton, Jana Shepherd, Samsung Lim, Paul Petrie, Gregory Dunn
Project duration:	1 August 2013 – 30 September 2017
Report submitted:	1 December 2017

Table of Contents

WINE AUSTRALIA 1
Abstract 8
1 Executive summary 9
2 Introduction 12
2.1 Background 12
2.2 Outline 14
3 Project aims and performance targets 15
4 Yield estimation and project nomenclature 19
4.1 Compensating factors 0
5 Experimental procedures 23
5.1 Study block background 23
5.1.1 Historical and actual yields 25
5.1.2 Harvest dates 26
5.1.3 Actual yield maps 26
5.1.4 PCD maps 30
5.1.5 EM38 maps 33
5.1.6 Weather data 35
5.1.7 Phenology 41
5.1.8 Management actions 45
5.2 Experimental setup 47
5.3 Data management 48
6 Manual yield estimation and component analysis 50
6.1 Shoot stage (Manual) 50
6.2 Flowering stage (Manual) 51
6.3 Pea-sized stage (Manual) 51
6.4 Harvest stage (Manual) 52
6.5 Results and component analysis (Manual) 53

6.5.1 Shoot stage results and component analysis 53
6.5.2 Flowering stage results and component analysis 54
6.5.3 Pea-sized stage results and component analysis 55
6.5.4 Harvest stage results and comparison of methods 56
6.6 Results from all three years 59
6.7 Comparison with long term average 62
6.8 Summary of manual yield estimation 62
7 Image processing elements 64
7.1 Shoot counting by image processing 64
7.2 Spatial variation map generation 66
7.3 Flower counting by image processing 68
7.4 Pea-sized berry estimation 70
7.4.1 Introduction 70
7.4.2 Methodology 70
7.4.2.1 Cascade Object Detection method 70
7.4.2.2 Estimating the final berry number via linear regression methods 71
7.4.3 Results 72
7.4.4 Conclusion 78
7.5 3D bunch reconstruction for berry counting at harvest 78
7.6 Berry diameter and weight measurement from bunch photos 78
7.6.1 Stripped berry diameter measurement 78
7.6.2 Berry weight versus diameter 79
7.6.3 On bunch berry diameter measurement 81
7.7 Map similarity analysis 82
7.8 Non-bearing and missing vine detection 84
8 Y1 method (GoPro) 86
8.1 System design for Y1 (GoPro) 86
8.2 Experimental design for Y1 (GoPro) 89
8.3 Theoretical method and results for Y1 (GoPro) 89
8.3.1 Shoot stage (GoPro) 90
8.3.2 Flowering stage (GoPro) 92

8.3.3 Pea-sized stage (GoPro) 93
8.3.4 Harvest stage (GoPro) 93
8.4 Overall summary of Y1 results 94
9 Y2 method (Manta) 96
9.1 System design for Y2 (Manta) 96
9.1.1 Hardware 97
9.1.1.1 Camera 97
9.1.1.2 Light Source 98
9.1.1.3 Data storage 99
9.1.1.4 Power source 99
9.1.2 System level design 100
9.1.3 Mount design 102
9.2 Experimental design for Y2 (Manta) 103
9.2.1 Hardware testing 103
9.2.2 Further GoPro analysis and determination of best stage to video 103
9.2.3 Harvest efficiency 104
9.2.3.1 Harvest efficiency Experimental Procedure 104
9.3 Results for Y2 106
9.3.1 Hardware testing results 106
9.3.2 Comparison between GoPro (Y1 and Y2) and Manta (Y2) systems 107
9.3.3 Further GoPro analysis and determination of best stage to video 109
9.3.4 Shoot stage yield estimation (GoPro) 110
9.3.5 Harvest efficiency experiment 112
9.3.5.1 Conclusion of harvest efficiency experiment 114
9.4 Overall summary of Y2 results 114
10 Y3 method 115
10.1 System design for Y3 (GoPro + Mobile) 115
10.2 Experimental design for Y3 118
10.3 Theoretical method for Y3 (GoPro + Mobile) 118
10.3.1 Shoot stage (GoPro + Mobile) 118
10.3.1.1 Shoot stage: Count shoots in Y3 video 118
10.3.1.2 Shoot stage: Bunch to shoot ratio 120

10.3.1.3 Shoot stage: Average bunch weight 120
10.3.1.4 Shoot stage: Shoot gain/loss factor 121
10.3.1.5 Shoot stage: Predict yield 121
10.3.1.6 Shoot stage: Yield component analysis 124
10.3.1.7 Shoot stage: Summary 125
10.3.2 Flowering stage (GoPro + Mobile) 126
10.3.2.1 Flowering stage: Inflorescences per shoot 126
10.3.2.2 Flowering stage: Accuracy of flower counting 127
10.3.2.3 Flowering stage: Flowers per inflorescence 128
10.3.2.4 Flowering stage: Fruit set ratio 129
10.3.2.5 Flowering stage: Berry gain loss factor 130
10.3.2.6 Flowering stage: Bunch gain/loss factor 131
10.3.2.7 Flowering stage: Flowers per shoot 131
10.3.2.8 Flowering stage: Predict yield 132
10.3.2.9 Flowering stage: Yield component analysis 135
10.3.2.10 Flowering stage: summary 136
10.3.3 Pea-size stage (GoPro + Mobile) 136
10.3.3.1 Pea-sized stage: Bunches to shoot ratio 136
10.3.3.2 Pea-sized stage: Berries per bunch 136
10.3.3.3 Pea-sized stage: Average berry weight 138
10.3.3.4 Pea-sized stage: Berry gain loss factor 139
10.3.3.5 Pea-sized stage: Bunch gain/loss factor 139
10.3.3.6 Pea-sized stage: Predict yield 139
10.3.3.7 Pea-sized stage: Yield component analysis 142
10.3.3.8 Pea-sized stage: Summary 143
10.3.4 Harvest stage (GoPro + Mobile) 144
10.3.4.1 Harvest stage: Bunch to shoot ratio 144
10.3.4.2 Harvest stage: Berries per bunch 144
10.3.4.3 Harvest stage: Berries per shoot 146
10.3.4.4 Harvest stage: Predict yield 146
10.3.4.5 Harvest stage: Yield component analysis 148
10.3.4.6 Harvest stage: Summary 150
10.4 Overall summary of Y3 results 150

11 Conclusions 152
11.1 Yield estimation 152
11.2 Project novelty 153
11.3 General learnings 153
12 Recommendations 155
12.1 Development 155
12.2 Testing 155
12.3 Policy 156
13 Bibliography 157
14 Appendices 161
A. Communication 161
List of Publications 161
Media Articles 162
Presentations 164
B. Intellectual Property 164
C. Staff 165
D. Other Materials 168
Historical Yield Values 168
E. Budget Reconciliation 169

Abstract

This project presented a system for yield estimation using image processing using consumer cameras and mobile phones to tackle high errors in yield estimation pervasive across the industry. The system was tested on four vineyard blocks and shown to outperform manual yield estimation at all stages, achieving 5.5% error at flowering. Image processing based shoot counting, flower counting and berry counting techniques showed high levels of accuracy and have great potential to reduce the manual labour required in Australian vineyards. However, to achieve this, improvements in automated data collection and management are crucial to drive the accuracy and uptake forward.

1 Executive summary

Industry practices for yield estimation in winegrape vines have been developed over many years, however they are still error-prone, time consuming and hence costly. Time pressures frequently prohibit detailed analysis of the data collected over many seasons, so understanding of the effect of different components on the final yield estimates is lacking.

This project developed several image processing-based systems for the purpose of yield estimation on an individual block basis. The systems were evaluated against manual yield estimates, using tonnage of fruit delivered to the winery as the objective. Analysis of non-bearing proportions of the block and harvester efficiency were included to provide inputs to all the yield estimates.

Experiments were conducted on two common varieties, Chardonnay and Shiraz, at two sites, Orange (NSW) and Clare (SA) over three growing seasons from 2015 - 2017. The blocks chosen were all spur pruned, with VSP trellis in Orange and 'Aussie sprawl' in Clare.

The final novel field-mobile system developed in the third year of the project was able to outperform the industry standard manual yield estimation method, relying predominantly on data available within the three project seasons. The system involves the use of GoPro cameras for videoing an entire block at the shoot stage in combination with mobile phone photos of marked bunches at flowering, pea-sized and harvest.

Shoot counting by image processing from consumer grade cameras mounted on farm vehicles such as Gators and quadbikes was demonstrated to have an accuracy of 88%. This translated to an error of 20% in final yield estimates, five months prior to harvest. The system can potentially be mounted on a tractor during an early spray pass, and the optimum time for filming was found to be E-L 9.

At the flowering stage, an average error of 5.5% was achieved across the four blocks, which is close to the winemaker target of 5%. The error increased to 14% and 12% respectively at pea-sized and harvest, as the approach is fundamentally based on counting florettes or berries per shoot. Variation in shoot number throughout the season influences the final result, hence later measurement of shoot or bunch density would further improve accuracy of yield estimation.

Of the many image processing components that went into the yield estimation, an improved flower counting system suitable for Australian varieties shows the most promise as a standalone output. An accuracy of 84% was achieved across 12 different datasets, and the limitations of the algorithm in respect of development stage and variety are discussed in the report.

Berry counting at pea-sized showed an accuracy of 90%, speeding up data collection and greatly reducing the manual labour needed at pea-sized estimates. Berry

counting at harvest using an existing 3D reconstruction algorithm achieved 88% accuracy on a single image without the need for any calibration and is applicable to multiple varieties. Across a few dozen images, the count error reduced to less than 10% and in two blocks was less than 2%, showing the feasibility of automated berry counting from mobile phone images.

Berry diameter measurement was briefly investigated and shown to have an accuracy of 95% from single images of bunches.

The project showed that achieving less than a 15% estimation error from industry standard manual sampling even at harvest is not realistic when relying on a purely data driven approach. In fact, using long term averages is often more accurate than manual estimates, which calls into question the effort put into making manual estimates. The addition of subjective farm-specific knowledge and longer term historical records can improve manual estimates in some cases, but all manual measurements are subject to bias.

Stratified sampling was shown to substantially reduce the number of samples required, and is a first step in improving accuracy without image processing. Bunch to shoot ratios and bunch to inflorescence ratios were found to contribute the most uncertainty to early season forecasts. Counts of berries per bunch were the cause of the greatest inaccuracy in forecasts at pea-sized, suggesting that methods for reducing bias in bunch selection are necessary. Estimated berry diameter at harvest was also poorly predicted, suggesting image processing methods for tracking this over time would be beneficial.

Improving data custodianship or management practices is critical to driving the accuracy of yield prediction up across the industry. Smartphone apps for flower counting and berry counting using image processing have the potential to not only improve accuracy by speeding up data capture but also provide a front-end for entering these data into a cloud-based yield estimation system.

Given the limited amount of data available to determine prediction factors, it is recommended that longer term trials be undertaken. Greater potential for improved accuracy exists in cane pruned vines due to greater visibility of shoots and fruit and industry is encouraged to implement cane pruning systems.

Finally, the report recommends further development and commercialisation of a number of image processing technologies that will improve yield estimation and provide key tools to reduce labour requirements. Shoot counting and early season mapping have the potential to greatly assist growers to manage blocks differentially and hence improve yield and quality across the Australian wine industry.

Acknowledgements

The contributions of Scarlett Liu (biological baseline, shoot counting, shoot mapping and 3D reconstruction for berry counting) and Julie Tang (non-bearing vine

detection) who independently developed a number of critical components used to generate the project outcomes are to be recognised.

In-kind contributions by Treasury Wine Estates and SeeSaw Wines were essential to the data collection and feedback process.

Thanks are also due to the industry reference group members who provided feedback and direction for this project: Keith Hayes, Paul Petrie, Mark Krstic, Alistair Dinnison, Justin Jarrett, Pip Jarrett, Brett McClen, Shelley Ray-Brennan, Philip Deverell, Angus Davidson, Catherine Wotton, Jana Shepherd, Chris Brodie, Brooke Howell and Hans Loder.

2 Introduction

2.1 Background

At various stages during each season, wineries ask grape growers to provide forecasts of yield. Differences between expected intake and actual delivery can lead to a chain reaction of problems spreading throughout the entire process of wine production and distribution, affecting harvest organisation, regional pricing negotiations, intake scheduling, tank space allocation, investment in winery capital equipment and the development of marketing strategies for domestic and export markets. Lately the demand for improved crop forecasting has intensified as major producers and purchasers of grapes are stipulating that particular yield targets should be met, in the belief that this will improve and maintain wine quality. Apart from the substantial economic benefits of improved crop forecasting alone, it is an essential first step to successful yield regulation.

At present, best practice systems used after fruit set, and based on manual measurements, are on average ± 15% out [1]. This is substantially higher than the error of ± 5% that winemakers and wine companies would like [2]. The level of accuracy, the cost of labour and training requirements of current systems are major impediments to adoption.

This project assembled a team to substantially improve block level forecasts after fruit set and early in the season through the application of appropriate image sensing technology.

This project tackled three major barriers to wider adoption of yield estimation techniques:

1. Accuracy of prediction: increased sampling accounted for the large spatial variability within vineyard blocks and reduced measurement bias.

2. Cost of sampling: the introduction of sensing technology led to a reduction in manual field measurements.

3. Ease of sampling: a mobile system to calculate potential yield was developed.

Many yield forecasting approaches have been tried [3] [4] [5] and found to be unsuccessful, for a range of reasons. Although remote sensing indices correlate well with yield, these approaches assess the canopy, not the fruit. As similar sized vines often have different yields from one season to the next, any remote sensing approach will require costly field calibration. Best practice 'block level' forecasting is still based on assessing yield components during the season [2] [1]. However, it is now clear that to significantly improve this approach, increased sampling is required above what is manually feasible to account for spatial variability. As early as 2004, Dunn and Martin showed the potential of digital imagery to estimate yield. Modern computer vision techniques can be used to estimate various canopy and

fruit characteristics [6], even when fruit and foliage are both green [7]. Although correlations between sensed data and harvest yield were described, these are likely to change depending on the time of sensing (stage of crop development), trellising system and from one year to the next.

This project explored the use of proximate sensing (primarily image analysis) to estimate fruit load directly between the shoot stage and harvest. This was combined with existing yield estimation techniques to make forecasts at a block level. Sensing technology to estimate inflorescence size was also explored based on studies investigating allometric relationships within grapevine inflorescences [8].

The specific objectives of the project were to:

1. Develop the ability to rapidly sense the amount of fruit or fruit potential on winegrape vines between the shoot stage and harvest for two cultivars and two commonly-used trellising systems at different times during the season.
2. Evaluate the performance of industry standard manual yield estimation techniques in the study blocks, with a specific focus on identifying the key prediction factors that introduce the greatest error.
3. Evaluate the ability of image-based sensing approaches to accurately assess berry size.
4. Explore the potential for image analysis to determine potential inflorescence size to improve 'early season' forecasts and identifying the best development stage to collect inflorescence imagery.
5. Describe the relationship between sampling frequency and the error of prediction for fruit sensing in vineyards with differing trellising systems and cultivars at a vineyard block level.
6. Develop a field-mobile system, that integrates into existing vineyard operations and is based on image analysis, to predict yield at several stages between budburst and harvest.

The major benefits of this project were envisaged to be:

1. Reducing the costs associated with yield forecasting in the vineyard.
2. Enabling growers to more quickly and efficiently intervene with management actions on a differential basis to improve quality and regularise yield by providing early season maps of yield potential variation.
3. Widespread adoption of accurate yield forecasting will lead to cost savings in wineries due to improved scheduling and improved wine quality from maximising fruit potential.
4. Providing complete vineyard imagery (a la Google Street View) as a basis for future work on detecting disease, vine water stress, dead vines and broken fence posts etc. with consequent economic benefits.

Large field experiments in both the Clare Valley, South Australia and Orange, New South Wales were conducted to address the aims of the project. Experiments

utilised existing Chardonnay and Shiraz vineyards blocks in each region. This report describes the experimental results and their implications for improving yield prediction in the Australian wine industry.

2.2 Outline

The report is structured as follows. Following listing of the project aims and performance targets, Chapter 4 introduces the nomenclature used in this report for both equations and project components. Chapter 5 then describes the four study blocks and shows their vital statistics along with general block and farm data collected during the project before briefly introducing the general experimental setup and data management system.

The results from manual yield estimation across the three project years have been collated in Chapter 6 along with analysis of the components that influence the final yield. A summary of several image processing algorithms used by or developed within the project is given in Chapter 7, with references to papers with more technical detail.

The key content of the report is contained in Chapters 8, 9 and 10, which follows the development of three systems for yield estimation broadly aligned to the three years of the project. Each chapter describes the system design, experimental procedures and results. Conclusions are drawn in Chapter 11 with recommendations for future research, development and extension in Chapter 12.

3 Project aims and performance targets

Table 3.1 Outputs and Activities 2014-15 (Y1)

Year 1	Output	Target Date	Activities	Report Section
a	Four experimental vineyards selected and characterised.	30/09/2014	Select and characterise four vineyards (Chardonnay and Shiraz) in the Clare Valley and Orange. This will include mapping spatial variability in soils (EM38) and accurate GPS surveys.	5.1
b	Prototype image analysis yield forecasting software. Prototype Sensor Suite for field use.	30/12/2014	Software development: develop image analysis software for evaluation in the vineyard. Hardware development: assemble and prepare Prototype Sensor Suite for evaluation in the vineyard.	8.1, 8.2
c	An evaluation of the potential of image analysis to assess branching patterns of inflorescences and predict inflorescence size.	31/05/2015	Collect inflorescences from vineyard blocks for laboratory analysis. Establish relationships between branching patterns and inflorescence size.	7.3
d	Yield forecasts after fruit set, at veraison and prior to harvest on all experimental vineyard blocks.	31/05/2015	Conduct best practice 'manual' yield forecasts including assessing yield components after fruit set, at veraison and prior to harvest. This will necessitate 'oversampling' to determine relationships between sampling intensity and	6.1 - 6.6

			error of prediction for image analysis. Collect remotely sensed imagery around veraison.	

Table 3.2 Outputs and Activities 2015-16 (Y2)

Year 2	Output	Target Date	Activities	Report Section
a	An evaluation of prototype image analysis-yield forecasting software and Prototype Sensor Suite using harvest yield data from four experimental vineyard blocks.	30/09/2015	Use harvest data including block yields, yield components and spatial yield patterns in the four experimental vineyard blocks to evaluate prototype forecasting system.	8.3, 8.4
b	Improved image analysis yield forecasting software. Low Cost Sensor Suite for field use.	31/10/2015	Further software development based on results from first season studies for evaluation in the vineyard in season 2. Select and develop Low Cost Sensor Suite for field evaluation.	9.1, 9.2
c	A report on the use of image analysis to measure the flower number on inflorescences across seasons and cultivars	31/12/2015	Collect inflorescences from vineyard blocks for laboratory analysis.	7.3
d	Stop/go decision (AGWA).	31/12/2015	Review and assess the viability of the technology development (software and hardware) in consultation with AGWA to determine whether the project will continue.	-

e	Yield forecasts after fruit set, at veraison and prior to harvest on all experimental vineyard blocks.	30/05/2016	Conduct best practice 'manual' yield forecasts including assessing yield components after fruit set, at veraison and prior to harvest. This will necessitate 'oversampling' to determine relationships between sampling intensity and error of prediction for image analysis.	6.1 - 6.6
f	Evaluation of improved image analysis-yield forecasting software and Low Cost Sensor Suite using harvest yield data from 4 experimental vineyard blocks. Harvest yield data from four experimental vineyard blocks	30/06/2016	Use harvest data including block yields, yield components and spatial yield patterns in the four experimental vineyard blocks to evaluate improved forecasting system.	9.3

Table 3.3 Outputs and Activities 2016-17 (Y3)

Year 3	Output	Target Date	Activities	Report Section
a	A prototype smart device for use with a tablet/phone developed for vineyard yield assessments.	30/09/2016	Evaluate image acquisition and analysis using smart devices for assessing vineyard yields. Develop software to support the acquisition and analysis of images to assess yield in vineyards using smart devices.	10.1, 10.2

b	An image analysis system comprising hardware and software with the ability to differentiate and count inflorescences in vineyards 4 to 6 weeks after budburst.	30/12/2016	Evaluate ability of image analysis to accurately differentiate and count inflorescences in vineyards 4 to 6 weeks after budburst. Develop software to analyse acquired images.	8.3.2
c	Data on the potential for image analysis to assess inflorescence number and size in vineyards 6 to 8 weeks after budburst.	31/03/2017	Analyse all field and laboratory data relating to assessing inflorescence number and size in vineyards 6 to 8 weeks after budburst.	7.3
d	Yield forecasts after fruit set, at veraison and prior to harvest on all experimental vineyard blocks.	30/05/2017	Conduct best practice 'manual' yield forecasts including assessing yield components after fruit set, at veraison and prior to harvest. This will necessitate 'oversampling' to determine relationships between sampling intensity and error of prediction for image analysis.	6.1 - 6.6
e	Evaluation of final yield forecasting software and a prototype smart device for use with a tablet/phone.	30/06/2017	Collect harvest data including block yields, yield components and spatial yield patterns in the four experimental vineyard blocks.	10.310.3.1 - 10.4
f	Final Report.	30/09/2017	Submit Final Report to Wine Australia.	-

4 Yield estimation and project nomenclature

Items	
S	Shoots
B	Bunches
b	Berries
f	Flowers / florettes
I	Inflorescences
q	Rachis

$\mathbf{S_{gl}}$	Shoot gain/loss factor
$\mathbf{B_{gl}}$	Bunch gain/loss factor
$\mathbf{b_{gl}}$	Berry gain/loss factor
Y	Yield (weight of fruit at harvest)

Functions	
f(.)	Function
c(.)	Count
w(.)	Weight
L(.)	Length
D(.)	Distance
V(.)	Volume
φ(.)	Diameter

r(.)	Radius
$\boldsymbol{\mu}$**(.)**	Average
∑(.)	Sum
σ(.)	Standard deviation
Q(.)	Quantile
%(.)	Percentage
R	Ratio

Subscripts (development or maturity stage)	
s	Shoot stage
f	Flowering stage
ps	Pea-sized
v	Veraison
h	Harvest

Times and estimates	
X	Current season or value
$\widehat{X}$	Estimate (current time)
X^*	Prediction / Forecast
$\overline{X}$	Long Term Average (LTA)

Locations or sources	
See Section 5.2	
SS	Sample Segment
SSS	Stratified Sample Segment
TL	Temporal Location
ATL	Anti-Temporal Location
BV	Block Video
MB/TB	Marked Bunch / Tagged Bunch
I	Image or frame
(*u*, *v*)	Image column, row in pixels

x^d	x detected
x^v	x visible
HE	Harvest efficiency
SP	Sampled percentage
MOG	Matter Other than Grape
ELXX or E-LXX	Modified E-L stage, as defined in Dry et al. [9]
O	Orange study site
C	Clare study site
M	Magill study site

FTX.Y-L = Field Trip Y in project year Y at location L, e.g. FT3.1-O means year 1, trip 1 at Orange. Trip numbers are not uniformly patterned across years.

Table 4.1 Study periods and project years

Study period	**Vintage**	**Abbreviation** **Y = Project Year**
July 2014 – June 2015	V2014	Y1
July 2015 – June 2016	V2015	Y2
July 2016 – June 2017	V2016	Y3

4.1 Compensating factors

AP = Active Percentage. Calculated from non-bearing length from UAV imagery. Section 7.8 shows the numerical values which were applied.

%(BV) = Percentage of recorded video. Calculated as proportion of rows actually filmed (not including frame subsampling if any), where the practicalities of field trips prevented complete data capture, or in the case of only recording every second row.

SP = Sampled Percentage. Proportion of the block that will be subsequently destructively sampled and not added to the final delivered tonnage and hence by which the yield estimate should be reduced. This is generally a very small proportion (<1%).

HE = Harvest efficiency. Calculated by experiment in Y2 only, see Section 9.3.5 and values have been adapted for use in other years (such as Clare in Y3 using a more efficient harvester than Y2).

For this report, losses due to transport (such as in spilt juice) were considered as part of the harvest efficiency.

AP, SP and HE have been applied consistently to all the yield estimation methods below, and have not been included in some formulas for clarity.

5 Experimental procedures

5.1 Study block background

All experiments were conducted on four blocks, two situated in Clare Valley (SA) and two situated in Orange (NSW). Each location contained one of each of two common Australian red and white cultivars, Chardonnay and Shiraz. More information about these four blocks is listed in Table 5.1 and their outlines are shown in Figure 5.1. Experiments were conducted across three seasons as listed in Table 4.1.

The properties of each block were obtained from the farm manager and verified where possible with manual measurements. This was particularly critical in the case of the block area. For all blocks, the original shapefiles used by the surveyor to set out the blocks provided one source of information, which was treated as the best estimate. The farm managers provided a separate number from their records. As a third source of information, the end row posts were tagged in Google Maps and the length of each row calculated, summed and multiplied by the row width to give another estimate of the area. The variation between all three measurements was significant, with a minimum of 4.1% and a maximum of 9.4%. Hence, having accurate information about the area of vines in each block is a critical first step for yield estimation.



(a) (b)



(c) (d)

Figure 5.1 The four block terrains in Google maps. (a) Clare 40A. (b) Clare 47A. (c) Orange B4. (d) Orange B12.

Table 5.1 Block dimensions and properties

Block Name	40A	47A	B4	B12
Variety	Chardonnay	Shiraz	Shiraz	Chardonnay
Location	Clare, SA	Clare, SA	Orange, NSW	Orange, NSW
Area (Ha) recorded by farmer	6.2	10.6	6.5	3.7
Area(Ha) from survey (used for all calculations in this report)	5.9986	10.1822	6.3184	3.5322
Pruning Type	Spur	Spur	Spur	Spur
Trellis System	Aussie Sprawl	Aussie Sprawl	VSP	VSP

Total vines in block	9472	17432	12482	6116
Total row length (km)	20.6	35.2	23.03	12.73
Row spacing (m)	3	3	3	3
Vine spacing (m)	2.17	2.02	1.87	2.08
Number of rows	84	134	78	83

5.1.1 Historical and actual yields

The final yield for each block was defined as the total tonnage of fruit delivered to the winery. This was measured differently depending on the site. At Clare, it was done by weighing a semitrailer at the winery before and after all the bins were emptied. Hence, the precision of the weighbridge was a limiting factor in the accuracy of the fruit harvested. At Orange, it was done by measuring each bin individually on a small weigh scale at the farm, so transport losses were not considered. However, in year 2, manual mislabelling of one of the bins may have occurred, indicating how easily human error can impact the final results. The final yields are shown in Figure 5.2 and for the three project years the actual values are given in Table 5.2 along with the Long Term Average (LTA). The actual values for the entire history are in the Appendix.

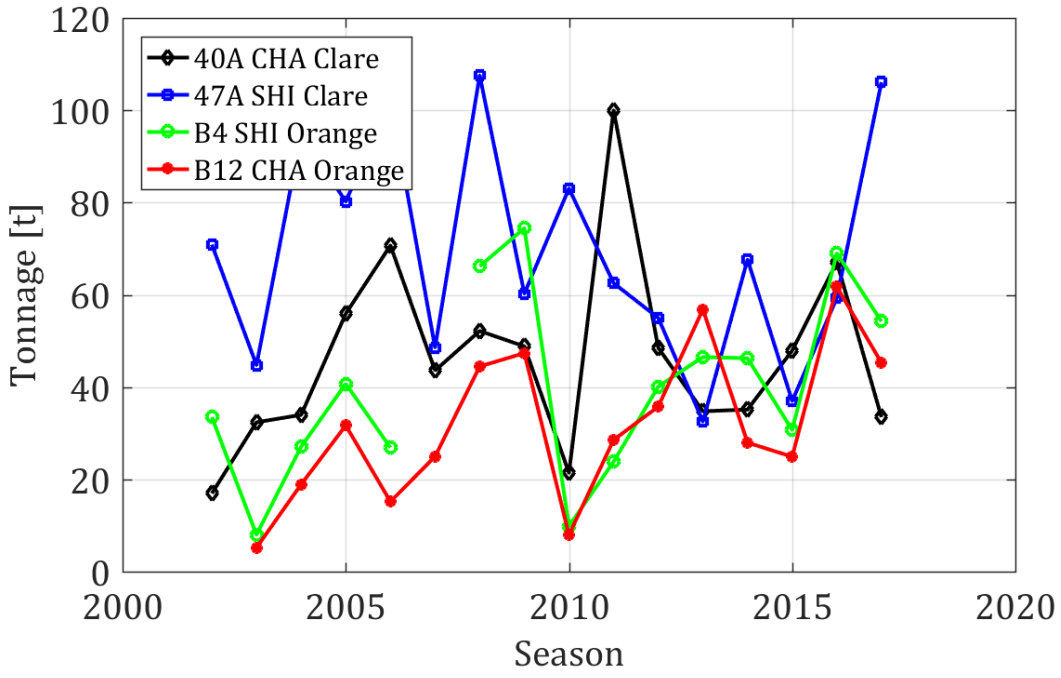


Figure 5.2 Actual yield history for each of the study blocks

Table 5.2 Actual yields (tonnes) and the long term average yield for each of the study blocks during the study period

Year	40A	47A	B4	B12
2015	47.92	36.98	30.702	24.912
2016	67.1	59.32	69.005	61.742
2017	33.5	106.09	54.254	45.272
LTA	46.43	69.55	39.83	31.79

The first season was noted as having below average yields in Clare and slightly below average yields in Orange. With the exception of 47A, the second season had above average yields, nearly double that of the first season. In the second season, substantial shrivel occurred on the bunches in the fortnight prior to harvest due to a couple of heatwaves, and logistical constraints delaying the harvest by about two weeks from when the harvest yield estimation field trip occurred. In the third season, block 47A had an outstanding yield, almost on par with the highest historically recorded value. 40A performed below average, possibly due to variability within the block, which meant it was harvested in three parts. The two blocks at Orange performed above average in the third year.

5.1.2 Harvest dates

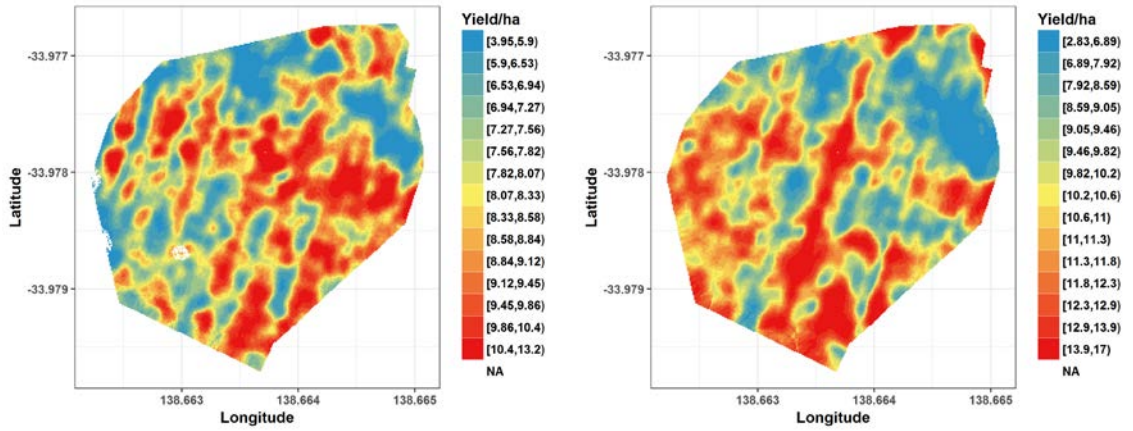
Table 5.3 presents the harvest dates for each block. Where the harvest took place over more than two consecutive nights, multiple dates are given.

Table 5.3 Harvest dates

Block Name	40A	47A	B4	B12
V2015	02/02/2015	18/03/2015	16/03/2015	23/02/2015
V2016	03/02/2016 + 08/02/2016	26/02/2016 + 01/03/2017	02/03/2016	23/02/2016
V2017	01/03/2017 + 02/03/2017	03/04/2017	19/03/2017 + 27/03/2017	15/03/2017

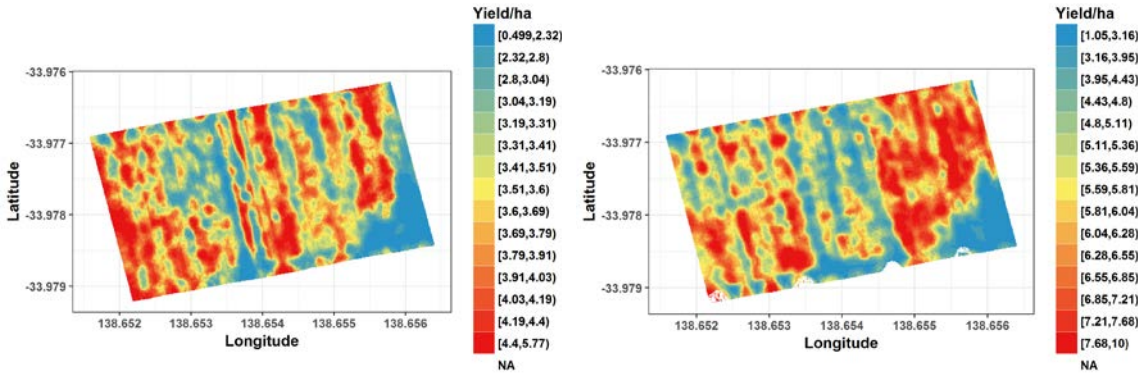
5.1.3 Actual yield maps

Actual yield maps for the four blocks over the three years are presented in Figure 5.3 to Figure 5.6. These maps were generated by a commercial on-harvester yield monitor utilising a weigh scale on the outflow belt, with values scaled to match the total yield in each block. Some year to year variation is evident within these blocks, in particular in block 12, which was influenced by water availability in a proximate dam.

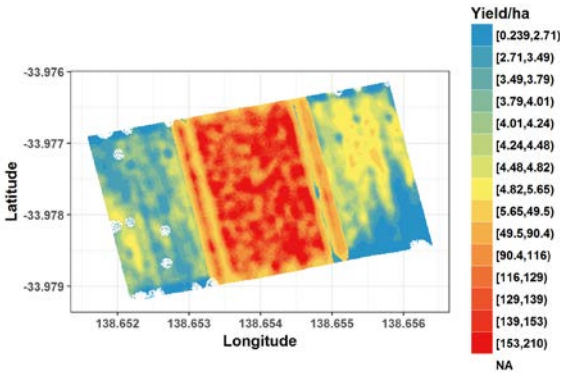


(a) (b)

Figure 5.3 Actual yield map for Clare 40A block. (a) 2015 harvest. (b) 2016 harvest. Note- Data for 2017 not available due to faulty yield monitor equipment.

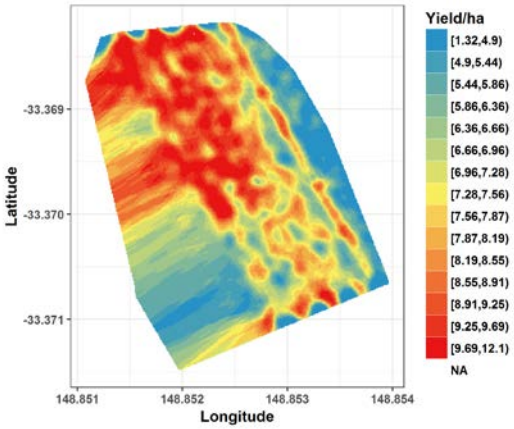


(a) (b)

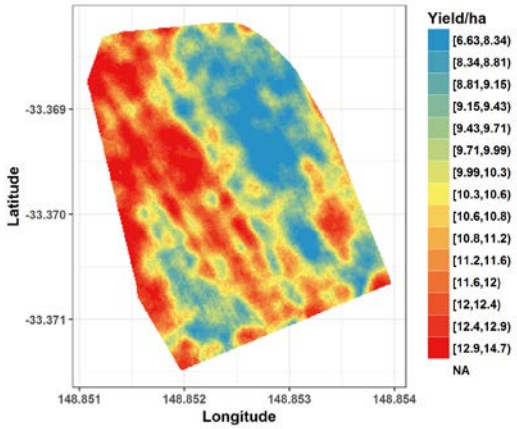


(c)

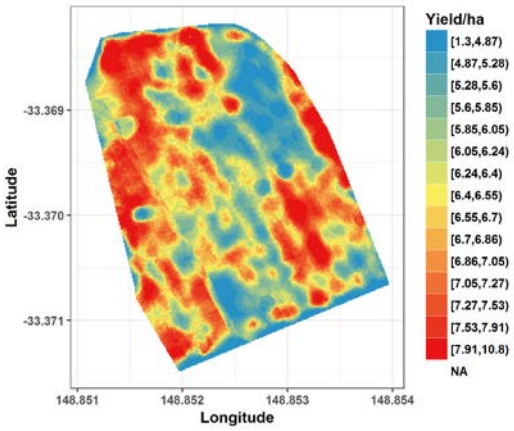
Figure 5.4 Actual yield map for Clare 47A block. (a) 2015 harvest. (b) 2016 harvest. (c) 2017 harvest – note mechanical problems with the proprietary yield monitor meant the 2017 map was composed of three sections that could not be reliably scaled together.



(a)

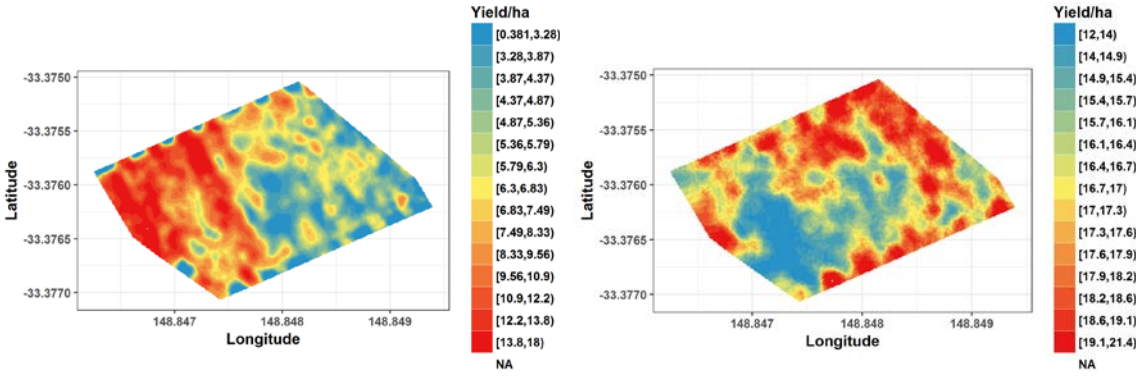


(b)

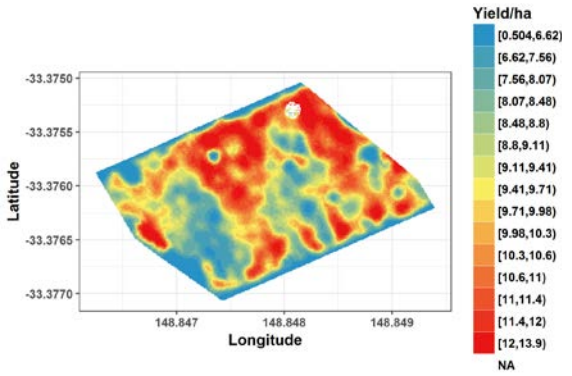


(c)

Figure 5.5 Actual yield map for Orange B4 block. (a) 2015 harvest – note the western third of the block was harvested by another harvester without a yield monitor. (b) 2016 harvest. (c) 2017 harvest.



(a) (b)



(c)

Figure 5.6 Actual yield map for Orange B12 block. (a) 2015 harvest. (b) 2016 harvest. (c) 2017 harvest. Significant differences between 2015 and 2016 are due to the presence of a dam on the North-Eastern side of the block, which was at a higher capacity in 2016 and 2017 and hence increased water availability to the Eastern portion of the block.

5.1.4 PCD maps

The PCD maps for the four blocks are presented in Figure 5.7 to Figure 5.9. These were captured at veraison and are a better indication of the growth of the canopy than of the variation in yield.

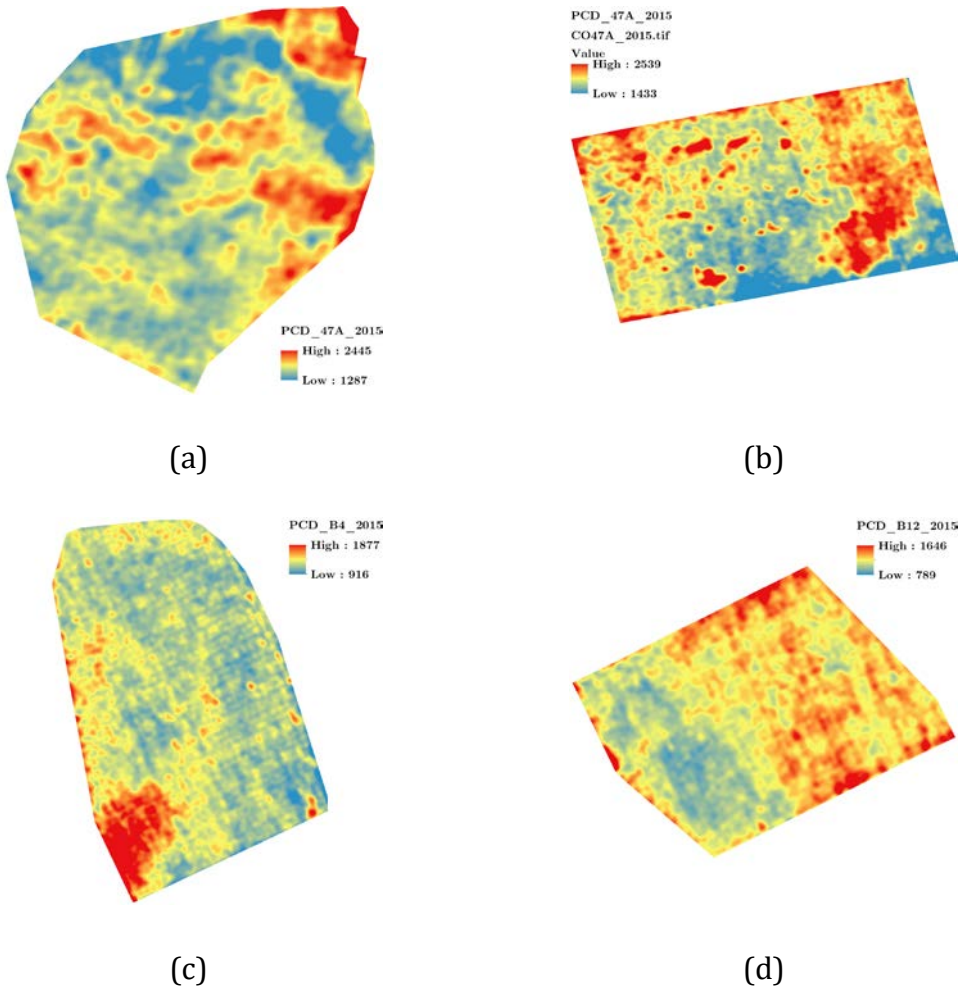
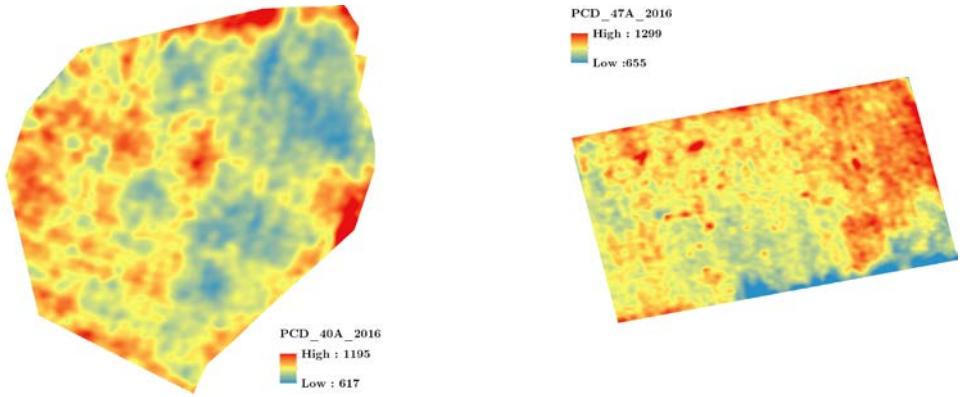
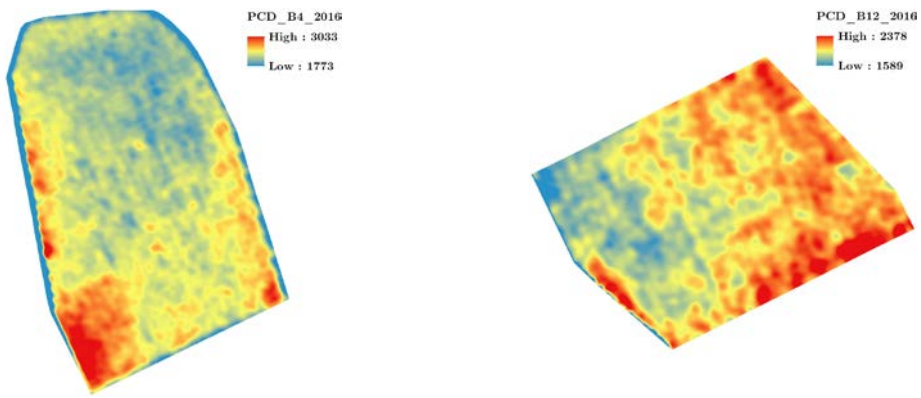


Figure 5.7 PCD maps for the four blocks in 2015. (a) Clare 40A. (b) Clare 47A. (c) Orange B4. (d) Orange B12.

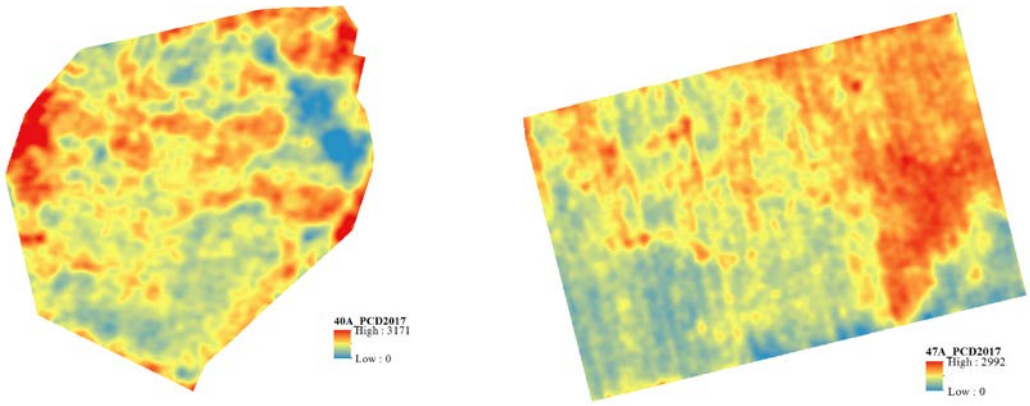


(a) (b)

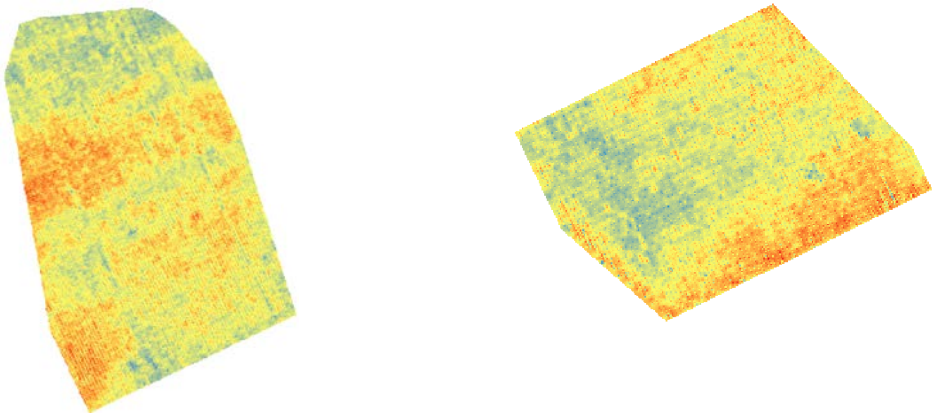


(c) (d)

Figure 5.8 PCD maps for the four blocks 2016. (a) Clare 40A. (b) Clare 47A (c) Orange B4. (d) Orange B12.



(a) (b)



(c) (d)

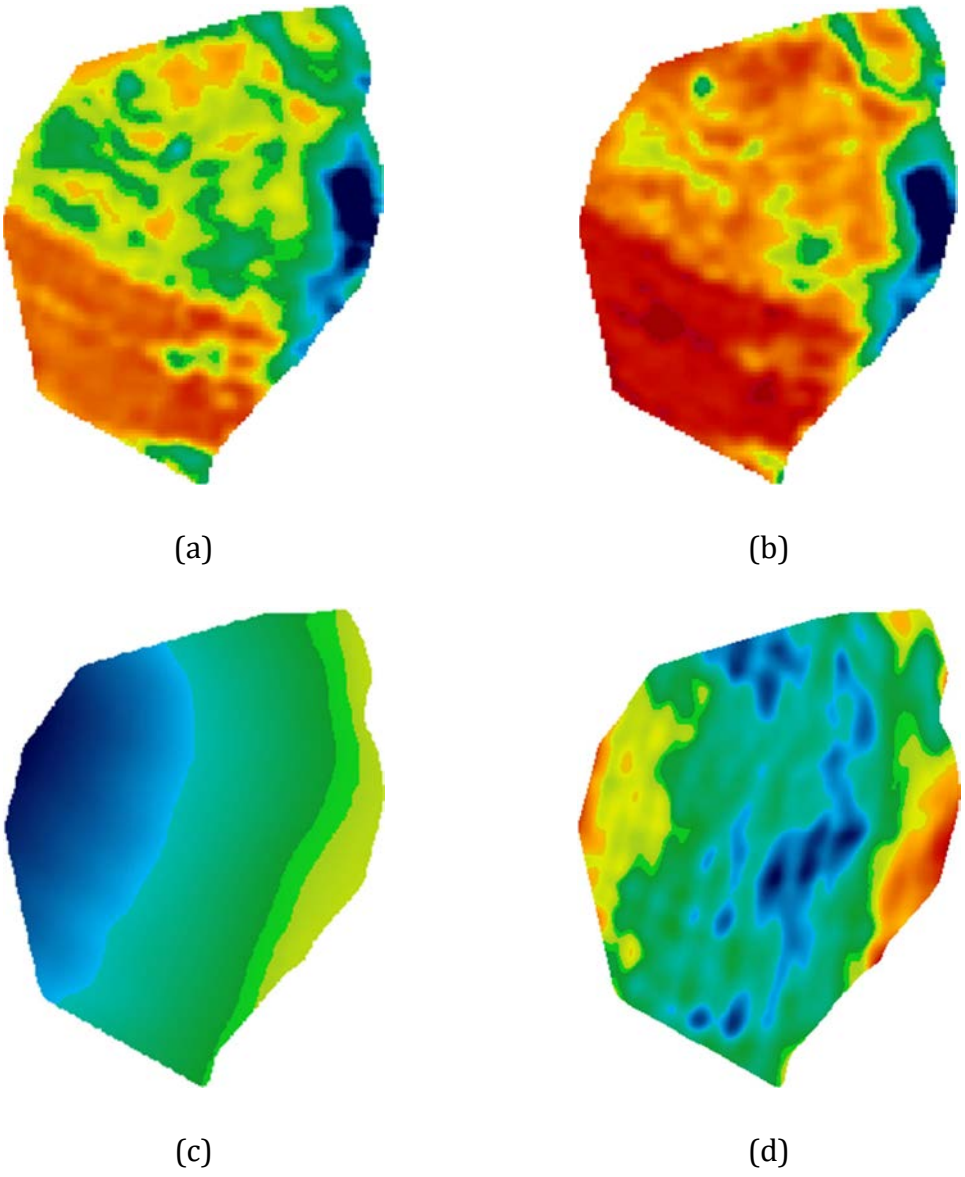
Figure 5.9 PCD maps for the four blocks in 2017. (a) Clare 40A. (b) Clare 47A. (c) Orange B4. (d) Orange B12.

The South-West corner of B4 is known to be particularly low-lying with poor drainage which has led to a very dense canopy detected in PCD maps. Comparison between Figure 5.7(c) and Figure 5.5(c) shows that the effect of this low-lying area on actual yield was less pronounced, as shading in the Shiraz reduces the crop level.

5.1.5 EM38 maps

Electromagnetic induction surveys were carried out in some of the blocks to gain an understanding of the moisture content of the soil. EM38 instruments were employed to conduct the survey. The survey was only conducted in 40A and 47A blocks in Clare, and the corresponding results are shown below. In both blocks, there was substantially higher moisture content at the lower sections of the block which were not well drained.

The survey was physically conducted at Orange by a commercial contractor, who was observed to collect the data but failed to supply the resulting maps.



(a) (b)

(c) (d)

Figure 5.10 EM38 plots for Clare 40A. (a) 0 – 50 cm depth. (b) 0 – 100 cm depth. (c) Slope. (d) Elevation. Red corresponds to lower values and blue to higher values.

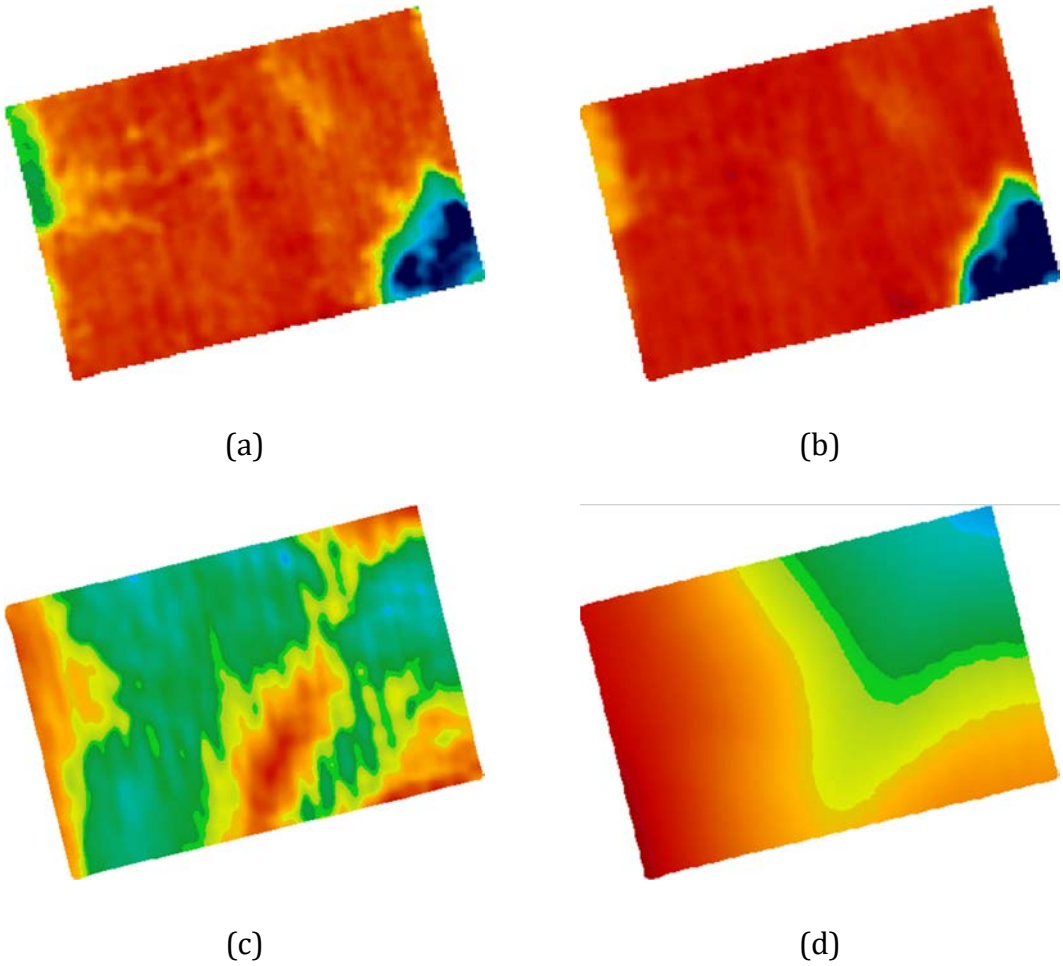


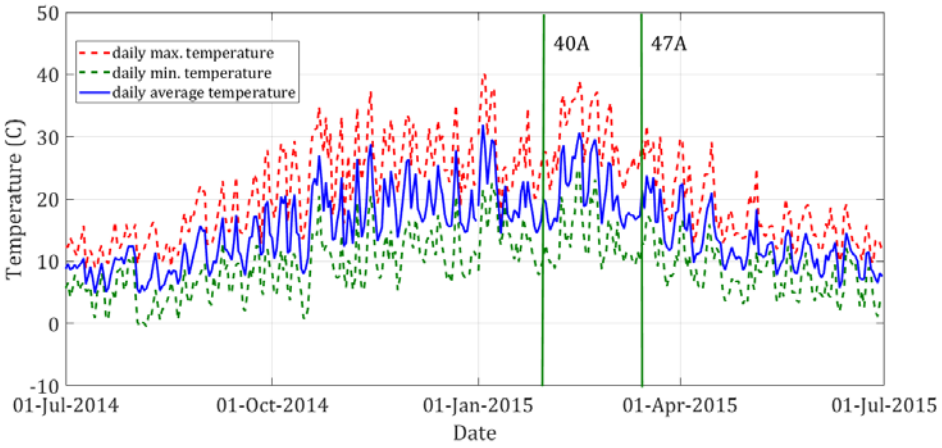
Figure 5.11 EM38 plots for Clare 47A. (a) 0 – 50 cm depth. (b) 0 – 100 cm depth. (c) Slope. (d) Elevation. Red corresponds to lower values and blue to higher values.

5.1.6 Weather data

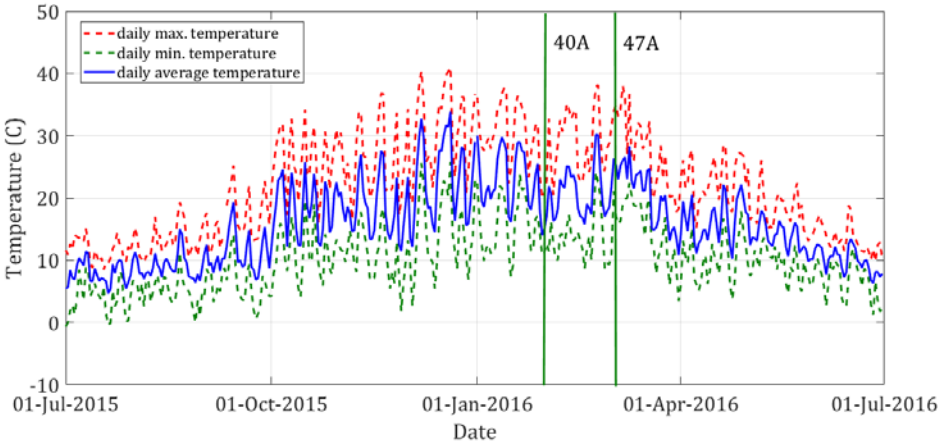
Next, weather data is plotted. Under this section, temperature values and rainfall are plotted for both Clare and Orange for the three seasons spanning from 2014 to 2017. The Clare data was from a weather station on the property, about 1km from the blocks. The Orange data was from a weather station on the property, about 1km from each of the blocks. Clearly Orange has a higher average rainfall than Clare.

Table 5.4 Total annual rainfall at each site [mm]

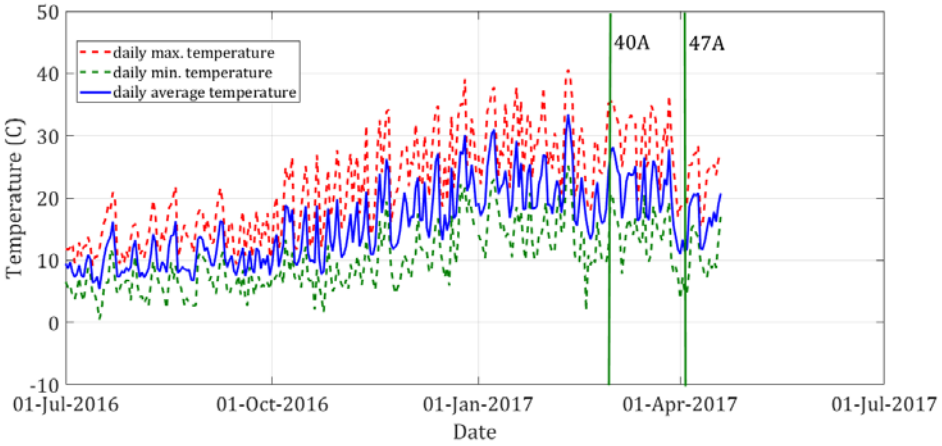
Location	Clare	Orange
July 2014 – June 2015	346.42	705.2
July 2015 – June 2016	430.52	932.0
July 2016– June 2017	636.7	763.8


daily max. temperature
daily min. temperature
daily average temperature
40A
47A
Temperature (C)
50
40
30
20
10
0
-10
01-Jul-2014
01-Oct-2014
01-Jan-2015
01-Apr-2015
01-Jul-2015
Date

(a)

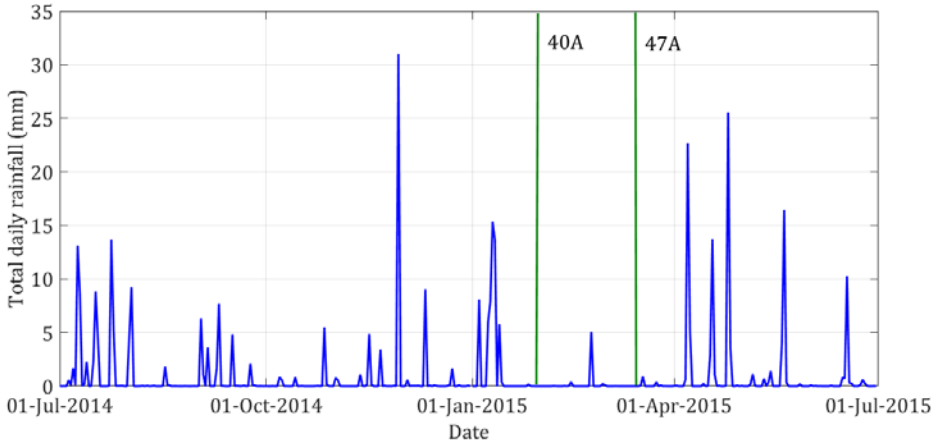

daily max. temperature
daily min. temperature
daily average temperature
40A
47A
Temperature (C)
50
40
30
20
10
0
-10
01-Jul-2015
01-Oct-2015
01-Jan-2016
01-Apr-2016
01-Jul-2016
Date

(b)

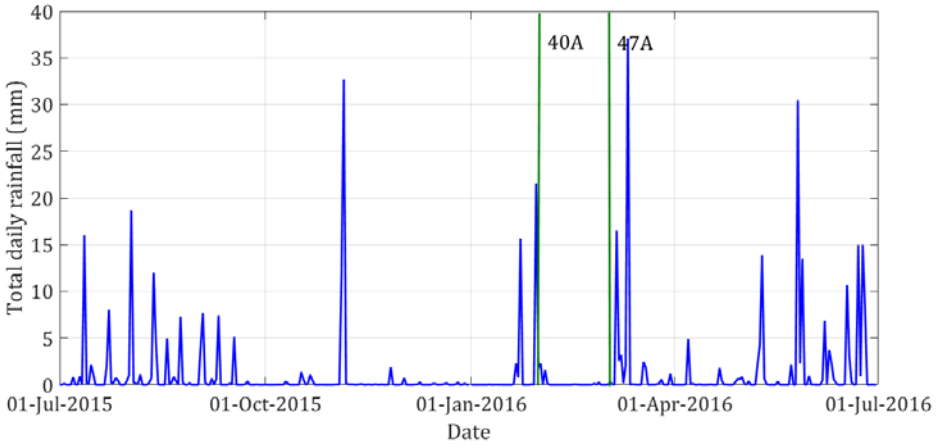


(c)

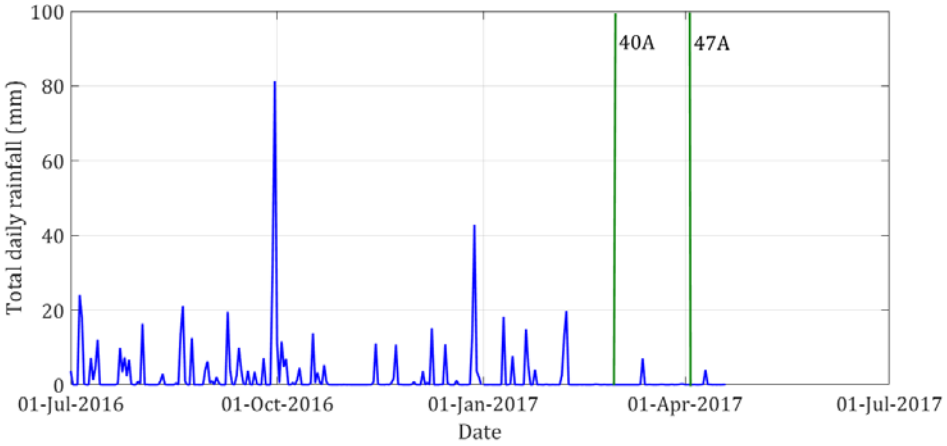
Figure 5.12 Temperature variation at Clare with harvest dates indicated by vertical lines. (a) 2014/15 season. (b) 2015/16 season. (c) 2016/17 season.



(a)

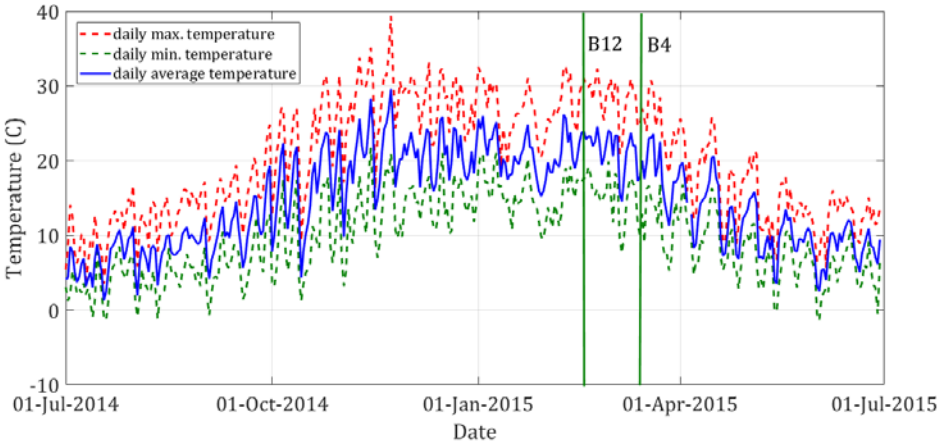


(b)

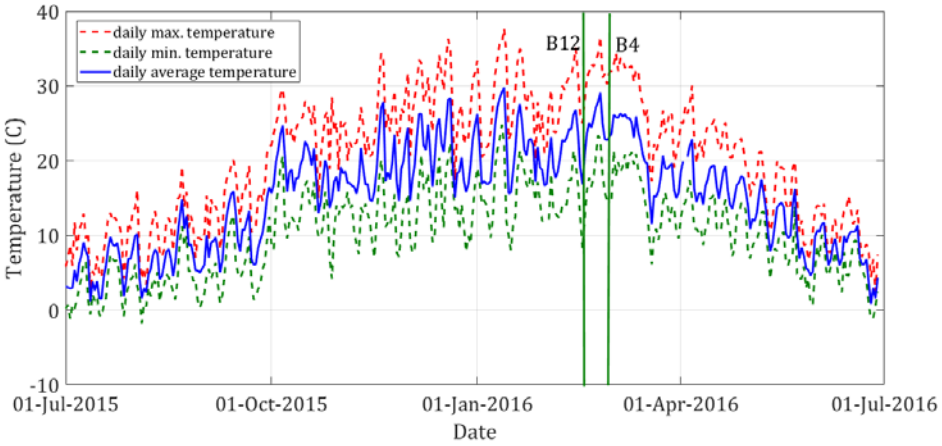


(c)

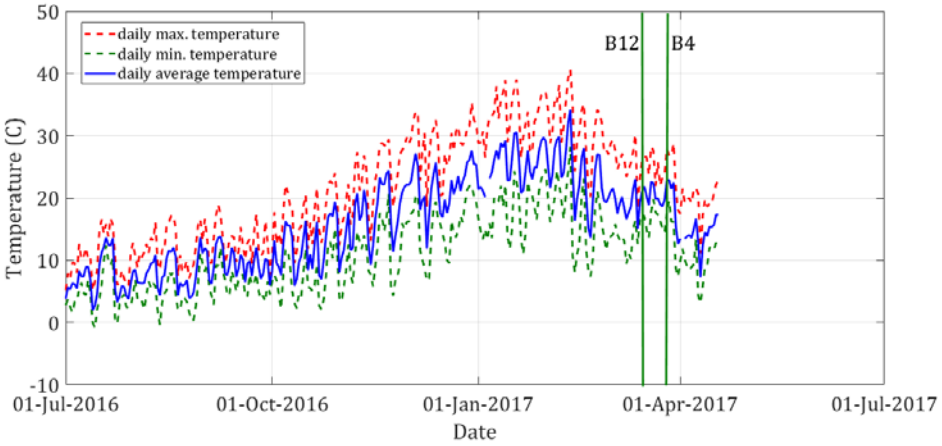
Figure 5.13 Daily rainfall at Clare with harvest dates indicated by vertical lines. (a) 2014/15 season. (b) 2015/16 season (c) 2016/17 season


daily max. temperature
daily min. temperature
daily average temperature
B12
B4
Temperature (C)
40
30
20
10
0
-10
01-Jul-2014
01-Oct-2014
01-Jan-2015
01-Apr-2015
01-Jul-2015
Date

(a)

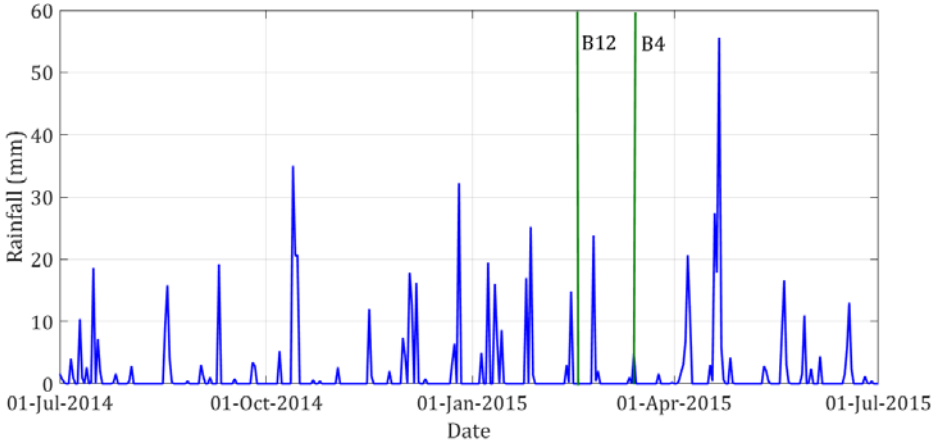

daily max. temperature
daily min. temperature
daily average temperature
B12
B4
Temperature (C)
40
30
20
10
0
-10
01-Jul-2015
01-Oct-2015
01-Jan-2016
01-Apr-2016
01-Jul-2016
Date

(b)

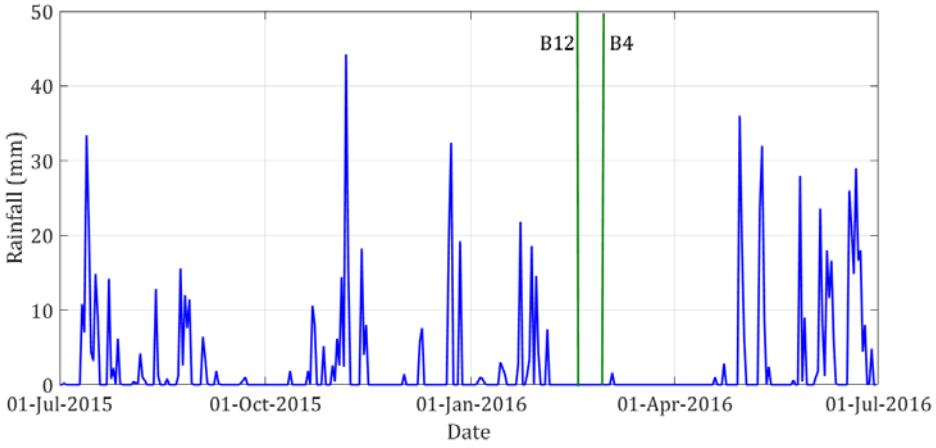


(c)

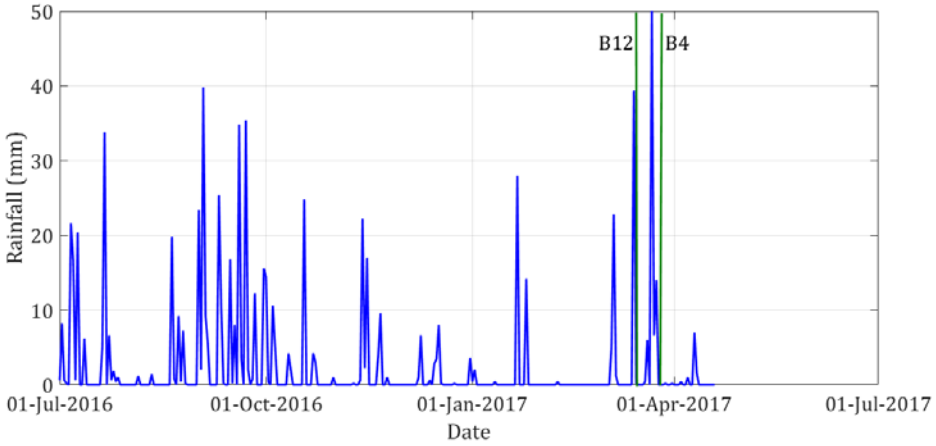
Figure 5.14 Temperature variation at Orange with harvest dates indicated by vertical lines. (a) 2014/15 season. (b) 2015/16 season. (c) 2016/17 season.



(a)



(b)



(c)

Figure 5.15 Daily rainfall at Orange with harvest dates indicated by vertical lines. (a) 2014/15 season. (b) 2015/16 season. (c) 2016/17 season.

5.1.7 Phenology

Manually collected data for key phenological dates in each block were entered into a centralised database and then visualised in the format shown in Figure 5.16, Figure 5.17, Figure 5.18 and Figure 5.19 below. Each EL stage shown is associated with a

particular colour in the colour gradient and the horizontal position denotes the calendar data in each season.

This visualisation enables growers to quickly identify the variation between seasons and begin to understand what impact weather effects had on phenology.

Clearly in 2017 the two Clare blocks were harvested far later than historically as a cooler start to the season meant that the bunches did not mature as quickly as usual. The much greater variation in the harvest dates of the Orange blocks as compared with the Clare blocks may be due to the flexibility allowed by a small contract grower as opposed to a large commercial grower as well as sensitivity to climatic effects at a higher altitude.

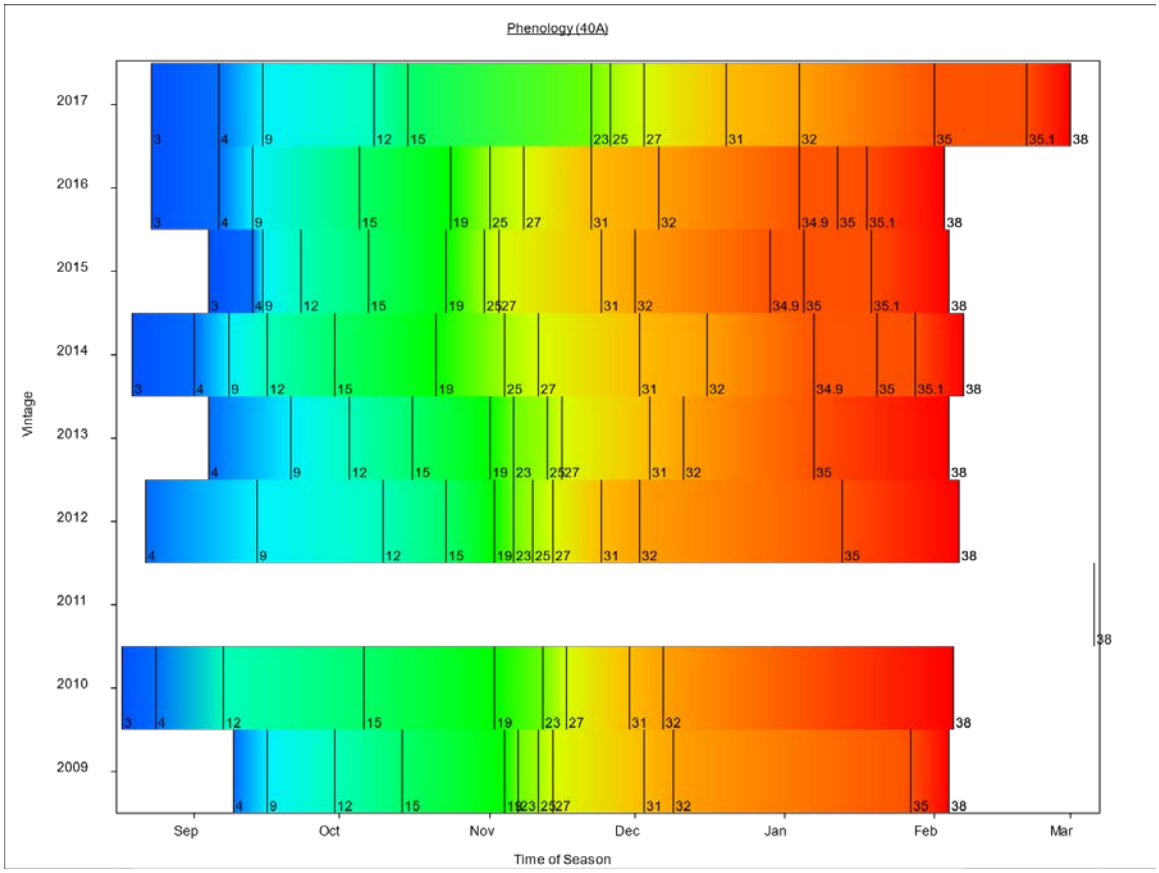


Figure 5.16 Phenology data for block 40A: 2009-2017

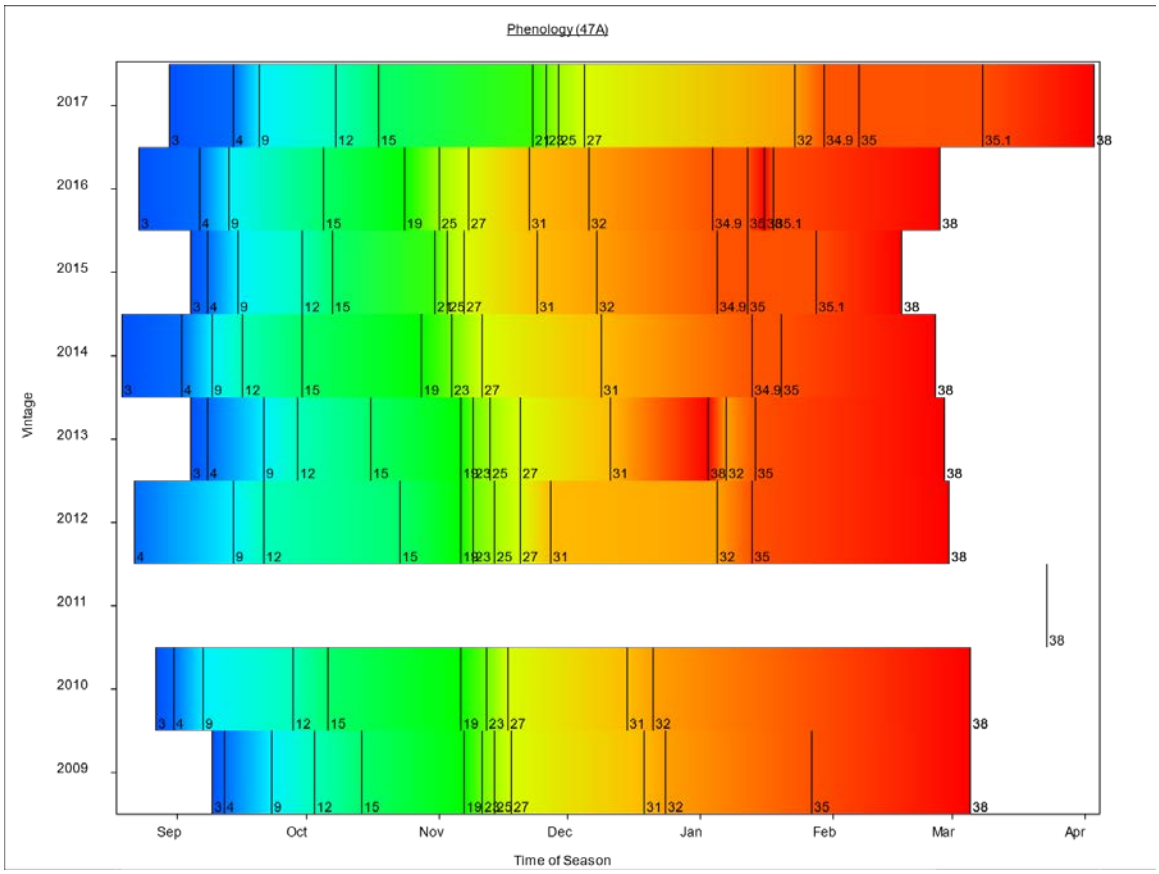


Figure 5.17 Phenology data for block 47A: 2009-2017

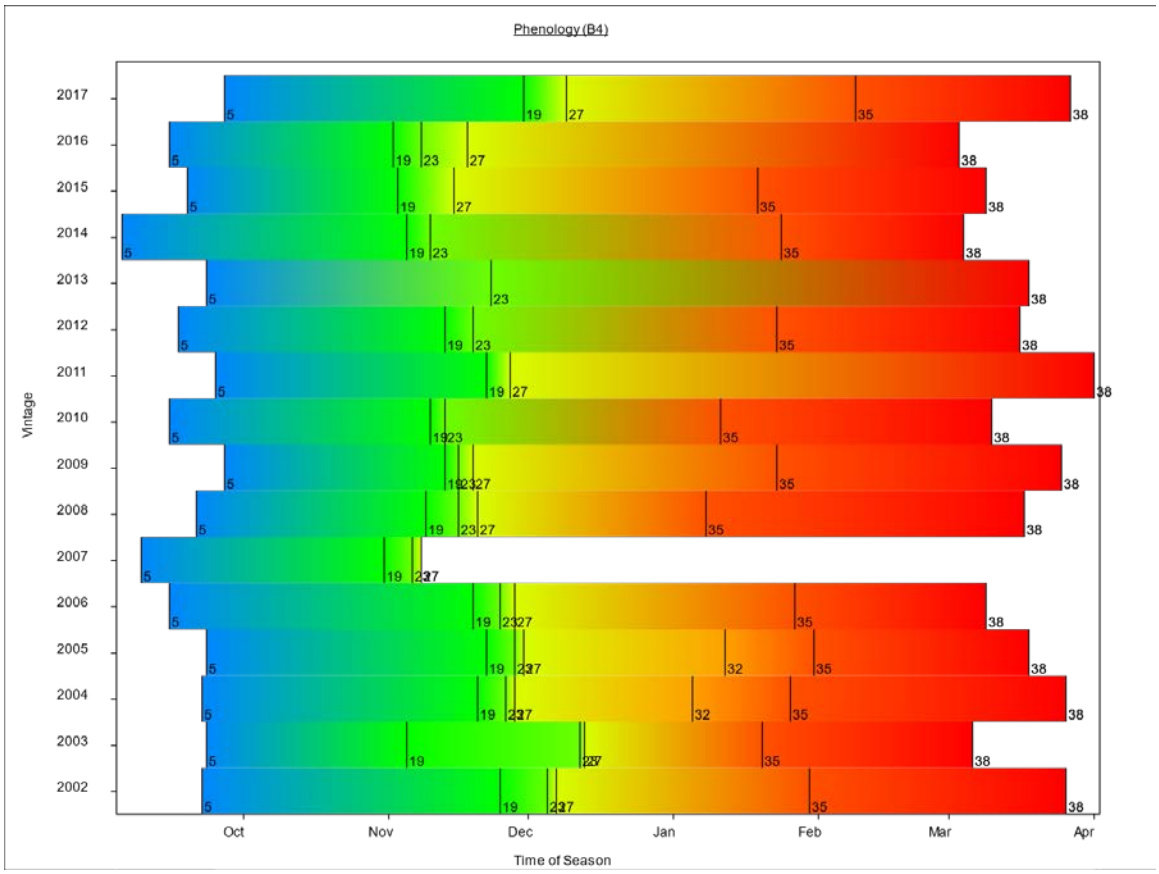


Figure 5.18 Phenology data for block B4: 2002-2017

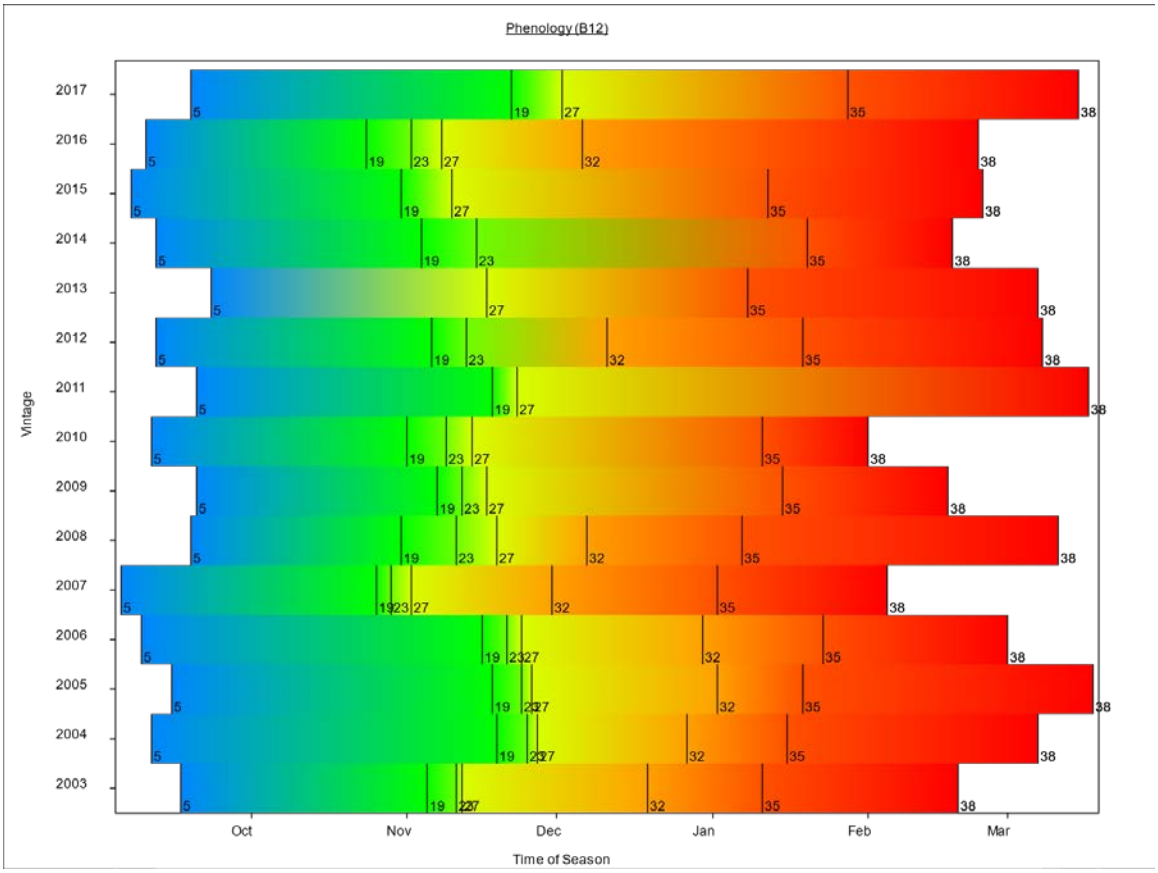
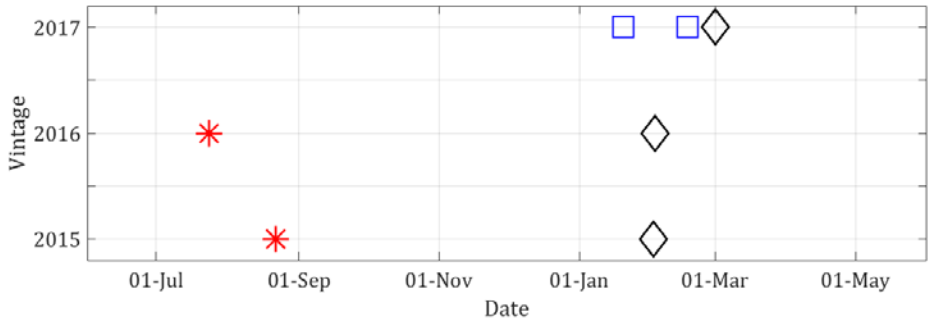


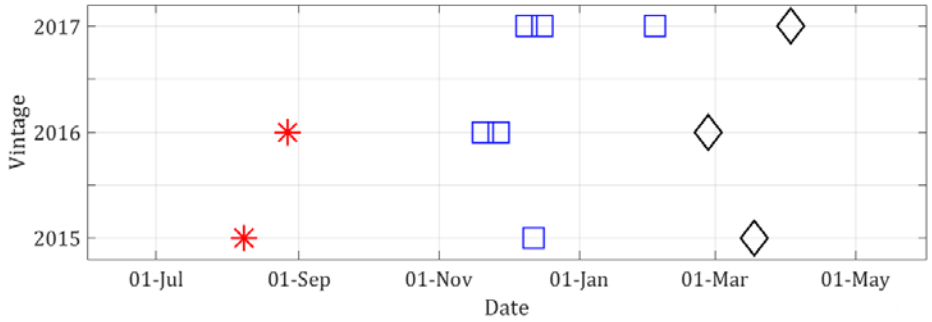
Figure 5.19 Phenology data for block B12: 2003-2017

5.1.8 Management actions

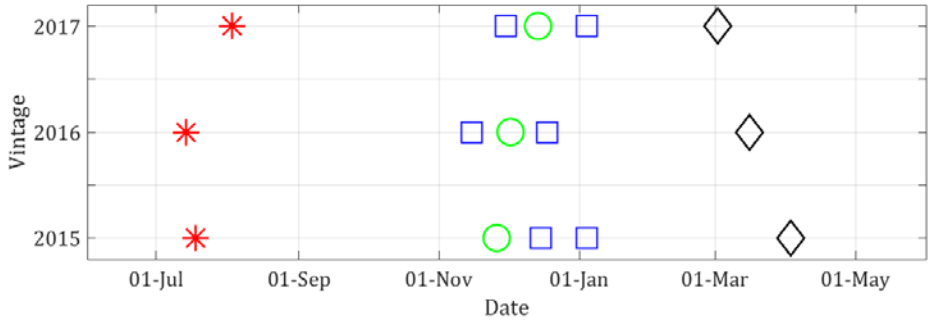
Management actions taken in each block that may have had impact on yield are presented in Figure and exact dates are in Table 0.2 in the Appendix. Trimming was generally undertaken without influencing the volume of fruit on the vines, although minor damage due to the passage of equipment may have occurred. No bunch or shoot thinning was undertaken in any of the blocks during the study period. The management actions and harvest dates have been plotted in Figure 5.20.


2017
2016
2015
Vintage
01-Jul
01-Sep
01-Nov
01-Jan
01-Mar
01-May
Date

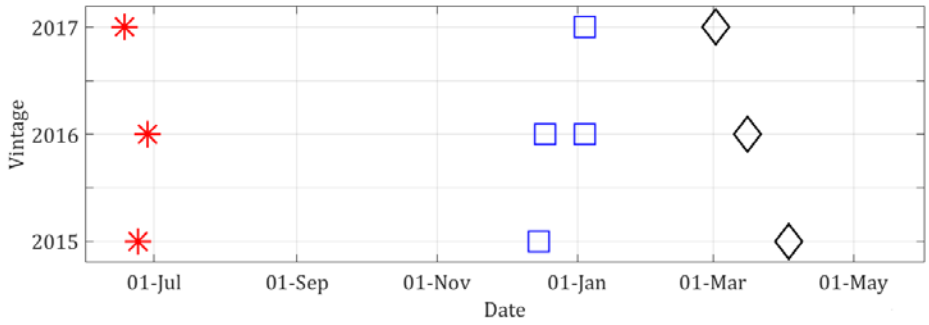
(a)


2017
2016
2015
Vintage
01-Jul
01-Sep
01-Nov
01-Jan
01-Mar
01-May
Date

(b)


2017
2016
2015
Vintage
01-Jul
01-Sep
01-Nov
01-Jan
01-Mar
01-May
Date

(c)



(d)

Figure 5.20 Management actions carried out in the four blocks from Y1 to Y3 (2015-2017) Legend – Red asterisk: Pruning, Blue square: Trimming, Green circle: Leaf plucking, Black Diamond: Harvest. (a) Block 40A. (b) Block 47A. (c) Block B4. (d) Block B12.

5.2 Experimental setup

Within each of the study blocks, several different arrangements for sampling were used, some shared between manual and visual yield estimation methods and some used for normal data collection while others were used for validation of parts of the algorithms. They have been abbreviated as follows:

- TL - Temporal Locations: 20 × 2 panel (3 post) segments in each block. The locations of 20 TLs were not changed from year to year. They are presented as pink short strips in Figure 5.21.
- SS - Sampling Segments: 30 or 60 × 0.6m segments, destructively sampled on each field trip in Y1 and Y2. The locations were randomly generated by best candidate sampling (2D) while checking for collisions with existing sample points. Yellow points in Figure 5.21 are examples of a set of SSs at one time.
- SSS – Stratified Sampling Segments: 30 × 0.6m segments, only used in Y3. These were positioned according to the previous year's actual yield map, which was classified into low, medium and high yield and 10 segments located in each classified region to improve sampling of the full variability within each block.
- HV - Harvest: Dense spatial sampling done immediately prior to harvest in Y1 and Y2 using 26 samples (SSs) per Ha, as recommended by Bramley [10].
- DC - Data Collection by mobile phone: Weekly or fortnightly images taken of marked bunches in each TL or SSS which were tracked through the growth cycle.
- FT - Field trips. FT1.2 means the second field trip in Y1 while FT2.5 means the fifth field trip in Y2.



(a) Block 40A



(b) Block 47A



(c) Block B4



(d) Block B12

Figure 5.21 Locations of TL (pink line) and SS (yellow points) on maps of four blocks.

5.3 Data management

To manage the large volume of collected data (see Table 5.5), a customised database was developed to store the data and allow easy retrieval through a web or application programming interface. A key learning from this project was that the time required to validate, input, store and manage data is enormous, sometimes greater than the time taken to collect the data. Hence, tools that enable more efficient data collection, validation, storage and backup are absolutely critical for future projects and for extension of the research solutions to growers. The skills required to do this are available but need to be applied for the direct benefit of growers and indeed across the entire supply chain.

Table 5.5 Statistics showing the scale of the data collected in the study blocks, not including analysis and processing time

Name	Y1	Y2	Y3	Total
Manual Measurements	27,463	35,881	8,481	71,825
Hours of video footage	65	97	15	177
Number of videos	2,288	4,283	379	6,950
Number of photos	15,079	10,963	1,482	27,524
Berries counted	46,014	100,587	81,166	227,767
Person days of field work	212	447	138	797
Field trips	46	137	16	199

6 Manual yield estimation and component analysis

To provide a valid basis for comparison, best practice manual yield estimation was undertaken at four times each season – at shoot stage, immediately prior to flowering ('flowering'), pre-veraison or pea-sized ('pea-sized') and immediately prior to harvest ('harvest'). The modified Eichorn-Lorenz ('E-L') scale [9] is used throughout this report to denote the development stage of the vines and bunches. The experimental procedures used are integrated with the description of the method at each stage. These stages correspond to those in which visual yield estimation was undertaken, for which the results are presented in subsequent chapters.

The stratified sample segments described in Section 5.2 and used only in Y3 were chosen based on the previous year's yield monitor map. Determining the best basis for stratifying samples is not trivial and is worth further investigation.

A comparison between different harvest yield estimation methods as well as sampling methods (TLs vs SSSs) was undertaken to better inform future fieldwork. A comparison with the long term average, effectively a 'do-nothing' plan, was performed in order to see the improvement possible using manual yield estimation.

A correction factor for rachis weight was not included for the shoot and flowering or harvest bunches method as this is not included in the best practice manual yield estimation used by industry (Martin 2003).

Historical estimates may be taken from any reliable source. In this project, very few prior data were available other than average bunch weights and total yields, so for all other values, an estimate was made for Y1, the values from Y1 were used for Y2 and the average of Y1 and Y2 was used for Y3.

6.1 Shoot stage (Manual)

To estimate the yield, we propose the following equation:

$$Y^* \text{ (shoot)} = c(S) \times (B_h/S_s) \times \mu(w(B)_h)$$

where c(S) is the number of shoots manually counted at each Sample Segment (SS) and extrapolated to the entire length of the block. The bunch to shoot ratio and the average bunch weight ($\mu(w(B)_h)$) are estimated from historical values.

Each of these terms has been estimated independently for this method, and the corresponding procedure for calculating the accuracy is given in Table 6.1 below.

Table 6.1 Calculation of yield components at shoot stage

Term	**c(S)**	**B_h/S_s**	**$\mu(w(B)_h)$**
Normal method of calculation (as	Manual counted at 30 x SSSs	Historical estimate	Historical estimate

would be applied in practice)			
Validation method for this project	As above	$c(S)_s$ and $c(B)_h$ both at 30 x SSSs	$c(B)_h$ and $w(B)_h$ for all bunches in each of 30 x SSSs

6.2 Flowering stage (Manual)

To estimate the yield, we propose the following equation:

$$Y^* \text{ (flowering)} = c(I) \times (B_h/I_f) \times \mu(w(B)_h)$$

where c(I) is the number of inflorescences manually counted at 30 Stratified Sample Segments (SSSs) and extrapolated to the entire length of the block. The bunch gain loss factor (B_h/I_f, also written as B_{gl}) and the average bunch weight ($\mu(w(B)_h)$) are estimated from historical values. Alternative approaches involving manual flower counting do exist, however they are not widely used in practice due to the tedium of counting.

Each of these terms has been estimated independently for this method, and the corresponding procedure for calculating the accuracy is given in Table 6.2 below. Historical estimates may be from any reliable source, at the discretion of the farmer.

Table 6.2 Calculation of yield components at flowering stage

Term	**c(I)**	**B_h/I_f**	**$\mu(w(B)_h)$**
Normal method of calculation (as would be applied in practice)	Manual counted at 30 x SSSs	Historical estimate	Historical estimate
Validation method for this project	As above	$c(I)_f$ and $c(B)_h$ both at 30 x SSSs	$c(B)_h$ and $w(B)_h$ for all bunches in each of 30 x SSSs

6.3 Pea-sized stage (Manual)

To estimate the yield, we propose the following equation:

$$Y^* \text{ (pea-sized)} = c(B) \times (B_h/B_{ps}) \times \mu(b/B) \times \mu(w(b)_h)$$

where c(B) is the number of bunches manually counted at 30 destructively harvested Stratified Sample Segments (SSSs) and extrapolated to the entire length of the block. The number of berries per bunch (b/B) is calculated from three bunches from each of 30 x SSSs. The bunch gain loss factor (B_h/B_{ps}, also written as B_{gl}) and the average berry weight ($\mu(w(b)_h)$) are estimated from historical values.

Each of these terms has been estimated independently for this method, and the corresponding procedure for calculating the accuracy is given in Table 6.3 below. Historical estimates may be from any reliable source, at the discretion of the farmer.

Table 6.3 Calculation of yield components at pea-sized stage

Term	c(B)	B_h/B_{ps}	μ(b/B)	$\mu(w(b)_h)$
Normal method of calculation (as would be applied in practice)	Manual counted at 30 x SSSs	Historical estimate	Manually counted from 3 bunches at 30 x SSSs	Historical estimate
Validation method for this project	As above	$c(B)_{ps}$ and $c(B)_h$ both at 30 x SSSs from destructive samples.	Manually counted from 3 bunches at 30 x SSSs	$c(b/B)_h$, $w(B)_h$ and $w(r)_h$ for at least 3 bunches in each of 30 x SSSs

6.4 Harvest stage (Manual)

To estimate the yield, we propose two equations and two methods, the bunches method and the berries method. The bunches method is calculated as:

$$\hat{Y}\,(\text{harvest})(\text{bunches}) = c(B) \times \mu(w(B)_h)$$

where c(B) is the number of bunches manually counted at several destructively harvested Stratified Sample Segments (SSSs) and extrapolated to the entire length of the block. The exact number of sample segments is shown in Table 6.11. The average bunch weight was measured using the total fruit mass in each SSS and divided by the number of bunches in that SSS.

The berries method is calculated as:

$$\hat{Y}\,(\text{harvest})(\text{berries}) = c(B) \times \mu(b/B) \times \mu(w(b)_h)$$

where $\mu(b/B)$ is the number of berries per bunch, manually counted from at least three bunches in each SSS. Average berry weight ($\mu(w(b)_h)$) was calculated by stripping and weighing five berries from each of the marked bunches, approximately 400 berries in total per block.

A comparison between the bunches and berries method is given in Section 6.5.4.

Each of these terms has been estimated independently for this method, and the corresponding procedure for calculating the accuracy is given in Table 6.4 and Table 6.5 below.

Table 6.4 Calculation of yield components at harvest stage (bunches method)

Term	c(B)	$\mu(w(B)_h)$
Normal method of calculation (as would be applied in practice)	Manual counted at 30 x SSSs	$c(B)_h$ and total $w(B)_h$ for all bunches in each of 30 x SSSs

Table 6.5 Calculation of yield components at harvest stage (berries method)

Term	c(B)	μ(b/B)	$\mu(w(b)_h)$
Normal method of calculation (as would be applied in practice)	Manual counted at 30 x SSSs	Manually counted from 3 bunches at 30 x SSSs	$c(b/B)_h$, $w(B)_h$ and $w(r)_h$ for at least 3 bunches in each of 30 x SSSs

6.5 Results and component analysis (Manual)

The following subsections describe the results when comparing the predicted yield against the tonnage delivered to the winery as well as the error in each component as calculated in the tables associated with each development stage above. The first row of the subsequent tables gives the percentage error averaged over all four blocks and three seasons. The second and third rows give the minimum and maximum percentage error over all four blocks and three seasons. The average percentage error calculated using absolute values – for comparison of the magnitude rather than offset follows, along with the standard deviation and coefficient of variation (standard deviation divided by the average). Columns with manual counts are left blank as they were physically counted rather than using prediction factors. However, that does not mean the counting was accurate and in many cases, is likely to be the greatest source of error.

6.5.1 Shoot stage results and component analysis

Table 6.6 shows that yield estimates at the shoot stage tend to be underestimates as the average is less than zero. This is quite likely due to undercounting of shoots manually, as the rapid growth at that time of the season means maintaining consistency is difficult and if left too late can be very challenging in spur pruned blocks.

Looking at the yield components, the bunch to shoot ratio had the greatest coefficient of variation, suggesting it needed to be calculated over a longer study period in order to understand the degree of variability from season to season. In Y3, this bunch to shoot ratio in blocks 40A and 47A was greatly influenced by a variation in shoot count between the shoot and harvest stages. Only 60-65% of shoots counted at the shoot stage remained when counted in the same SSS locations at harvest. No shoot thinning was undertaken in the block, only several passes of

trimming, which should not have affected the shoot count. No logical explanation of this has been found – the shoots were counted by the same people, both non-destructively.

Curiously, the average bunch weight was incorrect by 20%, so understanding bunch weight development would be key to improving the yield estimate.

Overall, an error of nearly 30% was obtained at the shoot stage across all cultivars and blocks.

Table 6.6 Yield and component errors [%] at the shoot stage across all four blocks and all three years

Term	Y* (shoot)	c(S)	B_h/S_s	$\mu(w(B)_h)$
Average % error (raw values)	-8.48	-	0.45	-2.69
Min % error (ABS values)	4.67	-	1.14	2.45
Max % error (ABS values)	60.74	-	47.40	52.10
Average % error (ABS values)	29.16	-	14.57	19.96
Standard deviation of % error (ABS values)	14.02	-	13.64	13.56
Coefficient of Variation of % error (ABS values)	0.48	-	0.94	0.68

6.5.2 Flowering stage results and component analysis

Table 6.7 shows that manual yield estimation at flowering is again an underestimate on average. The magnitude of the error is slightly lower than the shoot stage (22% versus 29%). The bunch to inflorescence ratio is again a larger contributor to the error than the average bunch weight estimate, suggesting that counting inflorescences more accurately would be helpful. This was shown to be exceptionally difficult in Section 8.3.2. The larger maximum error in bunch to inflorescence ratio as well as the greater standard deviation, as compared with the bunch to shoot ratio reflects the difficulty in obtaining this measurement.

Overall, an error of 22% was obtained at the flowering stage across all cultivars and blocks.

Table 6.7 Yield and component errors [%] at the flowering stage across all four blocks and all three years

Term	Y* (flowering)	c(I)	B_h/I_f	$\mu(w(B)_h)$
Average % error (raw values)	-13.99	-	-0.84	-2.69

Min % error (ABS values)	3.15	-	0.13	2.45
Max % error (ABS values)	46.90	-	74.22	52.10
Average % error (ABS values)	22.06	-	23.16	19.96
Standard deviation of % error (ABS values)	15.94	-	20.36	13.56
Coefficient of Variation of % error (ABS values)	0.72	-	0.88	0.68

6.5.3 Pea-sized stage results and component analysis

Table 6.8 shows that pea-sized estimates are particularly problematic, relative to all other estimates. The average error and even the minimum error in yield estimation are enormous. It was initially suggested that poor selection of representative bunches had led to bias in the number of berries per bunch, and with an average overestimate of 23% this is one leading factor.

However, the variation in berry weight has a dramatic impact on the error, with by far the largest coefficient of variation amongst the three predicted parameters. Within these study blocks, the berry weight was frequently an overestimate, and while in some instances, 47A Y2 in particular, substantial berry shrivel was observed, longer term data collection is needed to really understand the variation in berry weight. Providing tools to better predict berry weight at harvest would be useful.

The berry gain/loss factor between pea-sized and harvest was inaccurately estimated by 8.84% on average, although only contributing a bias of 3% in the results.

Table 6.8 Yield and component errors [%] at the pea-sized stage across all four blocks and all three years

Term	Y* (pea-sized)	c(B)	B_h/B_{ps}	μ(b/B)	$\mu(w(b)_h)$
Average % error (raw values)	93.99	-	3.14	23.45	13.08
Min % error (ABS values)	28.18	-	0.71	2.77	0.92
Max % error (ABS values)	272.08	-	21.36	69.87	111.21
Average % error (ABS values)	93.99	-	8.84	32.98	28.41
Standard deviation of % error (ABS values)	76.15	-	6.48	18.90	33.64
Coefficient of Variation of % error (ABS values)	0.81	-	0.73	0.57	1.18

6.5.4 Harvest stage results and comparison of methods

To determine the best method for manual yield estimates at harvest, multiple methods were tested. The bunches and berries methods were defined in Section 6.4.

Sampling location TL means that all fruit was destructively sampled from all the vines in each temporal location, of which there were 20 throughout the block, each of length approximately 13m, for a total of approximately 260m. Sampling location SS (see definitions in Section 5.2) was a 60cm segment, with 26 per Ha (as recommended by Bramley [10], with the total length varying from 60m to 166m depending on block size. Sampling location SSS was also a 60cm segment, but stratified, as described in Section 5.2. All the results are shown in Table 6.9.

Table 6.9 Absolute % error of manual yield estimations at harvest, compared with actual yield by using multiple methods of sampling and calculation

	Method	**Sampling location**	**40A**	**47A**	**B4**	**B12**	**Average**
Y1	Bunches	TL	0.29	11.74	22.19	9.29	10.88
	Bunches	SS	10.03	15.16	30.48	3.90	14.89
	Berries	TL	14.06	37.44	42.88	3.05	24.36
	Berries	SS	25.84	63.20	58.28	19.74	41.76
Y2	Bunches	TL	35.28	12.08	3.29	6.83	14.37
	Bunches	SS	10.04	21.88	19.72	11.16	15.70
	Berries	TL	42.22	5.55	24.26	60.23	33.07
	Berries	SS	10.53	32.00	40.59	69.64	38.19
Y3	Bunches	TL	-	-	-	-	-
	Bunches	SSS	10.34	24.43	20.08	2.88	14.43
	Berries	TL	-	-	-	-	-
	Berries	SSS	9.42	32.32	31.17	13.78	21.67

From Table 6.10 we can directly compare the different methods of sampling and measurement. The error for the berry based methods was substantially higher than for bunch based methods, because of the difficulty in finding representative berries to weigh and damage or deformity of the berry when being detached from the petiole to be measured.

There was a slightly smaller error for TL vs SS based sampling, primarily due to the larger length of vines sampled. The number of TLs was much smaller than the number of SSs, and thus thought not to represent the full range of variation across the block as well.

Hence, for attaining a single measure of accuracy for manual methods for each year, the bunches per SS or SSS method was chosen, in line with standard industry practice.

Table 6.10 Absolute % error of manual yield estimation methods at harvest, compared with actual yield by using multiple methods of sampling and calculation, summarised over all blocks and years

Method	Sampling location	Average
Bunches	TL	12.62
Bunches	SS/SSS	15.01
Berries	TL	28.71
Berries	SS/SSS	33.88

Table 6.11 Absolute % error of bunches and SS manual yield estimates, showing comparison between 26 samples per Ha in Y1 and Y2 and a total of 30 stratified samples in Y3

			Number of samples				
	Method	**Sampling location**	**40A**	**47A**	**B4**	**B12**	**Average error**
Y1	Bunches	SS	161	275	180	100	14.89
Y2	Bunches	SS	161	271	179	99	15.70
Y3	Bunches	SSS	30	30	30	30	14.43

Table 6.11 then shows the difference between SS and SSS measurements in terms of the number of samples and the corresponding accuracy. Despite the number of samples being much larger in Y1 and Y2 than Y3, the stratified samples were on average slightly more accurate. This suggests that using only 30 stratified samples is sufficient for yield estimation, at least for blocks in the range of areas used in this study (3Ha – 10Ha).

Finally, results from the bunches method over all three years are shown in Table 6.12. The yield estimate is an overestimate by 6% on average, suggesting that some of the common correction factors (harvest efficiency including transport losses, non-bearing percentage) are having a substantial influence on the result. It also means that the winemaker target of 5% error is not achievable by a purely data driven approach using industry standard sampling protocols. Improvements based on expert knowledge could be made, but are again subject to bias.

Overall, the magnitude of error to be expected by yield estimation using manual methods at harvest is 15%.

Table 6.12 Yield errors [%] at the harvest stage across all four blocks and all three years

Term	$\widehat{Y}$ (harvest)
Average % error (raw values)	6.41
Min % error (ABS values)	2.88
Max % error (ABS values)	30.48
Average % error (ABS values)	15.01
Standard deviation of % error (ABS values)	8.06
Coefficient of Variation of % error (ABS values)	0.54

6.6 Results from all three years

Figure 6.1 shows the manual yield estimation results for all four blocks in all three study seasons, with estimates shows as red circles and the final tonnage shown as a blue line. Several conclusions can be drawn from these results. The same data is represented in Table 6.13.

Table 6.13 Absolute % Error for manual yield predictions for all blocks and years

		40A	47A	B4	B12	Average
Y1	Shoot	5.34	37.44	60.74	34.40	34.48
	Flowering	6.97	10.84	3.15	12.09	8.26
	Pea-sized / pre-veraison	78.79	53.80	56.43	28.18	54.30
	Harvest	10.03	15.16	30.48	3.90	14.89
Y2	Shoot	36.00	25.71	27.04	32.10	30.21
	Flowering	5.59	28.78	41.11	39.37	28.71
	Pea-sized / pre-veraison	51.39	*149.66*	*227.54*	*272.08*	175.17
	Harvest	10.04	21.88	19.72	11.16	15.70
Y3	Shoot	28.93	25.16	4.67	32.36	22.78
	Flowering	7.26	46.90	42.58	20.02	29.19
	Pea-sized / pre-veraison	40.44	40.20	59.23	70.11	52.50
	Harvest	10.34	24.43	20.08	2.88	14.43
Average		24.26	40.00	49.40	46.55	**40.05**

Table 6.14: Absolute % Error per stage for manual yield predictions across three years

	40A	47A	B4	B12	Average all blocks
Shoot	23.42	29.44	30.82	32.95	29.16
Flowering	6.61	28.84	28.95	23.83	22.06
Pea-sized / pre-veraison	56.88	81.22	114.40	123.45	93.99
Harvest	10.14	20.49	23.43	5.98	15.01

Table 6.15 Absolute % Error per stage for manual yield predictions across three years, split by cultivar and location

	Chardonnay (40A + B12)	Shiraz (47A + B4)	Clare (40A + 47A)	Orange (B4 + B12)
Shoot	15.22	28.89	17.73	26.39
Flowering	8.06	21.96	15.32	14.70
Pea-sized / pre-veraison	90.16	97.81	69.05	118.93

Harvest	28.19	30.13	26.43	31.88
Average all stages	35.41	44.70	32.13	47.98

Firstly, there does not appear to be much consistency between estimates, either per cultivar, per site or development stage. The only exception is the pea-sized or pre-veraison (third point from the left on each plot), which is consistently an over-estimate. There was some variation between personnel and methods used in each season, and in Y2 in particular, the pea-sized estimates were wildly inaccurate.

Secondly, pea-sized estimation relies heavily on accurate counts of berries per bunch, this means that the selection of representative bunches is particularly critical, and easily biased by human selection. Even in Y3 when clear directions were provided to avoid choosing non-representative bunches, the difference between destructive berry counts at pea-sized and at harvest was 30% on average across the four blocks and ranged between 20 and 42%. This means that choosing a single bunch from a few dozen destructively sampled bunches is likely to result in a substantial overestimate than if all bunches on a randomly sampled shoot are considered. Additional factors such as berry loss or shrivel may have influenced this result, but the overestimate caused by poor bunch selection was notable in all four blocks.

In 40A, the berry count was similar, but the final berry weight was about 50% of the average berry weight in the previous year. It is likely that the marked bunches in Y2 were handled a number of times which may have influenced their growth as a substantial proportion of the bunches and berries were shrivelled.

Table 6.13 shows that overall, the average absolute value of error was 40%. This is somewhat skewed by the extreme values of pea-sized estimates, so if they are excluded the average absolute value of yield prediction using traditional manual methods was 22% across all development stages.

Table 6.14 shows that apart from the pea-sized stage, the error of prediction decreased from the shoot stage to the harvest stage, as expected.

Table 6.15 shows that estimates in the Chardonnay blocks were generally more accurate than in the Shiraz blocks, particularly at the shoot and flowering stages. Further analysis showed that apart from the prediction of bunch weight, all other predictions factors used were more accurate in Chardonnay than Shiraz. Errors were generally lower at Clare than at Orange.

At harvest, the average error was 15%, with all known contributing factors to the estimate being considered. This provides a baseline for all earlier predictions, as there are no prediction factors used (e.g. weather). Therefore, for yield estimation, we cannot reasonably expect to obtain better than 15% accuracy using manual methods.

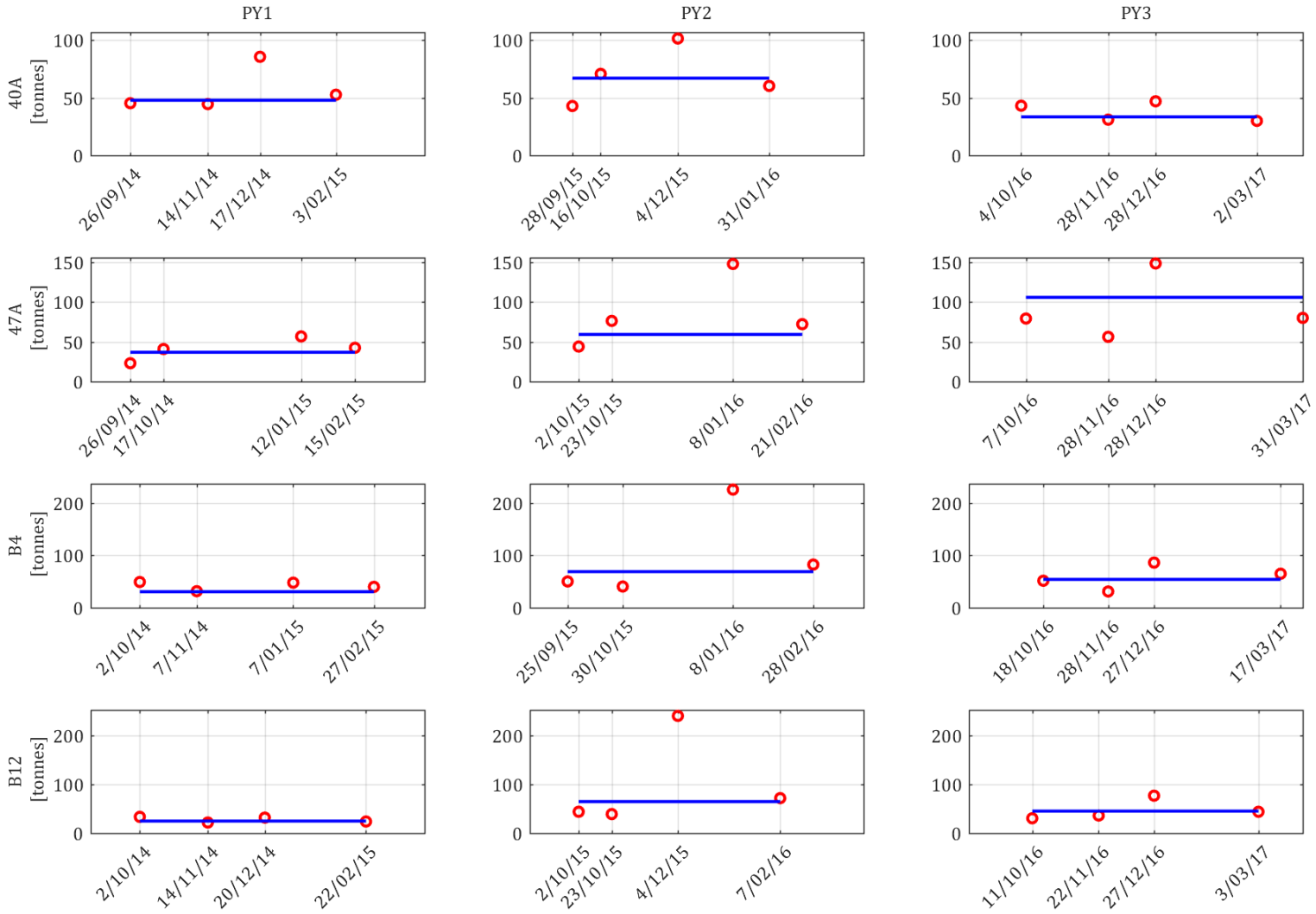


Figure 6.1 Manual yield estimates (red circles) and actual yields (blue line) for four blocks over three years.

6.7 Comparison with long term average

In order to give some context to the accuracy of manual yield estimation methods, a comparison was made with the Long Term Average (LTA) when used for yield prediction. This simply assumes that the grower took the average historical yield of the block as the predicted yield at each stage during the season, on the basis that the terroir remains constant, management actions are generally consistent and the only major factor influencing yield is the weather, which is difficult to predict.

Table 6.16 shows the percentage error in each block and season combination, with the average (of absolute values) being approximately 35%. This means that should a grower do no fieldwork whatsoever, they can expect to know their yield within ± 35% on average. Clearly this value is not very useful, but should the cost of undertaking yield prediction prove relatively high, it gives an upper bound on the expected error.

Table 6.16 Error in predicted yield [%], taking the long term average as the prediction

	40A	47A	B4	B12	ABS Average
Y1	-3.11	88.07	29.73	27.61	37.13
Y2	-30.80	17.25	-42.28	-50.90	35.31
Y3	38.60	-34.44	-26.59	-29.78	32.35
ABS Average	24.17	46.59	32.87	36.10	**34.93**

When these values were individually compared with the manual yield predictions, 40% (24/60) of the LTA predictions were more accurate, suggesting that traditional methods of yield prediction are very limited in their ability to predict yield. This may come to no surprise to some growers, but this study has characterised the magnitude of the error using four representative blocks over three years.

6.8 Summary of manual yield estimation

The key result here is that longer term records of yield components are necessary and grower knowledge needs to be integrated to improve accuracy. A purely data driven approach as taken in this project relies on a reasonable history of values, and the enormous variation between each component (± 100% in subsequent years) requires more than the two years of available historical data on which to make predictions.

The bunch to shoot and bunch to inflorescence ratios have been shown to contribute the greatest to errors in manual yield estimation at the shoot and flowering stages. This is subject to the assumption that the error due to manual counting is low, although many of the results point to an inability to count, hence making counting more reliable using image processing is a key target of this report.

At the pea-sized stage, our ability to manually predict berry diameter is very poor, contributing substantially to the error in yield prediction. However, the count of berries per bunch contributes even more to the inaccuracy and methods need to be devised to eliminate sampling bias in the selection of bunches for berry counting.

At the harvest stage, using a smaller number of stratified sample locations was shown to be more accurate than a large number randomly placed. This error was still in the order of 15%, forming a baseline for further analysis.

To further highlight the futility of manual yield estimation, it was shown that using the long term average was more accurate in 40% of the block and season instances. In short, industry standards for manual yield estimation are unprofitable and consideration must be given to automated solutions.

7 Image processing elements

This chapter presents a number of image processing algorithms and systems that have been developed either as part of this project or in parallel with it and which have been applied to varying degrees for yield estimation in the following chapters. Reference to external papers is given in several instances rather than a full inclusion of the theoretical content and method validation and the reader is encouraged to seek these out for further details.

7.1 Shoot counting by image processing

In parallel with this project, Scarlett Liu developed [11] a method for unsupervised detection, classification and counting of shoots from images in a vineyard which is shown in Figure 7.1 and further details have been published [12] [13]. Results from the application of this method to images captured using the hardware developed in this project (Section 8.1) are given in Section 8.3.1.

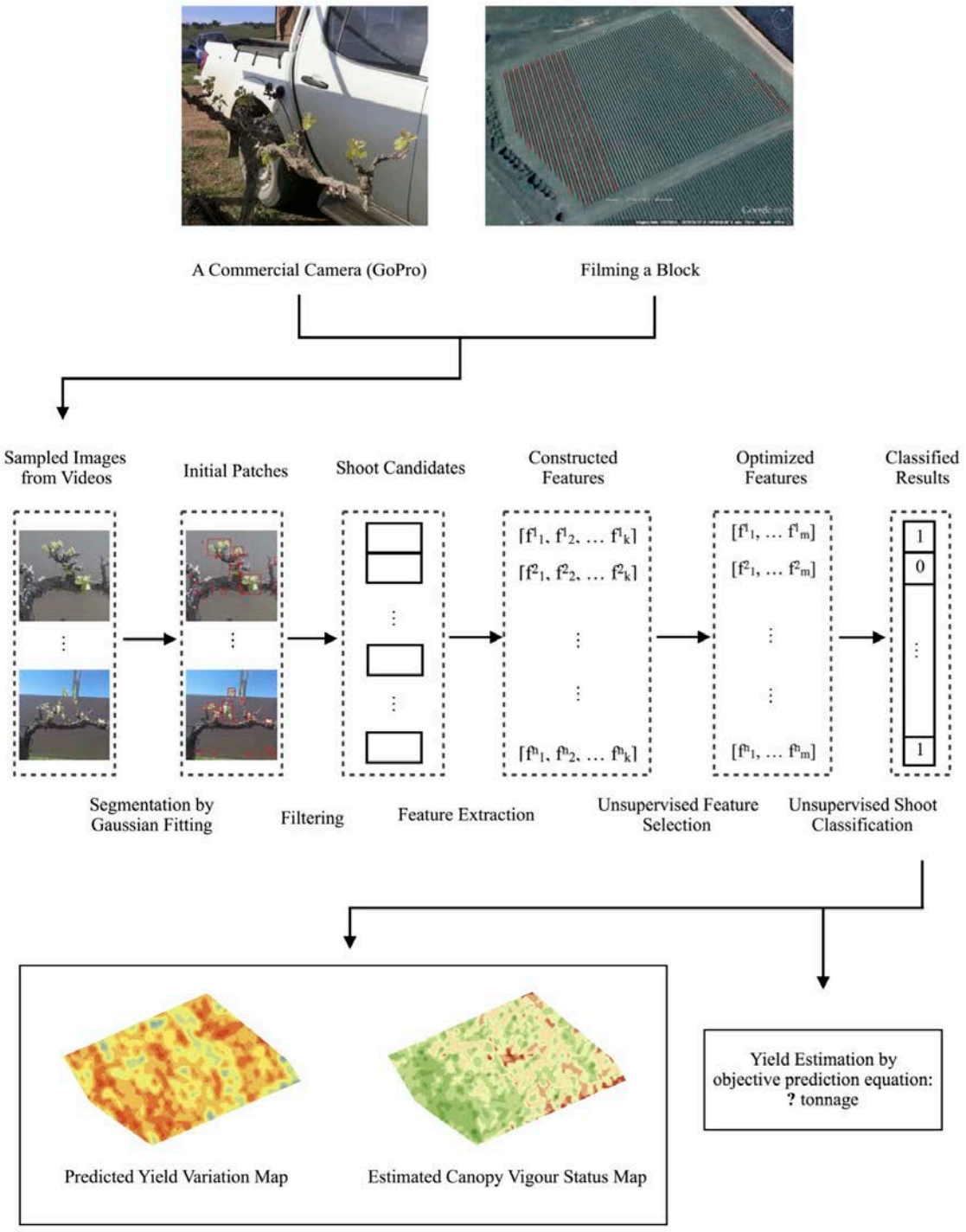


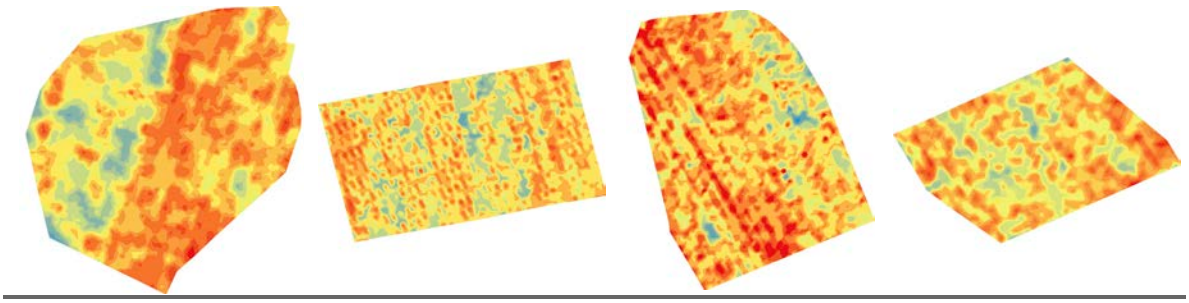
Figure 7.1 Flowchart of the procedure for yield estimation used in this report based on computer vision and data mining.

7.2 Spatial variation map generation

A method for generating a spatial variation map of visible objects without using GPS was proposed as part of this project and the results were published by Cossell [14] and Liu [12]. This method provides a GPS-free crop variation mapping solution in vineyards, which is economical for growers and is easily applied. It provides spatial information to generate a predicted yield variation map and estimated canopy vigour map. The values detected from video frames at discrete points in each block are kriged using the default settings in ArcGIS (v10.3) to generate a continuous surface across the entire block. A subset of 25% of the frames for each block in each E-L stage is used to match the spatial resolution of the provided yield monitor data, although this is only to aid in visualisation.

Based on the shoot counts processed from video frames, combined with the yield prediction formula, a predicted yield map can be produced across the entire block. *Figure 7.2* illustrates the predicted yield variation maps for four experimental blocks and compares them with actual yield maps from harvester monitors. Visually, there is some degree of correlation, so we posit that the shoot variation maps can be used as a guide to yield potential for growers, despite the imagery being captured five months prior to harvest. Having a predicted yield variation map early in the season can provide a clear tool for vineyard managers to adjust their management strategies to regularise yield and improve profit.

It is important to note that this prediction is being carried out five months prior to harvest, and assumes that the spatial variation of yield within a block will tend towards the final spatial variation at harvest. Variability in fruit set ratios, weather conditions, irrigation and other management practices will alter this result. The clear distinction between shoot growth as a result of mulch application on only the Eastern half of block 40A is evident in *Figure 7.2*, although the effect on yield was less pronounced by the harvest stage.



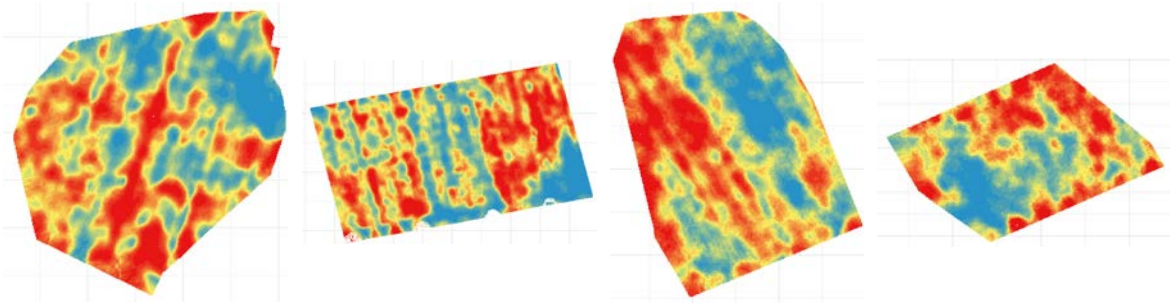


Figure 7.2 Predicted yield variation maps (Y2) from shoot counts (top row) against actual yield maps (bottom row), blocks 40A, 47A, B4, B12 from left to right. In both cases red indicates higher value in yield/Ha.

Plant Cell Density (PCD) maps can give information about canopy vigour which may be related to the final yield variation map, but this relationship is not guaranteed as seen in block B4 in *Figure 7.3*.

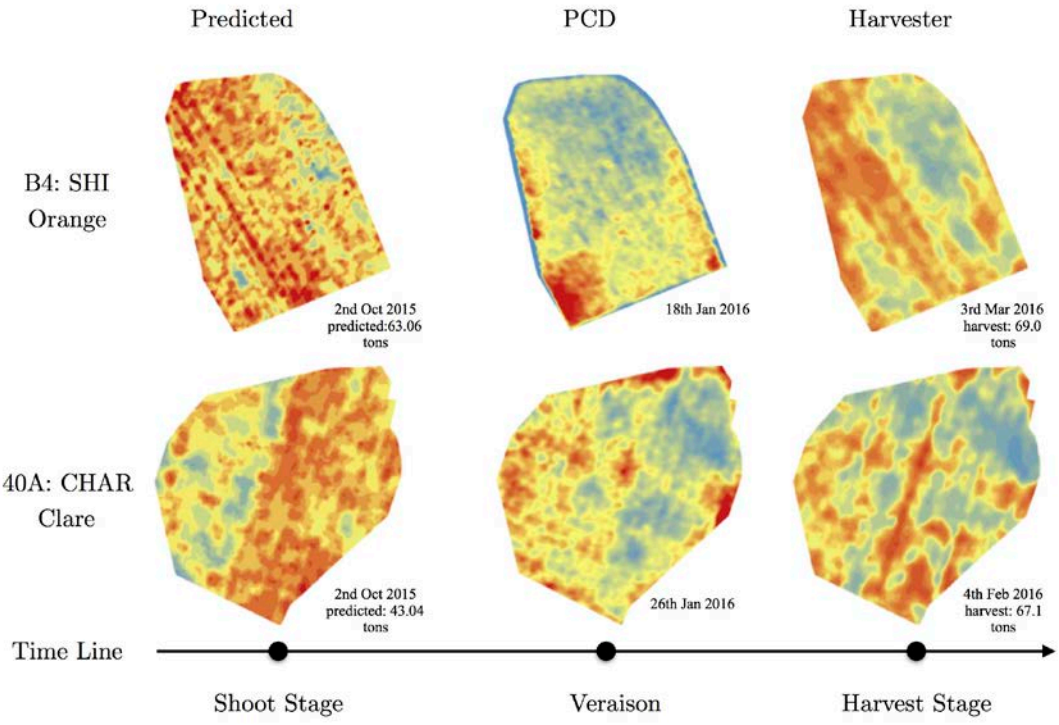


Figure 7.3 The comparison of timing to obtain yield variation map. Maps in the first column are generated by the proposed shoot counting method; maps in the second column are PCD maps collected by UAV at veraison; maps in the third column are generated by harvest monitor.

7.3 Flower counting by image processing

A flower counting method developed within this project was used to generate the results in Section 10.3.2.3 and the technical details will shortly be published [15]. An example of flower detection is shown in Figure 7.4.



Figure 7.4 Result of the flower detection algorithm applied to a single image – fine red spots show detected florettes

Automated flower counting systems have been developed to process images of grapevine inflorescences, assist in determining potential yields early in the season and measurement of fruitset ratios without arduous manual counting. We introduce a robust flower estimation system comprised of an improved flower candidate detection algorithm, flower classification and flower estimation by investigated calibration models. These elements of the system have been tested in eight aspects across 533 images with associated manual counts to determine overall accuracy and how it is affected by experimental conditions.

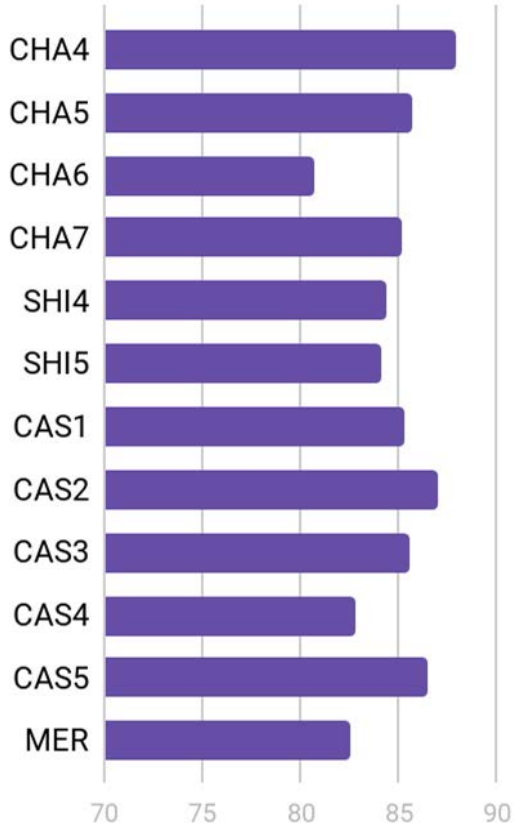


Figure 7.5 The accuracy of flower counting expressed in percentages for 12 datasets across four varieties: Chardonnay (CHA), Shiraz (SHI), Cabernet Sauvignon (CAB) and Merlot (MER)

The proposed algorithm for flower candidate detection and classification is superior to all existing methods in terms of accuracy and robustness when compared with images where visible flowers are manually identified. As shown in Figure 7.5 an accuracy of 84.3% was achieved both in-vivo and ex-vivo when tested against actual manual counts and found to be robust across the 12 datasets used for validation. Making the proposed flower estimation system applicable to in-field measurement of fruit-set ratios is vital for yield estimation. A single-variable linear model trained on 13 images outperformed other estimation models and had a suitable balance between accuracy and manual counting effort. Accurate flower counting is dependent on the stage of inflorescence development, but once they reach approximately E-L16, the importance of development reduces and the same estimation model can be used within a range of about two E-L stages. A global model can be developed across multiple cultivars if they have inflorescences with a similar size and structure.

7.4 Pea-sized berry estimation

7.4.1 Introduction

The main aim of this section is to present a robust approach to correctly estimate the berry numbers on bunches at pea-sized stage. The estimation is made by analysing close-up images of berry bunches. First, a machine learning based cascade classifier is applied to identify individual berries on the bunch image. The detected visible berry number from this approach is then used to estimate the final berry count of the bunch via linear regression methods.

A detailed description of the methodology followed in achieving this goal is presented in Section 7.4.2. The results obtained from this approach for Y2 and Y3 are presented in Section 7.4.3.

7.4.2 Methodology

The proposed methodology to count pea-sized berries consists of two stages.

1. Stage 1: Detect the visible berries in an image via a cascade object detection algorithm.
2. Stage 2: Build a relationship between the visible number of berries and the actual berry count in the bunch, via linear regression methods.

7.4.2.1 Cascade Object Detection method

The Cascade Object Detection (COD) algorithm is a multi-stage classification learner, where each stage is made up of a collection of weak learners. Each of these stages is trained using a technique called boosting. For the work presented in this chapter, a COD that uses the Viola-Jones algorithm for face detection is re-trained for the purpose of identifying pea-sized berries.

The COD approach is known for reliably classifying objects for which the aspect ratio does not change drastically. Furthermore, this method is better suited for situations where there are no out of plane rotations of the object. Thus, COD can be identified as a good candidate for pea-sized berry detection since all berries are nearly spherical in shape, which results in only minor aspect ratio changes. Also note that the COD method employed for this task uses Histogram of Oriented Gradients (HOG) as the main learning descriptor. The implementation procedure for the COD algorithm consists of two major steps.

a) Train the cascade object detection classifier using a set of positive images (images containing berries) and a set of negative images (images of rachis, backing board, ribbons, fingers etc.).

b) Slide a window over the closeup image and use the trained COD classifier to check for individual berries inside the window. The sliding window size

range should be adjusted roughly to match the size range of pea-sized berries.

Figure 7.6 presents the COD algorithm at work. Note that this approach is robust to differences in the berries from different blocks, as well as varying lighting conditions. Once the berries are detected, the next step is to estimate the final berry number of the bunch via linear regression methods. The approach followed is discussed in detail, next.

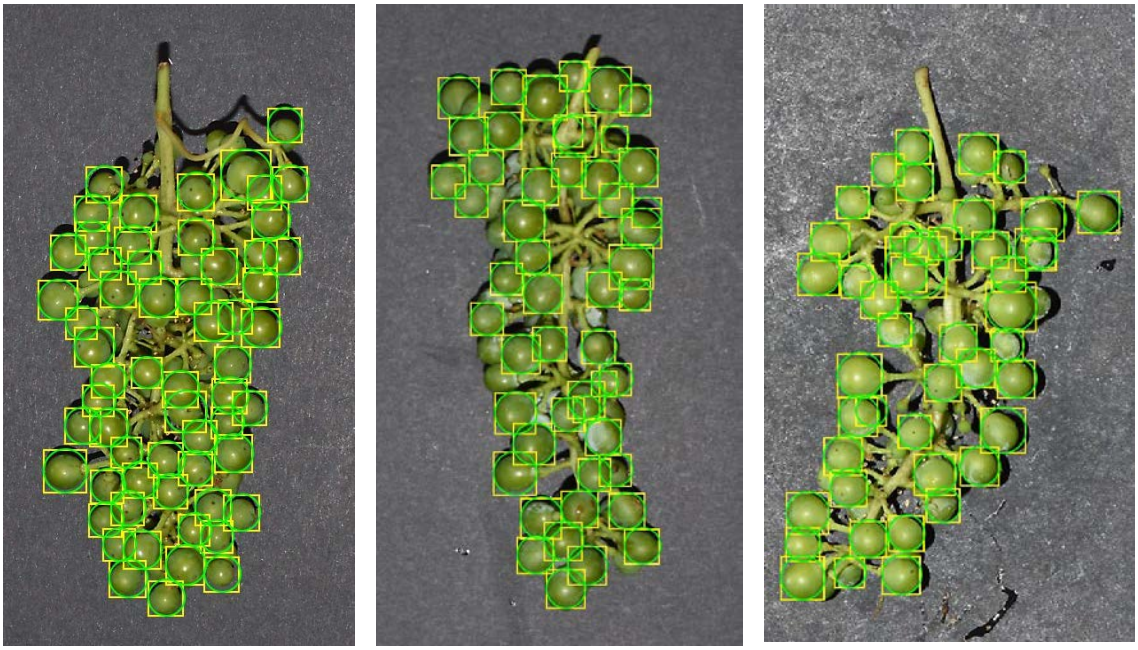


Figure 7.6 The cascade classifier at work. The method is robust to different lighting conditions and background reflection levels.

7.4.2.2 Estimating the final berry number via linear regression methods

Although the number of visible berries can be counted, a single image only captures around 40-60% of all berries present in a bunch. Thus, there should be a proper method to derive the final estimate of the berry number based on the visible berry number. The following method was implemented to estimate the final pea-sized berry counts for the four blocks in Y3.

a) The actual pea-sized berry count (ground truths) for over 150 bunches across three blocks was determined for Y2. These ground truthed numbers were determined using a special machine learning based GUI.

b) The number of visible pea-sized berries was counted using the COD approach for the same three blocks for Y2.

c) A linear regression model was built using the Y2 ground truths and Y2 visible berry counts.

d) The visible berries were counted for four blocks in Y3 using the COD approach.

e) The final estimate for the pea-sized berry number for each bunch in Y3 was derived using the regression model developed in step (c) and the visible berries detected in step (d).

More details on the results achieved for each step can be found in the next section.

7.4.3 Results

The COD algorithm was applied to count the visible berries in three Y2 blocks: namely 40A, 47A and B12. The actual berry counts for the same three blocks were found using a separate machine learning based GUI. The relationship between the detected visible berry number and the actual berry number for Y2 can be found in Figure 7.7. The linear fits generated via regression for each separate block are also presented in the same figure.

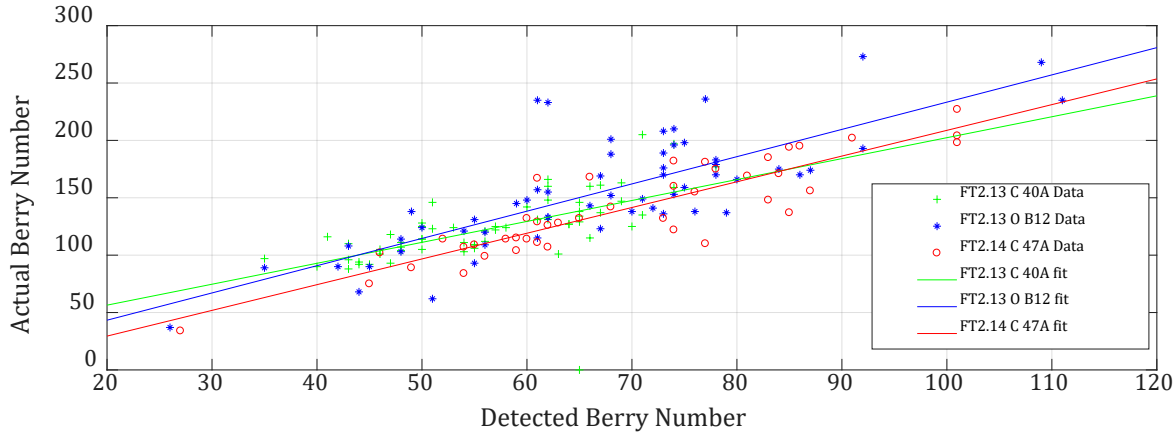


Figure 7.7 Variation of the actual berry number with the detected visible berry number. The linear regression fits for each block are also shown.

Figure 7.7 suggests that the linear regression models for the three blocks have similar characteristics. Such an observation indicates that the berry detection algorithm performs consistently across the three blocks. A simple cross-validation test presented in Table 7.1 further demonstrates this point. According to Table 7.1, the accuracy of the linear regression models varies between 86.1 % and 91.5 %, across the three blocks.

Table 7.1 Cross validation results for the linear regression models developed for each block.

Linear regression model	Weighted average accuracy of regression model (%)		
	Y2 Clare 40A	**Y2 Clare 47A**	**Y2 Orange B12**
Y2 Clare 40A	91.31	89.45	88.06
Y2 Clare 47A	88.56	91.48	88.42
Y2 Orange B12	90.78	86.19	88.43

However, the aim here is to derive a single linear fit which matches all blocks across all years, while using a minimum number of samples to generate the fit. To identify the correct sample size that generates an accurate model, different linear regression models were developed using different sample sizes. These linear regression models were then used to estimate the pea-sized berry number for bunches in each block. The estimates were compared with the ground truthed numbers to calculate the accuracy of the approach. Here, the accuracy is defined as,

$$Accuracy\ (\%)\ = \left[\frac{Y - \hat{Y}}{Y}\right] \times 100\ \%$$

where, Y is the actual value and $\hat{Y}$ is the estimated value. The corresponding results are presented in Figure 7.8. According to the figure, the accuracy levels reach their peak when the sample size exceeds eight samples. Thus, looking at the results, it is reasonable to assume that building a linear regression model using eight random samples from each block could result in a reliable model. The results also show that the response of the accuracy to the sample size is similar in all three blocks.

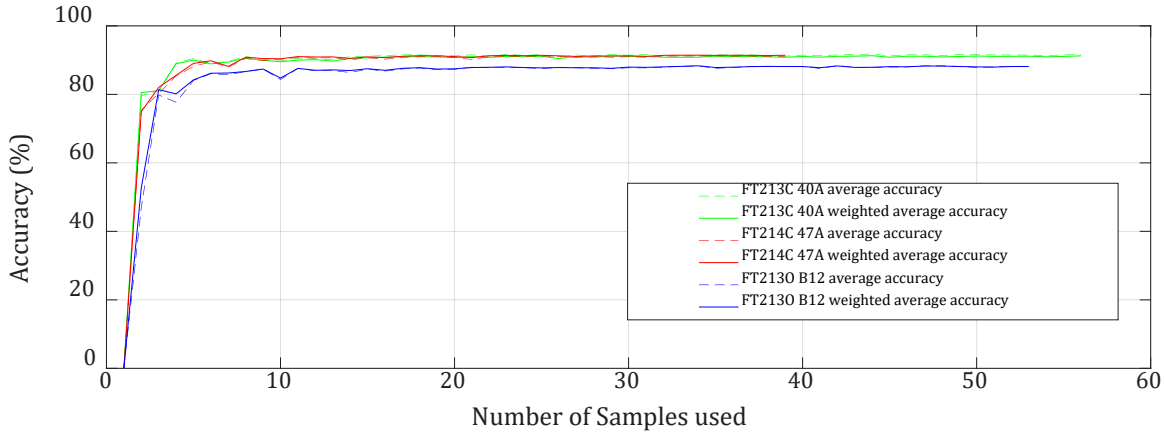


Figure 7.8 Variation of pea-sized berry estimation accuracy with the number of samples used to generate the linear regression fit.

Now that there is a clear indication of the sample size, the next step is to generate a single linear regression model using randomly selected samples from all three blocks. For this test, a linear regression model was developed using 30 randomly selected samples from the three blocks (10 samples from each block). The process was repeated 20 times. The corresponding results are shown in Figure 7.9.

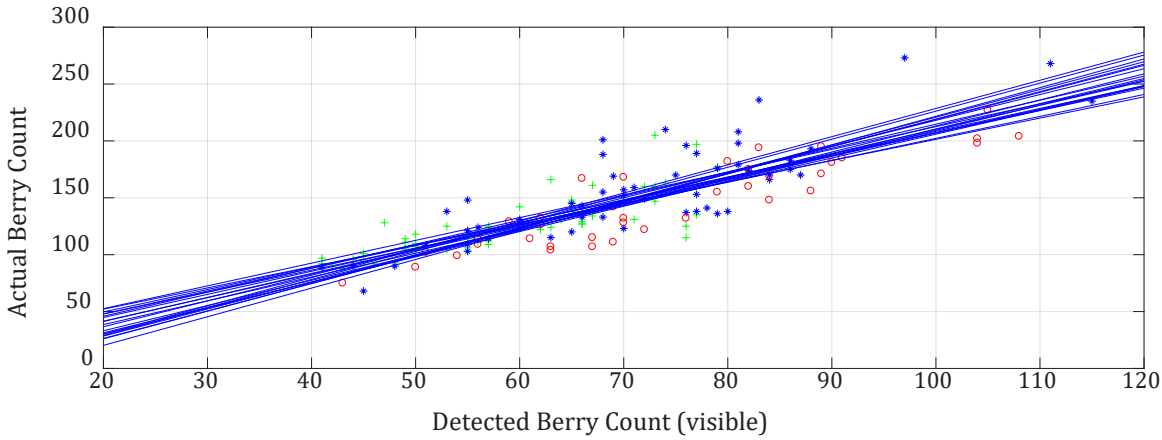


Figure 7.9 20 linear fits generated by randomly selecting 10 bunch photos from each dataset. The linear fits have similar gradients and intercept values in the region of interest.

As seen in the figure, the parameters of the linear regression model do not vary much for the 20 tests. In fact, the models behave similarly to each other when the actual berry number lies between 50 and 200. Based on these observations, it was decided to build a single model for the pea-sized berries using 30 bunch samples. The linear regression model used for the experiments conducted in this research is presented below,

$$\hat{Y} = 1.98 \times Y_{det} + 4.558$$

where Y_{det} is the detected berry number, and $\hat{Y}$ is the final estimated berry number. The above linear regression model developed using 30 samples was then used to estimate the final berry numbers of the three Y2 blocks. The corresponding results are presented in Table 7.2 Performance of the linear regression model developed using 30 samples.

Table 7.2 Performance of the linear regression model developed using 30 samples

Block	Weighted average accuracy of regression model
Y2 Clare 40A	91.73 %
Y2 Clare 47A	91.17 %
Y2 Orange B12	88.7 %

The next step is to estimate the pea-sized berry numbers for the Y3 datasets, using the above linear regression model. However, unlike Y2 bunch photos that were collected ex-vivo (indoor environment), the Y3 bunch photos were captured in-vivo. Thus, considerable differences can be observed in the images captured in Y3 as shown in Figure 7.10. Compared to ex-vivo images, the in-vivo bunch photos contain the following differences:

a) The in-vivo bunch photos contain background elements such as tree trunks, other berry bunches, leaves and calibration chequerboard patterns in addition to the backing board.

b) The distance between the camera and the bunch is subject to change in each photo.

c) The lighting conditions vary for the same dataset.

The following additional steps were taken to achieve robust pea-sized berry detection.

a) The in-vivo bunch was automatically cropped from the bunch photo. This action removes most of the unnecessary elements from the image.

b) A separate 'zoom-factor' parameter that relates to the rough distance between camera lens and the bunch was tuned for each block.

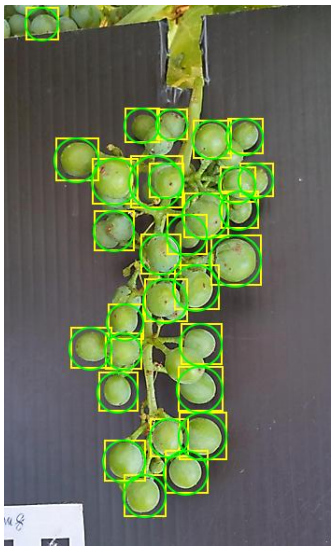
c) Additional positive and negative samples were introduced to the training dataset with the aim of reducing the false positive rate.



(a) (b)

Figure 7.10 The differences between an in-vivo and ex-vivo bunch image. (a) The ex-vivo bunch image is taken with a uniform background with consistent lighting conditions. (b) The ex-vivo bunch image has different background elements in addition to the varying lighting conditions.

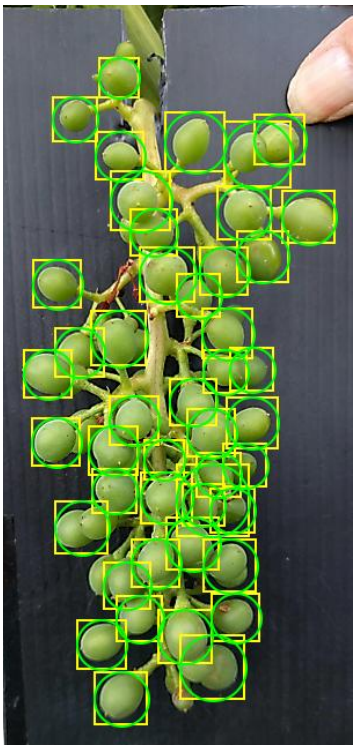
Figure 7.11 shows the performance of the pea-sized berry detection method on the Y3 datasets. Although most of the unnecessary elements are cropped out, it is difficult to remove certain elements from the image which may lead to false positive results. The detected berry number is then applied to the linear regression model developed to generate the estimates for the Y3 datasets. The estimated average pea-sized berry number per bunch for each Y3 block is presented in Table 7.3.



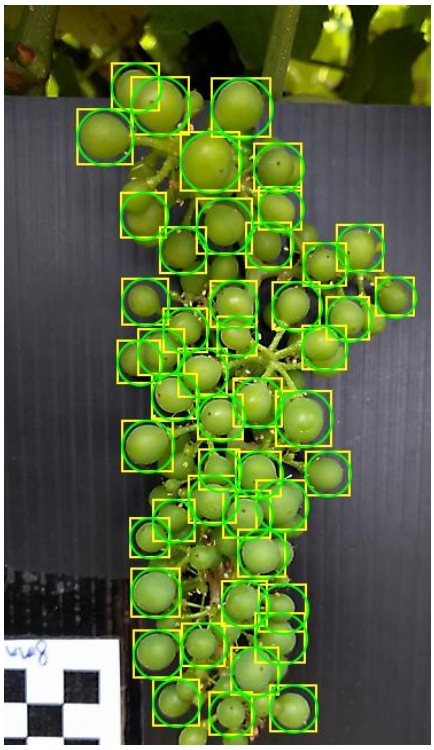
(a)



(b)



(c)



(d)

Figure 7.11 Visible berry counting with cascade classifier for Y3 datasets. (a) FT3.3-C 40A (b) FT3.3-C 47A (c) FT3.3-O B4 (d) FT3.3-O B12. Note that the bunch photos were cropped first to remove unnecessary background elements and to isolate the bunch.

Table 7.3 Final estimation for the average pea-sized berry number per bunch in each Y3 block

Block	Estimated average pea-sized berry number per bunch	Average manual count: pea-sized berries per bunch (Randomly selected destructive samples)	Average manual count: berries per bunch at harvest (Marked bunches)
Y3 Clare 40A	94	108.7	98
Y3 Clare 47A	110.07	108.4	100
Y3 Orange B4	121.45	104.7	132
Y3 Orange B12	198.06	176.6	228

7.4.4 Conclusion

A COD based approach was implemented to estimate the pea-sized berry number in a given bunch, for both ex-vivo and in-vivo cases. The COD based pea-sized berry identification method was then combined with a linear regression model to derive the final estimate for the average pea-sized berry number per bunch in a given block.

7.5 3D bunch reconstruction for berry counting at harvest

Prior to the commencement of this project, Scarlett Liu developed a method for estimating the 3D reconstruction of a bunch from a single image which was applied to generate the results in Section 10.3.4.2. Some aspects of the approach have been published [16].

7.6 Berry diameter and weight measurement from bunch photos

An investigation into the accuracy of berry diameter measurement was undertaken by Zhen Liu [17] for comparison with the methods by Kicherer [18], Cubero [19], Tardaguila [20] and Mirbod [21]. Mirbod's approach was most novel in that it was applied in-vivo and achieved an error of 5-6%.

7.6.1 Stripped berry diameter measurement

Using five marked berries that had been stripped from a bunch and photographed using a DSLR, the accuracy of berry diameter measurement was found to be 95.72% across three datasets. Table 7.4 shows the results for each dataset, with the accuracy calculated by Leave One Out Cross Validation.

Table 7.4 Results of berry diameter measurement by image processing

Field Trip and Block	FT1.7 B4	FT2.22 47A	T2.21 40A
Variety	Shiraz	Shiraz	Chardonnay
Number of images	75	60	75
Development stage	Harvest	Harvest	Harvest
Correlation coefficient (manual diameter vs image processing diameter)	0.91	0.94	0.95
Average error [%]	4.82	3.46	4.56

7.6.2 Berry weight versus diameter

Each berry was also weighed and the relationship between berry weight and berry diameter investigated, similarly to the analysis of Tardaguila [20]. Figure 7.12, Figure 7.13 and Figure 7.14 show the results from three blocks corresponding to columns in Table 7.4. The correlation coefficients for each of the curves were 0.92, 0.90 and 0.90 respectively, suggesting that a strong correlation between image processing measurements of berry diameter and actual berry weight can be obtained. Outliers in data from Block 40A were present, due to a notable and inexplicable change in the lighting conditions. Finally, a fourth dataset (FT2.22 B12) was tested, where the berries had a high degree of shrivel. The correlation between diameter and weight was found to be bimodal in that instance (figure not shown), presumably due to a large proportion of shrivelled berries. Further work is necessary to further validate the detection of shrivelled berries.

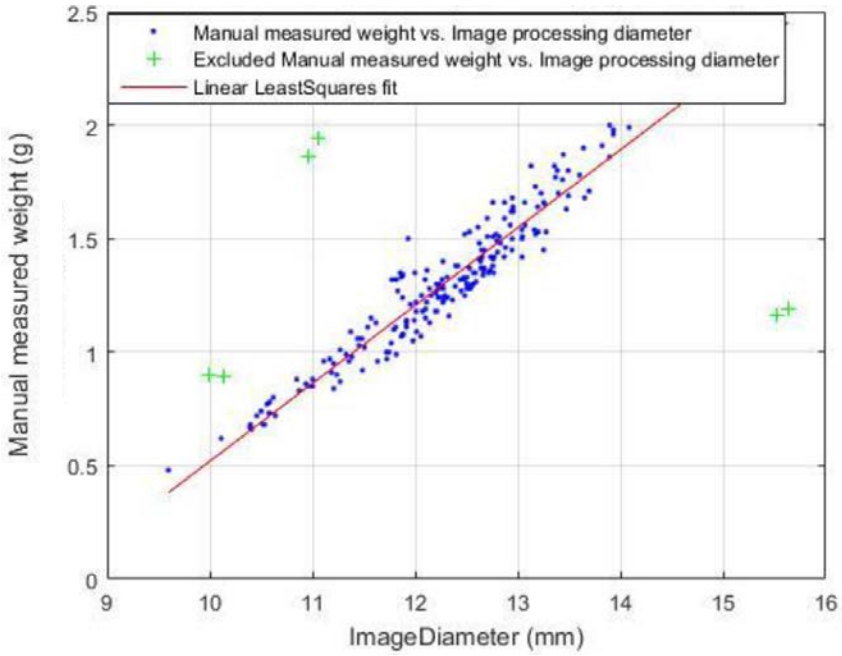


Figure 7.12 FT1.7 B4 Berry diameter from image processing against berry mass

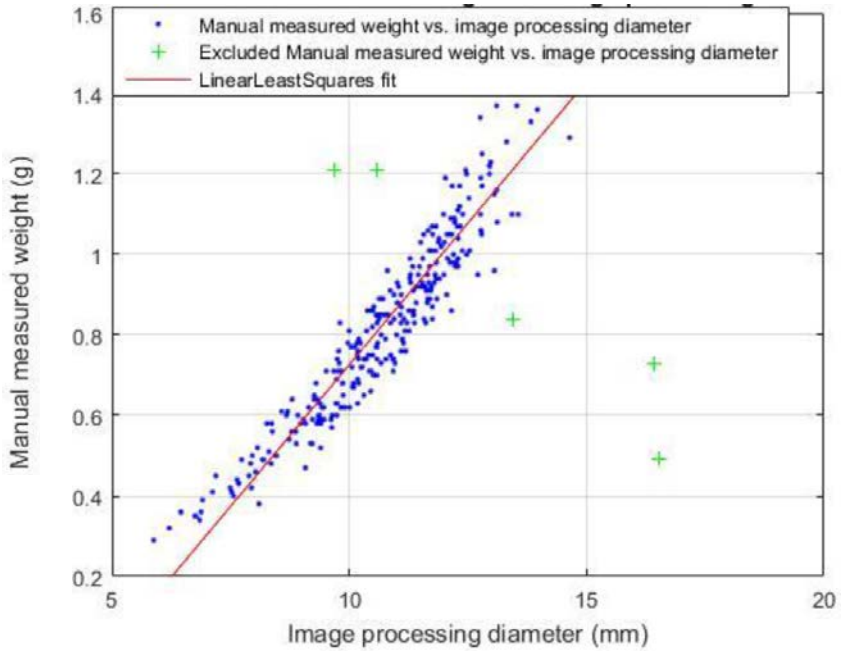


Figure 7.13 FT2.22 47A Berry diameter from image processing against berry mass

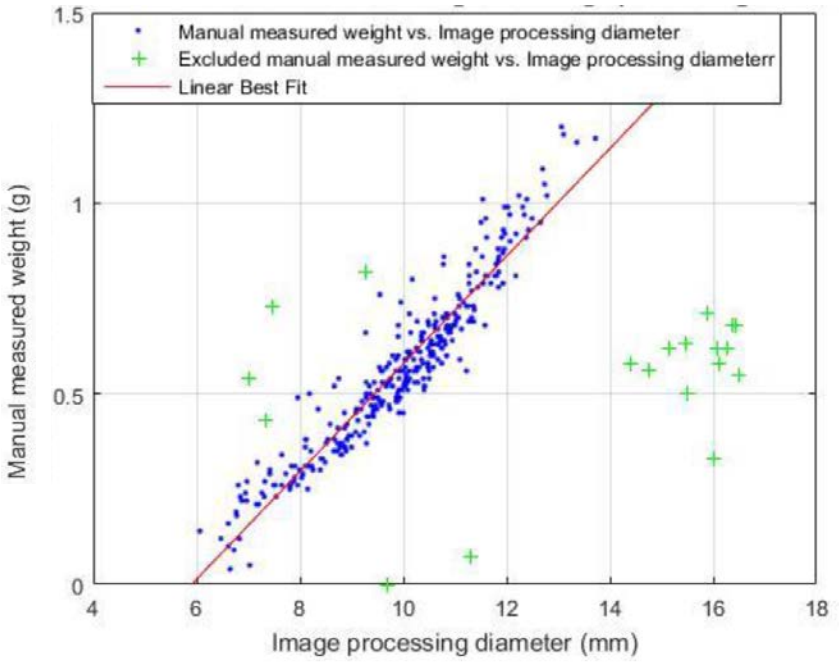


Figure 7.14 FT2.21 40A Berry diameter from image processing against berry mass

7.6.3 On bunch berry diameter measurement

The results in the previous subsections were from berries stripped from a bunch as a baseline for image processing. To test the accuracy of berry diameter measurement on complete bunches, the same berries were marked and the bunches photographed before the berries were stripped off. Compensation factors for the distance to the camera based on the position in the bunch were applied, using a model developed by Liu [22], and the accuracy of berry diameter measurement calculated. The process is shown in Figure 7.15. The error of berry diameter measurement on a set of 43 complete bunches was found to be 4.9%. This is in line with existing work [21].

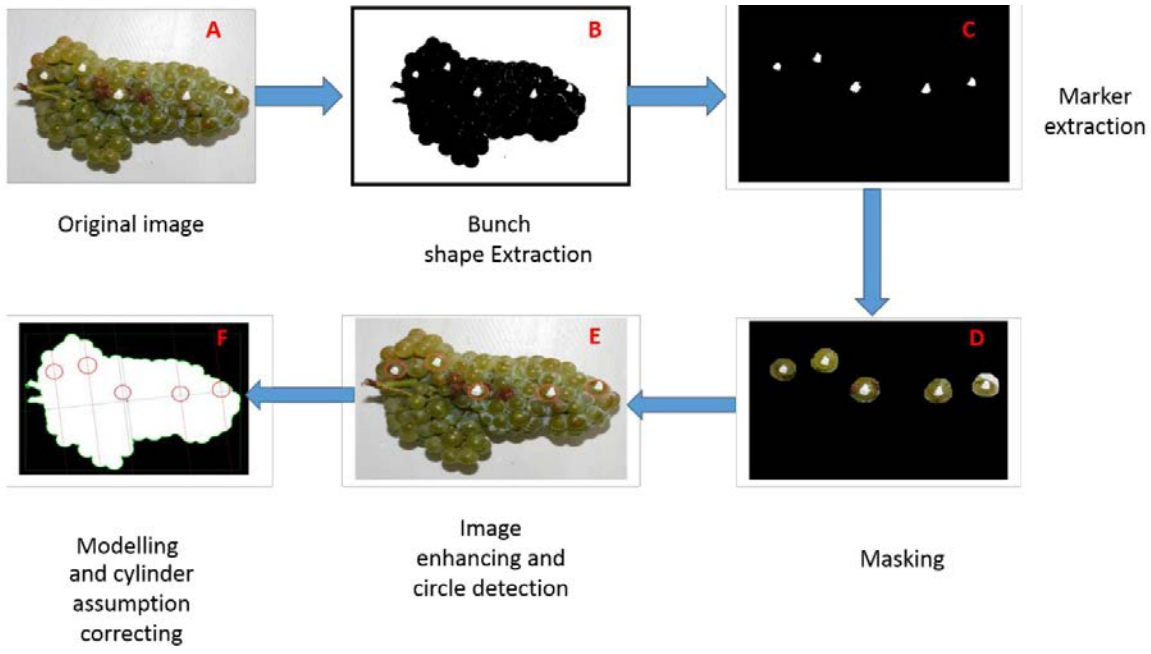
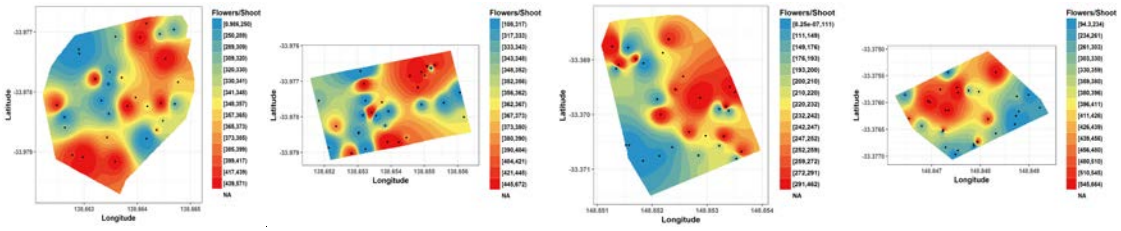


Figure 7.15 Experimental procedure for detecting and calculating berry diameter [17]

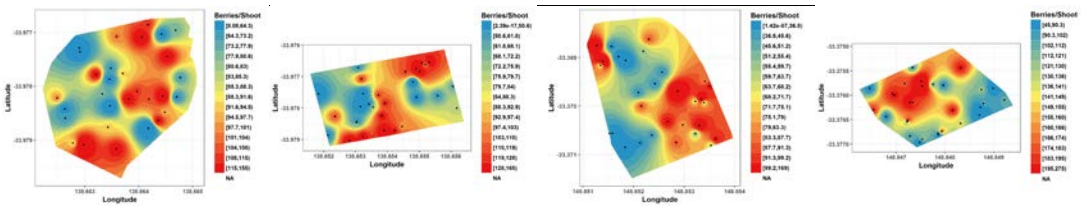
7.7 Map similarity analysis

One major component in traditional yield estimation methods is the count of flowers per inflorescence or berries per bunch. The counts are not stable and are biased by the sampling method and personnel. To explore the spatial consistency of those key counts we tracked the marked inflorescences from flowering until harvest and photographed them at each stage. Once the collected images were processed we plotted the spatial map by IDW and the results are shown in Figures 11.25, 11.26 and 11.27. The fruit weight per shoot at 30 SSSs was also interpolated in Figure 11.28 for investigating the correlation between berry counts immediately prior to harvest and fruit weight at harvest stage.



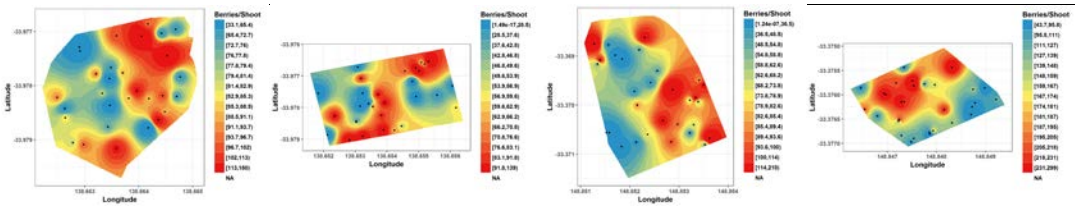
(a) 40A (b) 47A (c) B4 (d) B12

Figure 7.16 Flowering Stage: automated flower counts by computer vision/ shoots at 30 SSSs.



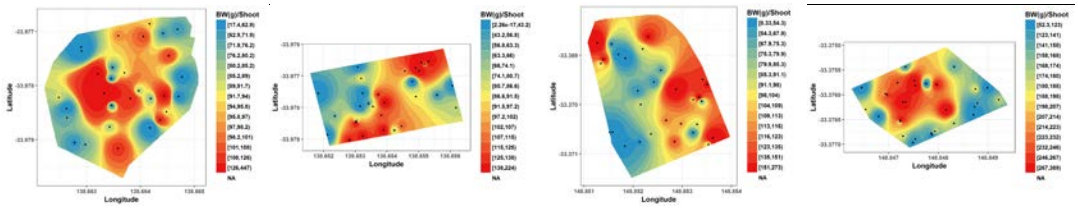
(a) 40A (b) 47A (c) B4 (d) B12

Figure 7.17 Pea Size Stage: automated berry counts by computer vision/shoot at 30 SSSs.



(a) 40A (b) 47A (c) B4 (d) B12

Figure 7.18 Harvest Stage: automated berry counts by computer vision/shoot at 30 SSSs.



(a) 40A (b) 47A (c) B4 (d) B12

Figure 7.19 Harvest Stage: bunch weight /shoot at 30 SSSs.

The spatial similarity between each of these maps over time was calculated using pixel-wise similarity as described by Liu [23] and the results are shown in Table 7.6. The spatial similarity between pea-size and prior harvest in terms of counts of berries poses the highest correlation, followed by the progression from flowering stage to pea-size stage. The latter suggests that fruit set ratios in these blocks tend to be spatially consistent.

Although one would expect the bunch weight and berry count to be highly correlated, it can be seen from G1:C3 in Table 7.6 that other than for B4, they are not as highly correlated as the previous two comparisons. We posit that this is due to variation in berry weights which suggests that tracking berry size along with berry

number would provide a more accurate method for crop mapping and yield forecasting.

In addition, by comparing the numbers presented in the second and third rows of in Table 7.5, the spatial variation has more significant change in Chardonnay (40A, B12) than Shiraz (47A, B4) between number of berries and bunch weight.

Table 7.6 Similarity quantification of intra-seasonal crop variation

Comparison	Stages	Objects	Similarity (%)			
			40A	47A	B4	B12
G1:C1	Flowering->Pea size	Flower/Shoot: Berries/ Shoot	88.36	81.83	83.13	93.67
G1:C2	Pea size->Prior to Harvest	Berries/ Shoot: Berries/ Shoot	88.50	92.69	91.82	94.18
G1:C3	Prior to Harvest->Harvest	Berries/ Shoot: Bunch Weight/ Shoot	72.40	88.60	94.00	85.72

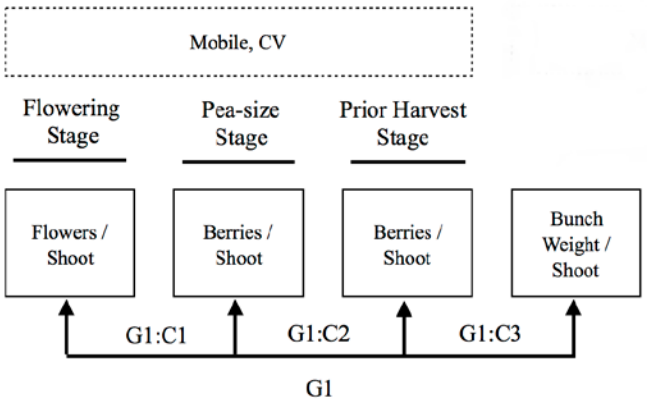


Figure 7.20 The chart for comparison in similarity between maps generated in different stages.

Comparing the flower distribution maps with the actual yield maps for B4 and B12, there is no obvious correlation between flower distribution and yield variation. In a general manner, the flower distribution pattern has the opposite trend compared with actual yield variation in some patches. However, these maps are only comparisons done at 30 points, which is insufficient for building a map of any spatial parameters [10].

7.8 Non-bearing and missing vine detection

In parallel with this project, Julie Tang developed an image processing method for detecting the proportion of non-bearing and missing vines in each row of a block, the results of which are presented in Table 7.7 and in a poster presented at AWITC

2016 [24] and Agricontrol 2016 [25]. These have been applied to all the yield estimation methods mentioned in this report. For two blocks and two seasons this was manually validated by workers manually mounting the total number of 0.6m segments of non-bearing canopy.

Table 7.7 Bare wire and non-bearing canopy as a proportion of entire row lengths in each block.

	40A	**47A**	**B4**	**B12**
V2015 Bare wire	-	-	0.065%	0.69%
V2015 Non-bearing %	3.47% (3.77% manual)	17.29% (18.48% manual)	4.09%	2.0%
V2016 Bare wire	-	-	1.46%	0.5%
V2016 Non-bearing %	5.52% (6.0% manual)	5.33% (6.74% manual)	6.75%	3.09%
V2017 Bare wire	2.42%	-	1.86%	0.84%
V2017 Non-bearing %	6.11%	6.17%	2.5%	10.96%

8 Y1 method (GoPro)

The system and methods proposed for yield estimation for year 1 were designed based on manual estimates, and experience from prior image based yield estimation [26]. The intention was to make a prototype system and gain experience with its deployment and experimental setup in field trials.

8.1 System design for Y1 (GoPro)

The Prototype system designed for the first year of experiments involved the mounting of a pair of GoPro Hero 3+ cameras on each side of a farm vehicle as it drove through the vineyard. The intention was to correlate detections of shoots, inflorescences and bunches with manual counts of these objects of interest at known locations in the block. Then from this to interpolate a map containing the total counts of each object across the entire block and use that to vastly improve the yield estimation. Prediction factors would remain the same (such as average bunch weight), while occlusion at later stages would require manual sampling to determine occlusion factors.

To tackle occlusion, the first experiments were designed for the shoot stage, as described in Section 8.2. To facilitate clear capture of the images, a pair of backing boards was mounted on the vehicle to fit over the rows to ensure only the nearest row was in the field of view of the camera and aid shoot segmentation. The vehicle setup at Orange is shown in Figure 8.1 and a similar setup was used at Clare except it was mounted on a Gator. Higher frame supports were needed at Orange relative to Clare due to higher posts. Improvements in the algorithm in Y3 were made to remove this cumbersome arrangement, as shown in Section 10.1. For videos at the later stages, the backing boards were unnecessary as the canopy had sufficient density to minimise visibility of distant rows. The vehicle was driven in a regular pattern through the rows, shown in Figure 8.2, capturing each row from one side.



Figure 8.1 Y1 setup at shoot stage at Orange with one GoPro circled and backing boards visible

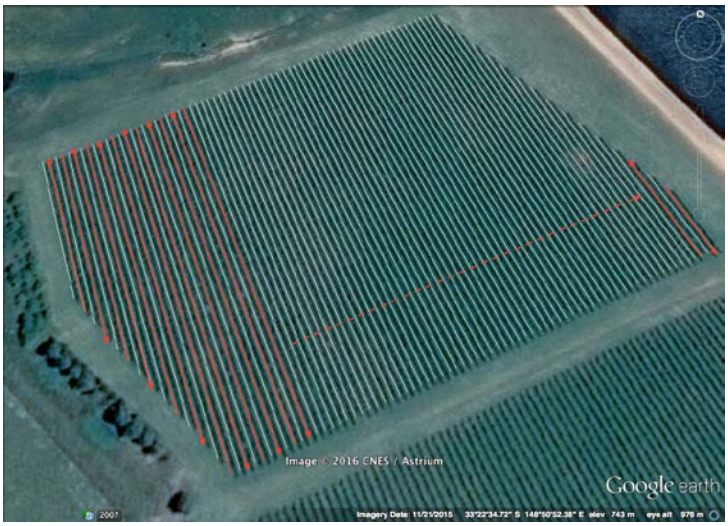
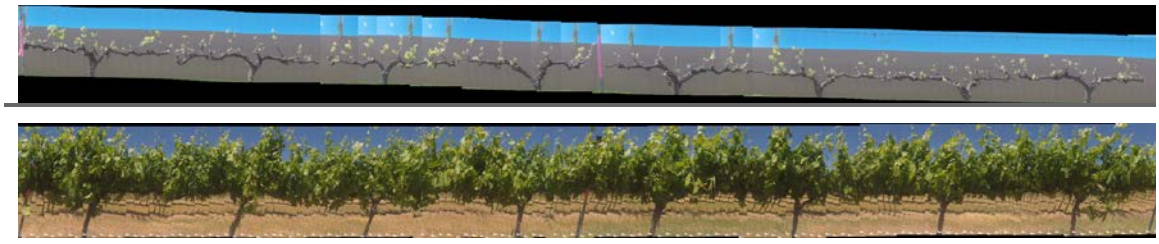


Figure 8.2 The driving pattern of vehicle mounted with a GoPro in a block for filming vines. Red line with arrows indicates the direction of driving paths.

A range of camera angles and settings was trialled, with the best results being found with the cameras mounted at cordon height, facing horizontally at the cordon and approximately 700mm from it, capturing at 30 frames per second with the 'Medium' field of view option. Image capture was recommended within four hours before or after solar noon to minimise sunlight causing lens flare, although this was not always practical. To drive a 6 Ha block at 10km/h took approximately two hours, with an additional half hour for setup and another hour for uploading images and video record sheets. The workflow for image capture, processing and yield estimation is given in Figure 8.3. A method for automatically locating the position of each image frame along the row given the end post locations was developed within this project [14]. A novel shoot detection algorithm [12] [13] was developed in parallel with this project and applied to the videos captured in this project.

Image stitching methods were applied with limited success, predominantly due to the unstructured foliage environment, wide field of view of the camera, minimal overlap between successive images and motion of the canopy as the vehicle passed – particularly in Clare where the shoots were less constrained. Examples of stitched images are shown in Figure 8.4, however, for the remainder of this report non-overlapping images were processed.



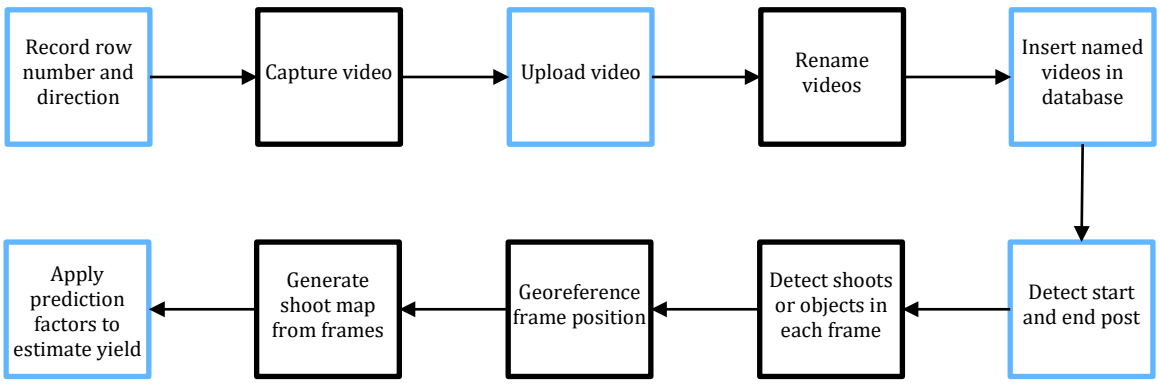


Figure 8.3 Flowchart of Y1 system for yield estimation. Processes in light blue involve a substantial degree of manual interaction whereas those in black are automated.



Figure 8.4 Stitched images from GoPro cameras in Y1 at a single temporal location at shoot stage (top – with backing board visible), inflorescence stage (middle) and pre-veraison (bottom)

8.2 Experimental design for Y1 (GoPro)

To determine the accuracy of shoot detection and counting using this system, the number of shoots in each of the 20 marked temporal locations (TLs) in the four blocks was manually counted within a day or two of filming. The sections of the videos correlating to these TLs were manually segmented and the shoot count algorithm applied to give a total shoot count which was then compared with the manual counts.

For a comparison with the final yield, the total number of shoots in the block was calculated by spatial interpolation across all counts from individually processed video frames and the yield calculation in 8.3.1 applied. This was directly compared with the reported tonnage of fruit delivered to the winery.

The manual shoot counts were extrapolated up to the total length of all rows in the block, subtracting the known length of non-bearing vines. Following the procedure in Section 6.1, this was also compared with the reported tonnage of fruit delivered to the winery.

Similarly, non-destructive counts of inflorescences and bunches in each of the TLs was undertaken at the later stages for direct comparison with the collected imagery. Finally, at harvest, all the bunches in each TL were manually harvested and counted and the weight per vine calculated.

In addition, destructive harvest sampling using 26 x 0.6m samples per Ha was undertaken to build yield maps in case the harvester monitor did not function. One bunch from each of these samples was chosen for ex-vivo analysis as the basis for determining average berry counts and weights.

8.3 Theoretical method and results for Y1 (GoPro)

The method for year 1 involved estimation at four phenological stages: shoot, flowering (immediately prior to flowering), pea-sized and harvest. The estimation

method in each stage is detailed in Sections 8.3.1 to 8.3.4 with a summary of the results being shown in Section 8.4.

8.3.1 Shoot stage (GoPro)

The number of shoots within each block was estimated using the hardware presented in Section 8.1 and the software in Section 7.1. Once the number of shoots has been estimated within a block, an early estimate of potential yield can be calculated. The proposed relationship between shoot counts and estimated yield is presented below.

$$Y^* = c(S) \times \%(BV) \times \overline{RBS} \times \overline{w(B)} \times \overline{RqB} \times H_e \times SP$$

where:

- Y^* is the total predicted block yield (mass of fruit delivered to winery)
- c(S) is the number of shoots detected from videos in block level
- %(BV) is the proportion of recorded video for the whole block
- $\overline{RBS}$ is the ratio of bunches to shoots from the previous season or historical data
- $\overline{w(B)}$ is the average bunch weight at harvest in previous seasons
- $\overline{RqB}$ is the proportion of a rachis weight to bunch weight
- H_e is the harvest efficiency factor – see Section 9.3.5
- SP is the proportion of all sampled fruit before harvest

The ratio of bunches to shoots can either be measured manually by counting the number of shoots in particular locations two weeks after bud burst and bunches in the same locations closer to harvest, or using automated methods such as the proposed solution by Liu et al. [27]. RBS varies among cultivars, the location of vineyards, the timing of water shoots and the weather. RBS was calculated based on the historical records provided the local vineyard managers.

The results from manual counts, to validate the image processing in each TL, are shown in Table 8.1. While these results are not perfect they show the promise of consumer grade cameras that are usable by growers to count shoots. It is likely that the better results from 47A and B4 are a consequence of the videos being recorded where individual shoots are sufficiently large to be detected, but not too large as to overlap and complicate the counting. Further technical details are in the paper by Liu et al. [13] and further results from Y2 are in Section 9.3.3.

Table 8.1 Shoot count error per TL in Y1, compared with E-L stages across the block

Error (%) /E-L-stage	**Season 1**			
Block	40A	47A	B4	B12
FT1.2	-36.10 E-L 4-9	-6.10 E-L 7-11	-10.31 E-L 9-10	-30.47 E-L 11-12

After getting the shoot number for a whole block, we can apply the yield prediction formula to calculate the final yield. *Table 8.2* provides a comparison of the predicted yield against the actual weighbridge values as well as that obtained by the manual counts given in Section 6.1.

Table 8.2 Comparison of the estimated yield at shoot stage against the weighbridge weights for fruit harvested in each block in Y1.

		Season 1: FT1.2			
Block		40A	47A	B4	B12
Yield (tonnes)	Imaging	45.04	13.40	49.46	25.20
	Manual	45.36	23.13	49.35	33.48
	Actual	47.92	36.98	30.70	24.91

To compare the yield estimation results accomplished by the proposed method and a manual sampling approach, *Table 8.3* demonstrates the error between actual final yield at the weighbridge and predicted yield by both methods. The Y1 yield estimate shows a similar trend to the manual estimate (both are either over or under-estimates), suggesting that weather effects and the prediction factors have more influence on the accuracy of the estimate than the accuracy of the image processing.

Table 8.3 Comparison of the error in yield estimation by the proposed method and the traditional manual approach in Y1

		Season 1: FT1.2			
Block		40A	47A	B4	B12
Error (%)	Imaging	-6.01	-63.77	62.12	1.18
	Manual	-5.34	-37.43	60.74	34.40

8.3.2 Flowering stage (GoPro)

Differentiating and counting inflorescences in the canopy by imaging is not feasible since the inflorescences are not visible in our four experimental blocks, both in VSP and Aussie Sprawl canopy styles. For example, in Figure 8.5, 19 inflorescences were counted within the sample segment frame. Hence the detection of inflorescences in-vivo was abandoned in favour of flower counting from individually marked or destructively sampled inflorescences, the results for which are shown in Section 10.3.2.



Figure 8.5 A sample segment immediately prior to flowering, showing the lack of visible inflorescences from a static camera view - 19 inflorescences were manually counted within this sample frame.

It should be noted that the four study blocks were all spur pruned, and a brief inspection of a nearby cane pruned block showed that inflorescences were far more visible, as shown in Figure 8.6. Hence it would be prudent to further investigate inflorescence or florette counting in cane pruned systems. Furthermore, it is suggested that adapting to more cane pruning systems in Australia would also increase the accuracy of shoot counts as there is less occlusion and greater uniformity which assists the image processing algorithms.



Figure 8.6 A cane pruned block at Orange (not included in this study), showing the greater visibility of inflorescences and florettes as compared with spur pruned blocks. Image processing on such blocks could be expected to produce improved results.

8.3.3 Pea-sized stage (GoPro)

Using the GoPro camera on a vehicle moving at up to 10km/h in each row was unsatisfactory in providing sufficiently clear images for detecting bunches at the pea-sized stage. The major challenges were the high variation in lighting conditions, between fully shaded and direct sunlight, the obscured nature of a large proportion of the bunches and blur or noise in the image from the GoPro cameras when moving in such an arrangement.

The GoPro camera parameters were varied extensively, however using the GoPro Hero 3+ models in Y1 was found to be ineffective in capturing clear images for robust bunch or berry detection and hence yield estimation. The suggestion was then to use a more advanced camera with higher dynamic range, controllable shutter speed and aperture and artificial lighting to improve the quality of captured images. This was used as feedback for the revised hardware system developed in Y2.

8.3.4 Harvest stage (GoPro)

A bunch detection approach [27] using traditional image processing techniques was implemented in parallel to this project, and found to detect bunches to an accuracy

of 87%. However, this required static images of high quality and was not successful on Y1 data.

A Convolutional Neural Network (CNN) approach using TensorFlow was implemented [28] to test more advanced visual bunch detection methods. The results were poor despite many images being manually labelled and used for training the classifier and detector. Figure 8.7 shows the results in two example images from both 40A and B12 at harvest. The enormous variation in brightness, the fact that most bunches were not visible to the naked eye and substantial blur in the images again highlighted that the prototype GoPro solution was not feasible for use once the canopy had grown.

The berry detection algorithm proposed by Nuske et al. [7] using the Radial Symmetry Transform was also investigated, but again the image quality was insufficient to give usable results in Y1.



Figure 8.7 40A (left) and B12 (right) at harvest, using GoPro Hero 3+ camera in Y1. The large variation in lighting in brightness within an image as well as blur and the highly occluded nature of bunches in both trellis styles (Aussie Sprawl at left, VSP at right) is evident. Overlaid boxes are the results from a CNN detector trained on a subset of the data.

8.4 Overall summary of Y1 results

This chapter has introduced a system and process for capturing and processing imagery of an entire vineyard block using consumer grade action cameras and turning this into a yield estimate and a map of the variation of the visible objects. While there are still several manual steps required in the process, the system is the first in the world to provide a map of spatial variability within a block at the shoot

stage. Being five months prior to harvest, this provides the grower with an opportunity to regularise yield and optimise quality by management actions such as variable rate mulching, leaf plucking, fruit thinning and chemical application.

In future work, a tool for automatically integrating GPS measurements with the videos to provide a way of interpolating the location of each frame would greatly reduce the amount of manual labour required to generate a shoot map and hence a yield estimate.

Results from Y1 indicated that at the shoot stage, a GoPro camera could reasonably be used to count the number of shoots in a block with an accuracy of 79%. This increased to over 90% on average where filming took place close to E-L 9, which vastly improved the stability of the results. Yield estimates from the shoot count varied from within ± 5% to ± 65% biased strongly by weather effects and the unpredictable nature of the growing season. This method was reapplied in Y2 and Y3, and further results are in the following chapters.

Beyond the shoot stage, the GoPro imagery failed to provide sufficient detail to differentiate inflorescences, the majority of which were severely occluded. The four study blocks were all spur pruned and while cane pruned blocks are less common in Australia, there is much greater potential for counting inflorescences and florettes in a cane pruned system.

The GoPro imagery was not sufficiently robust under varying lighting conditions, particularly once the canopy was grown and did not provide sufficient detail for segmenting grape bunches or berries for yield estimation purposes beyond the fruit set stage.

Consideration could be given to adapting training systems and pruning styles to make fruit more visible in Australian vineyards, however the costs and consequences on light exposure for the fruit are factors to be considered.

At the end of Y1, a Wine Australia supported study tour was undertaken by the Chief Investigator to review the performance of a similar system developed by Stephen Nuske in the US. A report from this visit [29] suggested that imaging with controlled lighting during daytime is feasible, as long as the camera is not pointing directly into the sun. This informed the hardware development for Y2.

Furthermore, the vine training methods used in the USA appeared to leave fruit far more exposed and hence easier to image reliably. It was noted that Nuske's 9.8% error in harvest yield estimation [7] was when compared against manual samples in a small number of discrete locations, rather than the entire block yield. Hence the results are not directly comparable with those in this report as they do not allow for harvesting or transport losses. This led to the implementation of the harvest efficiency experiments in Y2.

9 Y2 method (Manta)

The system and methods proposed for yield estimation for year 2 were designed based on experience from Y1, and the desire to implement a more complex and accurate system for imaging the vines. In particular, the issue of motion blur and sensitivity to challenging lighting conditions were addressed through the use of a higher quality camera and flash arrangement.

9.1 System design for Y2 (Manta)

Several image processing techniques have been proposed to automate the yield estimation process. Berry detection methods which involve imaging in the visible spectrum have had success in the field; however, their impact has been limited due to the tightly controlled image acquisition parameters and small sample spaces selected. The success of these methods depends highly on the quality and consistency of images captured. A study by a US research team [30] has vastly improved the accuracy of grape vine yield estimation through the use of a well-designed image acquisition and illumination system.

The system design for Y2 focused on the design and testing of an automated image acquisition system mounted on a mobile vehicle in the field to capture high resolution, consistently lit images of vines for future image processing.

The system requirements of the design were derived from a detailed and in-depth understanding of the required performance of the system, the interaction with the user, the environment in which it will operate and the deficiencies of the original low-budget image acquisition system which was based on GoPro cameras. For example, the image acquisition system needs to function outdoors and in all weather conditions, from 40 ^{o}C summer days to subzero temperatures during winter.

After a thorough requirement analysis, the following set of specifications were derived for the proposed system.

1. Ability to capture high resolution images 1 - 1.5 metres from the vines while travelling at least 10 km/h through the rows.
2. Operate continuously for up to four hours.
3. Capture clear images during day and at night.
4. Ability to be reliably mounted onto the back of a utility vehicle.
5. Withstand a range of weather conditions.
6. Capability of vibration isolation.
7. Device should be portable.

9.1.1 Hardware

9.1.1.1 Camera

To source the appropriate hardware, each of the system requirements was translated into a set of technical specifications. Since lead times for custom hardware can be lengthy, sourcing the correct equipment early in the project was crucial. Imaging experts from Adept Turnkey were consulted in order to find a camera, flash and lens unit that would meet our system requirements. The camera recommended was the Manta G-235C, pictured in Figure 9.1, an industrial machine vision camera by Allied Vision Technologies which featured a 1/1.2" Sony IMX174 CMOS global shutter, with a resolution of 1936 x 1216 and a maximum frame rate of 50.7 frames per second (fps) at full resolution. The camera sensor had dimensions of 10.67 mm x 8.00 mm.

A lens with an appropriate focal length was chosen so that the images of the grapes were sharp and in focus. The focal length of the lens is a function of the sensor height, the field of view height and the working distance between the camera and the subject. For our imaging requirements, a 16 mm lens was determined to be sufficient.

For analysis purposes, it was decided to capture images such that there is a 50% overlap between two adjacent images captured. To achieve the required 50% overlap needed for stitching, images must be captured every 300 mm. At a speed of 10 km/h, or 2.78 metres per second (m/s), a distance of 300 mm is traversed every 0.108 seconds. A period of 0.108 seconds between consecutive images corresponds to an acquisition rate of 9.3 frames per second (fps). Since the Manta G-235C has a maximum frame rate of 50.7 fps, it was capable of capturing vine images with sufficient overlap.



Figure 9.1 Allied Vision Technologies Manta G-235C Camera

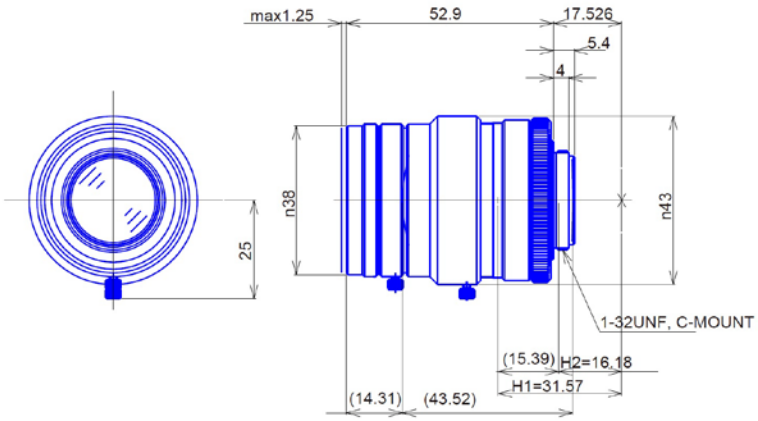


Figure 9.2 Goyo Optical 1 inch Format High Resolution Lens with 16mm focal length and F1.4 to F16 iris range.

9.1.1.2 Light Source

For the image acquisition system to take clear images in the day and at night a powerful source of illumination was required. As outlined earlier, the minimum capture rate for the system is 9.3 fps, so the light source must also trigger at that rate. An illumination range of 1 - 1.5 m was also essential to ensure images of the grapes were well exposed and evenly illuminated. A Gardasoft VCT6-W-50-ETH high intensity LED strobe light, pictured in Figure 3.6, was recommended by Allied Vision Technologies as a suitable illumination source. The flash unit can supply up to 500 Watt (W) pulses at a maximum trigger frequency of 10 kHz, has a beam angle of 50 degrees and is housed in a IP65 rated enclosure.



Figure 9.3 VCT6 High Intensity LED Strobe Light

9.1.1.3 Data storage

A target run time of four hours placed further technical constraints on a number of subsystems. At a minimum capture rate of 10 fps, a four-hour runtime will result in 144,000 images. The data acquisition and storage system was designed to handle this data load. The Manta G-235C camera has a Gigabit (Gb) Ethernet port on board which can transfer data at a rate of 1 Gb/s, which ensured that the image transfer and storage rate did not act as a bottleneck for the high image capture rate. A Gigabit Ethernet switch was required to ensure no loss in data throughput when connecting the camera and the flash to the laptop.

As the primary interface for the user and the default storage device for the captured images, the laptop was the crucial component of the data acquisition and storage system. The ASUS F555LD was chosen because of its high performance processor (Intel Core i7-5500U) and sufficient memory (4GB RAM) but mostly due to the 512 GB solid state drive (SSD) and USB 3.0 ports included.

9.1.1.4 Power source

The required runtime of four hours also placed constraints on the power system, which needed to be portable and powerful enough to last for the entire filming session. At 12 volts (V) direct current (DC), the camera unit consumed 2.8 W of power, with an average current draw of 0.23 amperes (A). The flash was significantly more powerful than the camera and required an average current draw

of 2.5 A, with up to 5 A being drawn during start up, it consumes approximately 60 W. A generic laptop transformer outputs 19VDC at a current of 3 A (57 W), whilst a generic Gigabit Ethernet switch is powered by 1.5 A at 12VDC (6 W). In total, the combined subsystems have an average current draw of 2.75 A and will consume approximately 125 W. For a runtime of four hours, this system would need a battery with a minimum capacity of 11 Ampere-hours (Ah).

An alternate power source such as a generator would require an expected runtime of more than four hours, and can produce at least 125 W of power. Since battery systems can only output DC, customised power circuits would need to be designed for each component, to ensure it received the correct current from the single 12 V source. To simplify the power system design and to ensure that only approved manufacturer-supplied transformers were utilised, a generator with AC and DC outputs was selected as the power source. The chosen generator, a Ryobi RGN1200A had an AC output of 3.9 A at 230 V, a DC output of 5.3 A at 12V, a power output of 900 W and a run time of 6 hours at full load, it had more than enough power to meet the system requirements.

9.1.2 System level design

An analysis of the system requirements of the design resulted in the creation of separate subsystems grouped by core functionality: image capture, illumination, data storage and power. Each of these separate subsystems had their own requirements, individual components, inputs and outputs. Clearly defined boundaries for each subsystem were created so that interfacing requirements between each system could be accurately outlined. A simplified system level design is illustrated in Figure 9.4.

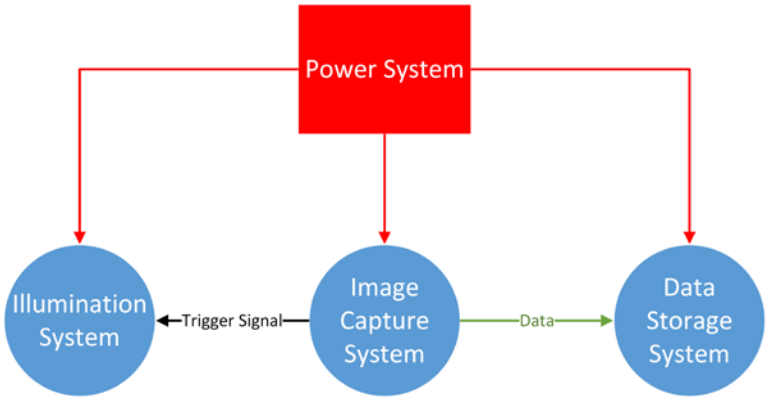


Figure 9.4 Simplified system level design for the Automated Image Acquisition System

The power system obviously provided electrical power for the other subsystems and consisted of the generator and a four outlet residual current device, which can be safely used to share power amongst several electrical appliances. The image

capture system consisted of the camera and lens, which imaged the vine at a specified rate. One of the outputs of this system was a trigger signal to the illumination system, which was required to sync the illumination output with the exposure of the camera, while the other output was the processed data to the data storage system. The data storage system consisted of the laptop, a Gigabit Ethernet switch, and an external hard disk drive. A detailed system level design is illustrated in Figure 9.5.

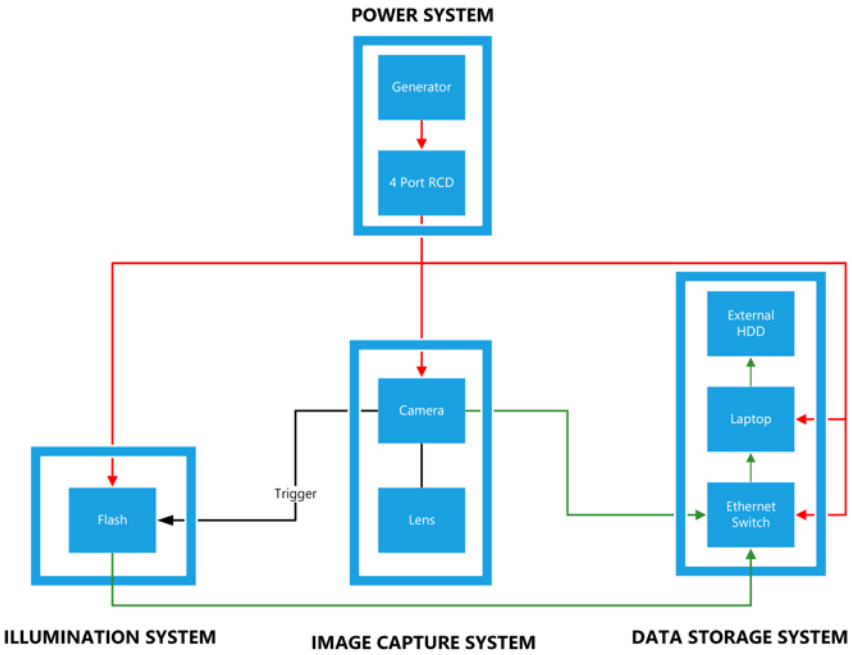


Figure 9.5 Detailed system level design for the automated image acquisition system. Red lines signify the electrical power transfer whilst the green lines signify data transfer.

The next step was to assemble the system as a final product. To simplify manufacturing and weather-proofing of the design, an off-the-shelf plastic enclosure was utilised as the main shell. Modifying a general purpose weather-proof enclosure to suit our needs was considered simpler and more time efficient than sealing a custom manufactured design. The chosen enclosure was IP66 rated and was made of glass fibre reinforced polyester, an easy to machine plastic. The enclosure was modified to house the strobe unit flush against the wall, aluminium brackets were made up to secure the camera power supply and the Ethernet switch and a camera mount was made out of RenShape. A transparent polycarbonate cover was chosen for better user visibility and troubleshooting. The completed image acquisition system can be seen in Figure 9.6.



Figure 9.6 Final assembled image acquisition system

9.1.3 Mount design

Custom mounts were designed to attach the image acquisition systems to the vehicles that would be driving through the vineyards and capturing images. Different mounts were needed for the different vehicles available at the Orange and Clare vineyards. The mount was designed to be sturdy, reduce the vibration experienced by the image acquisition system while driving through bumpy vineyards and provide an attachment surface for the camera enclosure to the ute.



Figure 9.7 Final mount for image acquisition system at Orange, NSW



Figure 9.8 Final mount for image acquisition system at Clare, SA.

9.2 Experimental design for Y2 (Manta)

9.2.1 Hardware testing

A detailed testing plan was developed to outline the tests that individual components and subsystems would need to pass to ensure the final automated image acquisition system would meet its requirements. Each section of the testing plan was linked to an entry in the system requirements of the design. The testing plan was developed in a way such that basic functionality was tested first with increasing levels of complexity and interfacing until whole subsystems could be marked as functioning. Field testing was performed at SeeSaw wines, a vineyard located approximately 30 km from Orange. Results from each round of testing were used to improve the design in an iterative process. Failed tests were investigated and in some cases troubleshooting was performed until the appropriate system parameter was adjusted in order to pass the test.

9.2.2 Further GoPro analysis and determination of best stage to video

In total, we collected videos in two successive growth seasons: 2015 and 2016. In season one, we only collected footage once for each block at shoot stage. During this time, we found that it was difficult to define the optimal timing to capture video of shoots. Hence in the second season, we collected multiple datasets for each block before the inflorescence stage to identify the optimal time for filming.

9.2.3 Harvest efficiency

Harvest efficiency can be defined as the proportion of the crop that is collected during the harvest process relative to what is left in the vineyard. A good understanding of harvest efficiency is important since it is a key component of uncertainty in the process of yield estimation. In addition, improving harvest efficiency can increase vineyard productivity as there are very few additional costs associated with a yield increase due to harvesting a higher proportion of the fruit.

This section focuses on estimating the harvest efficiency in four machine harvested vineyard blocks; a Chardonnay and Shiraz vineyard in each of Orange and the Clare Valley. The data gathered through these experiments would pave the way to developing more efficient harvesting practices. A small improvement in harvest efficiency can translate to a significant increase in the absolute yield.

The experimental procedure followed in estimating the harvest efficiency is discussed next and was also presented at a poster at AWITC 2016 [31].

9.2.3.1 Harvest efficiency Experimental Procedure

Two different types of harvesting machinery were utilised in the two vineyards. The vineyard in Clare employed a towed harvester, while the vineyard in Orange used a self-propelled harvester. The two types of machinery are shown in Figure 9.9. The harvest efficiency experiment consisted of the following steps.



(a) (b)

Figure 9.9 (a) Towed harvester used in Clare. (b) Self-propelled harvester used in Orange.

a) Mark out a set of Anti Temporal Locations (ATLs):

   An ATL can be defined as a sample location chosen to manually count the grapes left behind after the harvesting process, in this instance comprised of a two-panel segment. ATLs were marked on the ground using the pattern

shown in Figure 9.10. 20 ATLs were defined across the block to achieve a better representation of the harvest efficiency.

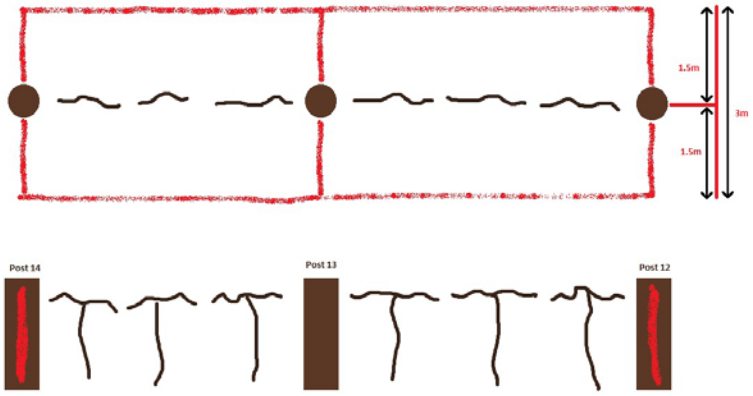


Figure 9.10 An ATL mark-out

b) Wait until the harvesting process is finished.

c) Pick up ground fruit at ATLs:
   i. All loose berries on the ground within the mark-out of a single panel were picked up, leaving bunches on the ground.
   ii. The total amount of individual berries collected at each ATL was weighed.
   iii. For the same panel, all loose bunches from the ground were picked up and counted, with a bunch defined as having at least one berry on it and empty rachises were not included.
   iv. The total weight and count of bunches for that panel were measured.
   v. All loose bunches from the other panel in an ATL were picked up, weighed and counted.

d) Harvest remaining bunches at ATLs:

   For each anti-temporal location,
   i. All remaining bunches having at least one berry on each of the vines between the marked posts were manually harvested
      - The number of bunches was counted
   ii. The total weight of manually harvested bunches was recorded.

These recorded values were then compared with the harvest data to derive the harvest efficiency.

9.3 Results for Y2

9.3.1 Hardware testing results

Individual image capture using the Manta system was successful. However, despite extensive planning involved in developing the Manta system, several hardware issues persisted during continuous capture.

1. Data collected was too large for a 1TB SSD HDD. Data compression was implemented to overcome this issue, but then the system failed to operate in real time.
2. Transferring the data from the laptop to the HDD was limited in speed, despite using USB3 external HDDs, hence video capture needed to be paused within a block to allow the HDD cache to clear.
3. The resolution of the Manta was 1936x1216 at best, below that of the GoPro (3000x4000).
4. The flash trigger control was not well synchronised with the camera, despite the supplier claiming it would work well – technical support was exceptionally slow.
5. The flash was not found to be powerful enough at the capture rate of >10 fps required for imaging all the vines.
6. The flash control parameters written in the firmware were randomly reset in the middle of data collection (with no operator feedback), meaning reversion to inappropriate default settings.
7. The software used to test and check the camera settings was extremely cumbersome to use.
8. The lens depth of field was too small in practice and variation in the distance to the vines meant many bunches were out of focus.
9. The camera and flash required a generator for a power supply to run for several hours, and the generators used required maintenance too frequently.

In addition, transferring data back from the field to the lab was only possible using a mail service, as internet bandwidth was insufficient. Debugging on-site was severely affected since it took many days for the data to arrive in the lab. Even the installation of the NBN on both sites in 2016 did not solve the data transfer problem due to the large file sizes involved. Data were uploaded into a state-of-the-art central university data archive, but this proved buggy and took months before a programmable interface that functioned correctly became available.

Extensive efforts were made to resolve the technical issues generated by the Manta camera and flash arrangement, however these were only resolved in time for the final harvest data collection at Orange. Ultimately, the Manta system lacked in usability and did not deliver the expected image quality.

9.3.2 Comparison between GoPro (Y1 and Y2) and Manta (Y2) systems

To analyse the improvements introduced by the Manta setup, images captured via the Manta system were compared with those from the GoPro cameras used in the previous season. As seen in Figure 9.11, both GoPro Hero3+ and Hero4 exhibit glare and motion blur. However, compared to GoPro Hero3+, the Hero4 images show less motion blur. Of the three camera systems, the Manta system produced images with the highest quality. The lighting condition is better due to the separate flash and the blur is minimised. Even individual berries can be seen in the images captured by the Manta system. However, due to its narrow field of view, the Manta system is required to capture more images per row, compared to the GoPro cameras. Furthermore, GoPro systems are configured to maximise the contrast for the entire image, including the sky and other bright objects like the leaves, whereas the Manta is configured to ignore these aspects of the image and instead focus on the shaded and darker bunches



(a)



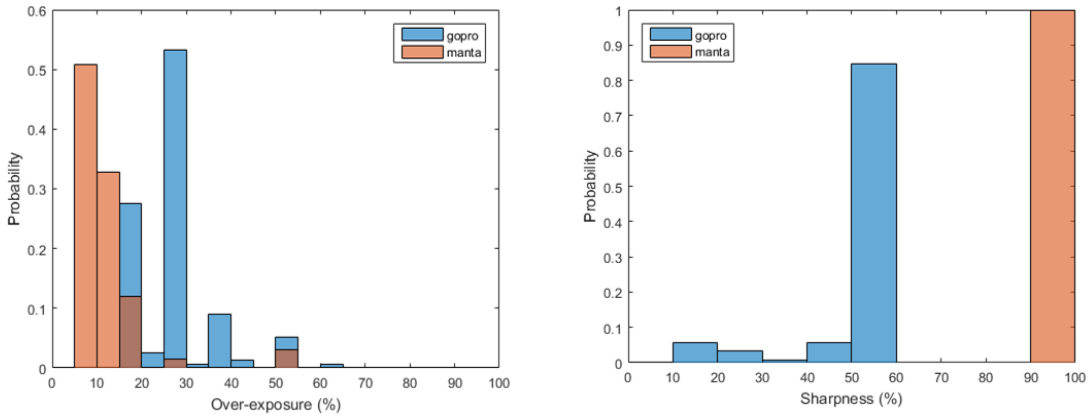
(b)



(c)

Figure 9.11 Images captured by different camera systems at the same location. (a) GoPro Hero3+. (b) GoPro Hero4. (c) Allied Vision Manta.

Next, parameters such as over-exposure and sharpness were measured for the images captured via the GoPro Hero4's and the Manta. The results are shown in Figure 9.12. These results show that the Manta systems surpasses the GoPros with less over-exposure and significantly improved image sharpness.

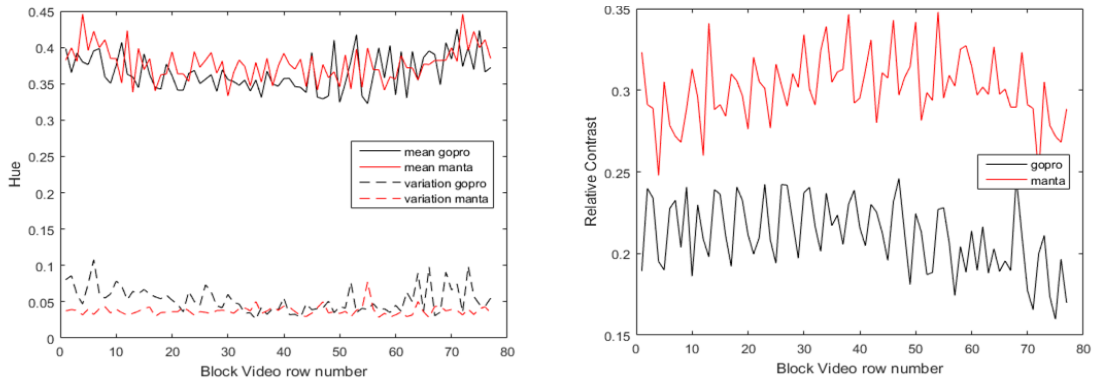


(a) (b)

Figure 9.12 (a) Over-exposure % against the probability of over-exposure for a given dataset. (b) Sharpness % for a given dataset

It was also observed that the variation between GoPro and Manta video data is strongest with the contrast for each frame, where there is greater contrast in the Manta videos. Furthermore, the colours detected between the GoPro and Manta videos were very similar, both tracking approximately the time of the day, with the

GoPro having a greater variation in the colour. More results on this are shown in Figure 9.13.



(a) (b)

Figure 9.13 (a) Hue values for GoPro and Manta. (b) Relative contrast values for GoPro and Manta.

9.3.3 Further GoPro analysis and determination of best stage to video

Table 9.1 Shoot count error per TL in Y2, compared with E-L stages across the block

Error (%) /E-L stage	**Season 2**			
Block	FT2.3	FT2.4	FT2.5	FT2.6
40A		-28.58 E-L 9-12	-29.54 E-L 12-15	
47A	19.37 E-L 6-7		-2.46 E-L 9-12	
B4		-13.71 E-L 7-9		-67.54 E-L 13-15+
B12		-9.74 E-L 8-10		-21.64 E-L 13-15+

The eight shoot stage dataset results for Y2 are listed in *Table 9.1* along with the corresponding E-L stages. It is clear that the early and later results for shoot counting are less reliable.

The datasets collected in block 40A at FT1.2 and block 47A at FT2.3 were too early, with approximately half of block 40A at E-L 4, which is budburst. Buds are usually filtered as noise and this is the reason that the counts generated by image processing are much lower than expected. Thus, videos recorded at or prior to E-L 6 were removed from the accuracy comparison.

The substantial variation in E-L stage of the vines in block 40A is due to that block being on a steep hillside, with a substantial variation in altitude and thus temperature from one side to the other. The western side develops much more rapidly as it is higher.

The datasets collected beyond E-L stage 12 (40A-FT2.5, B4-FT2.6, B12-FT2.6) were also discarded, as at this stage the shoots had grown rapidly and overlapped and interleaved with one another and it was completely unfeasible to distinguish them by image processing.

For the remaining five datasets, the average accuracy of shoot detection was found to be 14.8%, validating the overall shoot counting procedure and laying the groundwork for an early stage yield estimation.

Block 12, FT1.2 was notably poorer in accuracy than the other dataset for this block (FT2.4), as in the first field trip the lighting conditions were exceptionally challenging. The sun was at an altitude of 26-37°, shining into the camera lens and causing lens flare and huge variation in light levels, depending on which direction the camera was facing.

In conclusion, the method of shoot detection, in combination with the algorithm and method for extrapolating these to real shoot counts is able to count the number of shoots to within 15% of the real value, using only a GoPro camera, backing board and vehicle. This holds true for blocks from E-L 7-11, with a shoot density of less than 40 shoots per metre. Further work is necessary to improve the counting where the shoot density is higher or where extremes in lighting conditions are observed. This marks the first time shoots have been counted automatically in vineyards and lays the foundation for early stage yield estimation as well as mapping of the spatial variation across a block at such an early stage.

9.3.4 Shoot stage yield estimation (GoPro)

To validate the system proposed in Section 7.1, we repeated the data process procedure conducted in Y1. The same yield calculations were applied on eight datasets we collected in Y2. The predicted yield results are demonstrated in Table 9.2 and Table 9.3.

Table 9.2 Comparison of the estimated yield at shoot stage against the weighbridge weights for fruit harvested in each block in Y2

Yield (tonnes)		Season 2			
Block		FT2.3	FT2.4	FT2.5	FT2.6
40A	Imaging	39.96	43.04	60.86	
	Manual	42.942			
	Actual	67.1			
47A	Imaging	57.41		67.38	
	Manual	44.066			
	Actual	59.32			
B4	Imaging		63.06	61.09	82.91
	Manual	50.346			
	Actual	69.0			
B12	Imaging	46.89	46.46	41.42	75.42
	Manual	43.962			
	Actual	64.74			

Table 9.3 Comparison of the error in yield estimation by the proposed shoot counting method and the traditional manual approach in Y2

Error (%)		Season 2			
Block		FT2.3	FT2.4	FT2.5	FT2.6
40A	Imaging	-40.44	-35.86	-9.30	
	Manual	-36.00			
47A	Imaging	-3.22		13.59	
	Manual	-25.71			
B4	Imaging		-8.61	-11.47	18.97
	Manual	-27.03			
B12	Imaging	-27.57	-28.24	-36.02	16.49
	Manual	-32.09			

The comparison between the proposed yield estimation based on shoots counts by computer vision and the manual method illustrates that the proposed method has better performance than the manual method in general. For videos captured

between E-L 7 and E-L 11, the average absolute value of yield estimation in Y2 was 13.5%.

9.3.5 Harvest efficiency experiment

The results for the overall harvest efficiency for the four blocks are presented in Table 9.4.

Table 9.4 Harvest efficiency for the four blocks in Y2

Block	Grape Type	Harvest efficiency
Clare 40A	Chardonnay	90.69 %
Clare 47A	Shiraz	84.12 %
Orange B4	Shiraz	96.12 %
Orange B12	Chardonnay	95.72 %

A further breakdown on the form of the berries that were left behind, can be found in the pie charts presented in Figure 9.14.

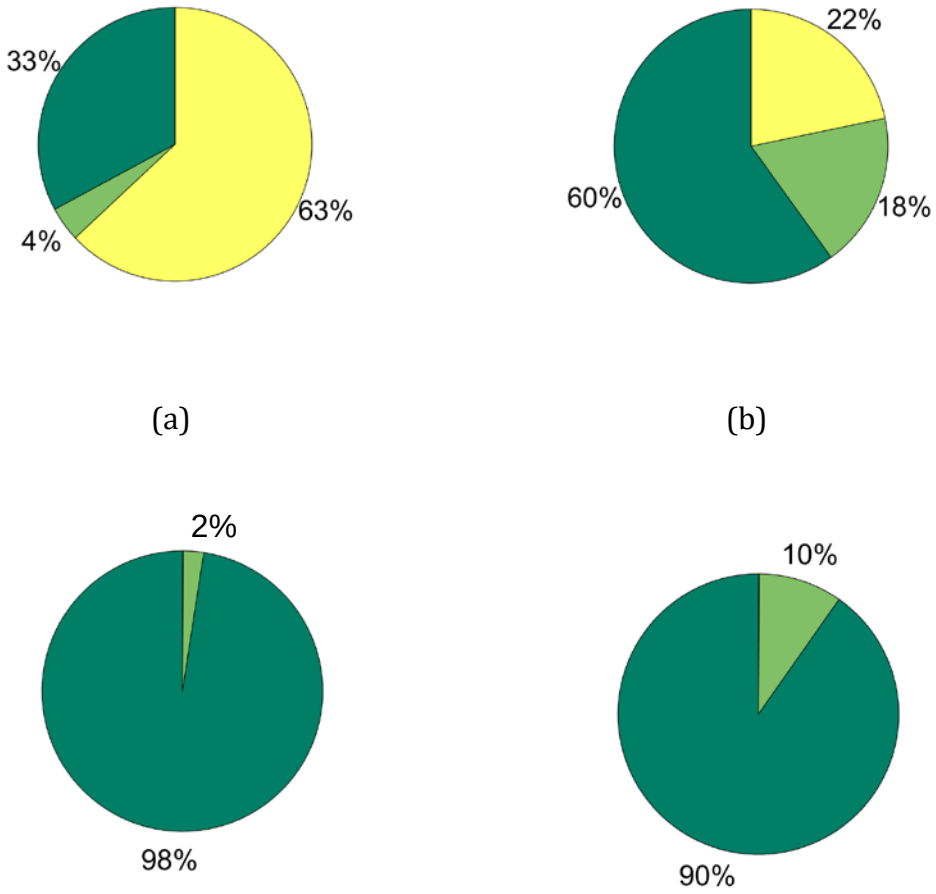


Figure 9.14 A breakdown of the berries left behind after harvesting. Yellow – Left on vine, Light Green – Left on ground (bunches), Dark Green – Left on ground (berries). (a) Clare 40A block. (b) Clare 47A block. (c) Orange B4 block. (d) Orange B12 block.

Harvest efficiency varied between sites and varieties due to the variety, pruning and canopy training systems and the type and setup of the harvester. Harvest efficiency ranged between 84.12 % and 96.12 %. These agreed with the harvest efficiency factors proposed by Martin *et al.* [32]. In three of the vineyards, the greatest proportion of uncollected fruit was individual berries that dropped onto the ground during harvest, with the exception being Chardonnay at Clare where most of the uncollected fruit remained on the vine. Compared to the towed harvester used in Clare, the self-propelled system employed in Orange was able to harvest with a higher efficiency while leaving only a negligible percentage of berries on the vines. Further trials are required to verify the most significant contributors to the harvest efficiency.

9.3.5.1 Conclusion of harvest efficiency experiment

The results suggest that substantial variation in harvest efficiency exists among the four Chardonnay and Shiraz blocks. In addition, the self-propelled system used in Orange exhibits a higher efficiency. Since most of the fruit left in the vineyard was loose berries dropped on the ground, improvements to mechanical harvester design are recommended. Other mechanical improvements may also help to reduce the amount of fruit on the vine. A small improvement in harvest efficiency can translate to a significant increase in absolute yield. These harvest efficiency values were applied to the calculations in this report.

9.4 Overall summary of Y2 results

The results from the development of the Manta system in Y2 were entirely disappointing. The objective was to make a field-robust system able to capture high quality images at a higher price point than consumer cameras. Despite the quality of individual images being better than GoPro imagery, the inability of the system to reliably capture large scale imagery of vineyard blocks was a major impediment. Additionally, extremely poor usability of the system meant that much time was spent debugging on site and remotely which detracted from analysis of the data captured.

Hence, at the reference group meeting held in August 2016 (in conjunction with AWITC 2016), the recommendation to cease development of the Manta system was endorsed by the reference group.

The decision was made to repeat the GoPro filming of rows, albeit with GoPro Hero 4 models, having a slightly improved image quality over the Hero 3+ models used in Y1. Experiments were specifically designed to identify the best time for filming shoots, and E-L 9 was found to be optimal, although the approach will work reasonable in the range of E-L 7–11. From videos collected at this stage, an average error in yield estimation of 13.5% was obtained.

Although extensive sets of videos were collected between flowering and harvest, the GoPro image quality was still insufficient for either traditional [27] or CNN [28] image processing results to generate reasonable outcomes.

Finally, experiments were conducted to determine harvest efficiency in each block, and notable variation was observed, ranging from 84% to 96%.

10 Y3 method

The system and methods proposed for yield estimation for year 3 were designed based on experience from Y1 and Y2 and the desire to implement a proof of concept of a mobile solution which could readily be deployed by growers.

10.1 System design for Y3 (GoPro + Mobile)

To track the crop variation map and hence forecast the yield variation map at harvest, we begin by tracking the yield components throughout the season. The key components for forecasting yield are counts of berries and bunches and their weights, so methods for tracking their development in-vivo through the season were designed in the experimental procedure. Flower and berry counting was conducted by processing images of marked bunches in-vivo, hence allowing correlations between these bunches to be examined. The technical details of detecting shoots, flowers and berries will not be explained in this report (references are given in appropriate sections below) but instead the proposed tracking system to analyse the progression in crop variation across a block is presented.

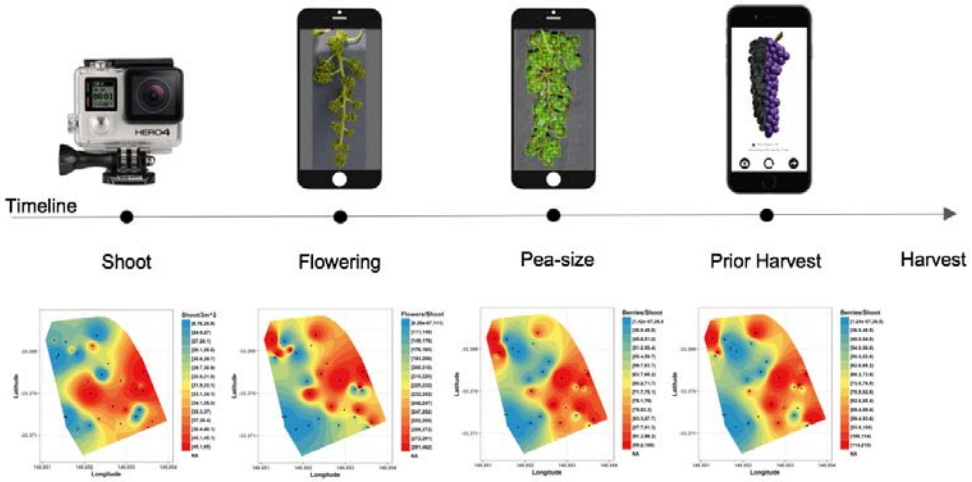


Figure 10.1 The designed data collection system for tracking the crop variation progression over the season. The maps at the bottom are generated based on the data collected in block B4 in 2017.



Figure 10.2 Mounting locations for GoPro cameras and USB power supplies, showing each of mounting on an existing farm vehicle



Figure 10.3 Gator and backing board solution used at Clare at the shoot stage in Y3. Backing boards were not used at Orange in Y3 or in either location after the shoot stage.

Improvements were made to enhance the battery life of the GoPro cameras without relying on temperamental cigarette lighter sockets. A simple solution was to purchase several USB power packs (commonly used for recharging mobile phones) and plug one into each camera, thus ensuring battery life well beyond the two hours required for a 10 ha block. The arrangement used is pictured in Figure 5.21 which shows how easily such a setup could be deployed on any existing farm vehicle.

GoPro Hero 4 Models were used instead of the GoPro Hero 3+ models used in Y1 due to a slight improvement in image quality as discussed in Section 9.3.2.

The overall data collection procedure is presented in Figure *10.1*. At the beginning of the season, a GoPro solution was used for counting the shoots and generating a map of shoot density across the entire block. At the flowering, pea-size and harvest stages, mobile phones were used to photograph all the bunches on three randomly selected and labelled shoots within each of 30 x 60cm wide segments. The bunches were marked to allow them to be tracked throughout the season. The position of each segment was chosen by stratified sampling (10 each in low, medium and high yield zones) using the prior year's yield map as a basis. The images were processed

by the developed computer vision algorithms to extract counts of shoots, flowers and berries.

From these counts, the corresponding crop variation maps were generated by Inverse Distance Weighted (IDW) interpolation [33] using R-Studio [34]. IDW was chosen over Kriging methods, due to the small number of Stratified Sampling Segments (SSSs). Hence a progression of crop variation maps was quickly generated in an automated manner and the correlations between these studied in Section 7.7.

10.2 Experimental design for Y3

In addition to the data collection described in the previous section, validation of each of the yield components was undertaken. As per Y1 and Y2, manual counts of the shoots in each TL was undertaken for direct comparison with the shoot counting method. The TLs remained constant over the three years of the project.

At the flowering stage, the number of inflorescences within each SSS was counted non-destructively, although this was known to be prone to manual error.

At the pea-sized stage, another set of 30 SSSs was generated and destructively sampled. The number of inflorescences was counted. From this, three 'average sized' bunches were chosen at random and the number of berries per bunch counted destructively.

At the harvest stage, the initial 30 SSSs were destructively harvested. The number of bunches in each SSS was counted along with a non-destructive count of the number of shoots in each SSS. This was to validate the shoot counts from earlier in the season and proved to be a major complicating factor for the Clare blocks in Y3. Each of the marked bunches was then weighed, the number of berries counted manually and the rachis weighed. This allowed calculation of the average berry weight for comparison with the predicted value.

10.3 Theoretical method for Y3 (GoPro + Mobile)

The method for year 3 involves estimation at four phenological stages: shoot, flowering (immediately prior to flowering), pea-sized and harvest. The estimation method in each stage is detailed in Sections 10.3.1 to 10.3.4 with a summary of the results being shown in Section 10.4.

10.3.1 Shoot stage (GoPro + Mobile)

10.3.1.1 Shoot stage: Count shoots in Y3 video

Each block was filmed by a set of GoPros installed on a quadbike or Gator (see Figure 10.2 and Figure 10.3) at the early growing season. In Clare, the backing board was still utilised, although we removed the backing board for data collection in Orange.

The shoot detection approach proposed in paper [13] was modified for adapting the film view without backing board in block B4 and B12. Some shoot detection results are demonstrated in Figure 10.4.

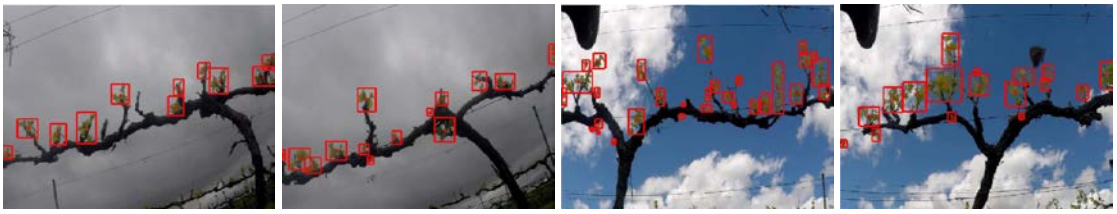


Figure 10.4 Shoot detection results from videos by the modified image processing algorithm, showing robustness to different lighting conditions.

The number of shoots detected from images was recorded and georeferenced [14]. The data for each block was cleaned by excluding outliers regarding shoot counts across a block.

Following pre-treatment of the data, the discrete points in each block were kriged by R[1] to generate a continuous surface across the entire block. A subset of 25% of the frames for each block in each E-L stage was used in order to match the spatial resolution of the provided yield monitor data, although this was only to aid in visualisation. Kriging also allows interpolation across any missing data.

Compared with the shoot estimation method used in previous years [13], the developed shoot number calculation is based on Kriging method. The shoot counting results based on processing filmed videos are illustrated in Table 10.1.

Table 10.1 Total shoot counts generated by computer vision based on videos captured by GoPro

Shoot Count	**40A**	**47A**	**B4**	**B12**
Proposed Method (Y3)	881088	2004147	667533	305000
Liu [13]	873576	1932242	555279	286705

To validate the accuracy of the proposed shoot detection approach we manually counted all shoots at 20 labelled temporal locations (TL). By comparing the counts calculated by computer vision with the real count within 20 TLs, the absolute average error of shoot counting was approximate 12.39%, which agrees with the results presented by Liu [13].

[1] R language, https://www.r-project.org/about.html

Table 10.2 Error in video shoot count against manual counts at TLs

Shoot Count Error (%)	**40A**	**47A**	**B4**	**B12**	**ABS Mean**
	2.32	-3.09	-15.46	-28.68	12.39

Note that errors from B4 and B12 in Orange are worse than the accuracy we obtained in Clare and lower than the actual shoot count in 20 TLs. This is likely due to the removal of the backing board in the Orange datasets and further testing is necessary.

10.3.1.2 Shoot stage: Bunch to shoot ratio

The comparison of bunch *c(B)* to shoot *c(S)* ratio *($R_{B/S}$)* is illustrated in Table 10.3*:*

- $R_{B/S1}$. This ratio is assumed as 1 for four experimental blocks
- $R_{B/S2}$. This ratio is calculated from the historical records of bunch *c(B)_h* to shoot *c(S)_s* ratio in 2015 and 2016. Numbers were collected at 20 TLs, per vine.
- $R_{B/S3}$. This ratio is calculated from the records of bunch *c(B)_h* to shoot *c(S)_s* ratio in 2017. Numbers were collected at 30 SSS, per shoot. The shoot counts were collected at **shoot stage** while the bunches were counted at **harvest stage**.
- $R_{B/S4}$. This ratio is calculated from the records of bunch *c(B)_h* to shoot *c(S)_s* ratio in 2017. Numbers were collected at 30 SSS, per shoot. Both shoot and bunch counts were collected at **harvest stage**.

Table 10.3 The bunch to shoot ratio at different stages

Ratio	**40A**	**47A**	**B4**	**B12**
$\mathbf{R_{B/S1}}$	1	1	1	1
$\mathbf{R_{B/S2}}$	1.014	1.349	1.142	1.130
$\mathbf{R_{B/S3}}$	0.725	1.083	1.257	1.151
$\mathbf{R_{B/S4}}$	1.290	1.649	1.357	1.261

The bunch to shoot ratio increased by around 65% in 40A and 47A, by comparing $R_{B/S4}$ to $R_{B/S3}$. The reason for this is the shoot number dramatically decreased in both blocks. This can be verified the shoot gain/loss factor in Table 10.5.

10.3.1.3 Shoot stage: Average bunch weight

Bunches were manual sampled and weighed at harvest.

- ABW_1 is the average bunch weight collected from 2015 and 2016, at SS.
- ABW_2 is the average bunch weight collected from 2017, at SSS.

Table 10.4 Comparison of average bunch weights

Average Bunch Weight (g)	40A	47A	B4	B12
ABW₁ (Y1 & Y2)	53.86	62.22	83.83	109.66
ABW₂ (Y3)	55.21	81.47	93.43	144.54

10.3.1.4 Shoot stage: Shoot gain/loss factor

At 30 SSSs, the shoots were counted manually in four experimental blocks at the shoot stage and before harvest, to investigate the gain/loss factor of shoots. The results are illustrated in Table 10.5.

Table 10.5 The shoot gain/loss factor between shooting stage and harvest in 2017

Ratio	40A	47A	B4	B12
shoot gain/loss factor	0.620	0.659	0.923	0.955

It is obvious that the shoot number per SSS declined by about 40% at the end of the season in two blocks in Clare Valley while it remained the same in two blocks in Orange. According to the vineyard managers, there was no major shoot thinning operation conducted through the season. Other than inaccurate non-destructive counting at either the shoot or harvest stage, no reason for this discrepancy could be found.

10.3.1.5 Shoot stage: Predict yield

To estimate the yield by computer vision and mobile solution, we propose the following equation:

$$Y^* = c(S) \times R_{B/S} \times \mu(w(B)_h) \times R_r \times HE$$

Where c(S) is the number of shoots estimated from GoPro video of the entire block, $R_{B/S}$ is the average number of bunch per shoot at shoot stage at 30 SSSs, $\mu(w(B)_h)$ is the average berry weight at harvest, R_r is the ratio of rachis weight to bunch weight, HE is the harvest efficiency. The detailed calculation is demonstrated in Table 10.6 .

Table 10.6 Yield Estimation at shoot stage by combining related yield components for 2017

Object	Source	Option	Year	40A	47A	B4	B12
c(S)	Shoot Counts by Kriging	1.1	2017	873576	1932242	555279	286705
	manual shoot counts (SSSs)	1.2	2017	975328	1174724	594730	327666

$R_{B/S}$	historical records	2.1	2016	1.01	1.35	1.14	1.13
	shoot at shoot stage, unit SSS	2.2	2017	0.73	1.08	1.26	1.15
$\mu(w(B)_h)$ (g)	History records	3.1	2015 +2016	53.86	62.22	83.83	109.66
	manual, harvest	3.2	2017	55.21	81.47	93.43	144.54
R_r	History records	4.1	2015 +2016	0.04	0.05	0.05	0.05
	manual, harvest	4.2	2017	0.06	0.05	0.06	0.05
HE	History records	5.1	2016	0.91	0.84	0.96	0.96
	Current records	5.2	2017	0.95	0.90	0.96	0.96
AP*	Active percentage	6	2017	0.9982	0.9987	0.9983	0.9969
NB*	Non-bearing area	7	2017	0.061	0.062	0.025	0.110
	Combination						
Yield Estimation (t)	1.1+2.1+3.1+4.1+5.1+6+7	P1		38.99	122.04	47.05	28.61
	1.2+2.1+3.1+4.1+5.1+6+7	P2		43.53	74.20	50.39	32.69
	1.1+2.2+3.2+4.2+5.2+6+7	A1		29.38	136.83	57.13	38.61
	1.2+2.2+3.2+4.2+5.2+6+7	A2		32.80	83.19	61.19	44.12
Actual Yield (t)				33.50	106.09	54.25	45.27
Error (%)	P1**			16.38	15.04	-13.27	-36.81
	P2			29.94	-30.06	-7.11	-27.79
	A1**			-12.30	28.98	5.30	-14.73
	A2			-2.09	-21.59	12.78	-2.54

* AP is active percentage (fruit removed for experiments) and NB is non-bearing area (calculated in Section 7.8)

** P means yield prediction based on the records only available at the current stage. A means yield estimation by real value in the harvest stage.

Table 10.7 Yield estimation absolute error at shooting stage for four experimental blocks in 2017

Yield Estimation ABS Error (%)	40A	47A	B4	B12	Average
P1	16.38	15.04	13.27	36.81	20.38
P2	29.94	30.06	7.11	27.79	23.73
A1	12.30	28.98	5.30	14.73	15.33
A2	2.09	21.59	12.78	2.54	9.75

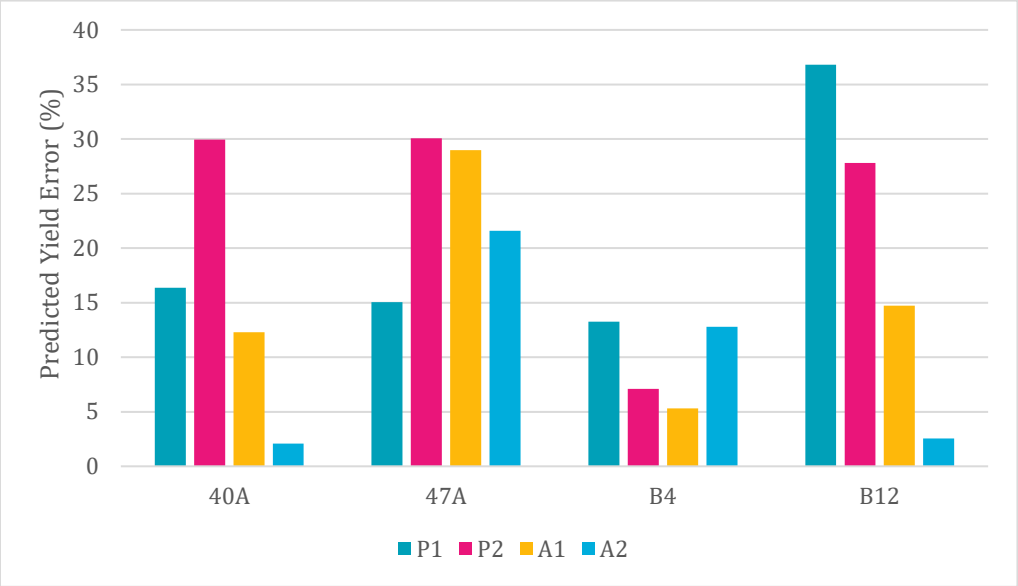


Figure 10.5 The bar chart of Yield estimation absolute error at shooting stage for four experimental blocks in 2017. P1 and A1 are the proposed yield estimation method (GoPro + mobile). P2 and A2 are the manual yield estimation (manual + mobile).

The average yield estimation error shown in Table 10.7 indicates that the prediction of yield based on the shoot numbers calculated by kriging (P1) has better performance than the yield generated based on the shoot numbers calculated by manual calculation (P1) in general.

Comparing A and P, the overall performance of the yield estimation has better performance in terms of final accuracy by multiplying all real yield estimation components calculated at harvest stage.

10.3.1.6 Shoot stage: Yield component analysis

As to the yield component analysis, given the shoot counts generated by computer vision combined with Kriging interpolation has better performance than that manual shoots counts cross a block, we replace each key yield component by its real value to check the significance of changes it caused.

Table 10.8 Yield estimation error (%) caused by key yield components at shoot stage

Combination		**Key Components**	**Yield Estimation Error (%)**				
			40A	47A	B4	B12	ABS Mean
P1	1.1+2.1+3.1+4.1 +5.1+6+7		23.96	22.60	-11.05	-29.04	20.38
C2	1.1+2.2+3.1+4.1 +5.1+6+7	Bunch to Shoot Ratio	-16.75	-7.62	-4.53	-35.67	16.14
C3	1.1+2.1+3.2+4.1 +5.1+6+7	Bunch Weight	19.30	50.62	-3.34	-16.72	22.50
C4	1.1+2.1+3.1+4.2 +5.1+6+7	Rachis Ratio	14.18	14.65	-14.18	-36.46	19.86
C5	1.1+2.1+3.1+4.1 +5.2+6+7	Harvest Efficiency	21.91	23.08	-13.27	-36.81	23.77

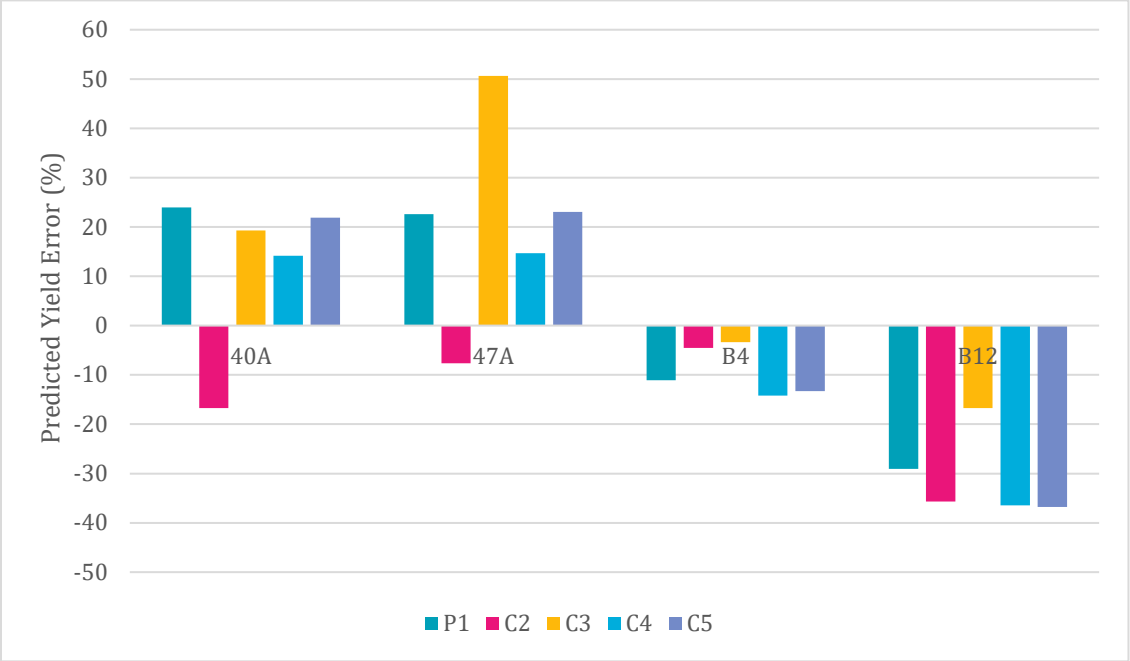


Figure 10.6 Yield components analysis at shoot stage in 2017.

By observing Table 10.8 and Figure 10.6, the bunch to shoot ratio and average bunch weight have critical influence in terms of yield estimation. By applying the real bunch to shoot ratio instead of historical records for four blocks yield average estimation error has decreased to 16.14% from 20.38%, which is close to the real average yield estimation error 15.33% (A1). The average bunch weight indeed plays a vital role (C3) since it changes the yield forecasting performance a lot according to Figure 10.6. Except for block 47A, the yield estimations have been improved by applying real bunch weight for the remaining three blocks according to the number shown in Table 10.8.

10.3.1.7 Shoot stage: Summary

In this section, an early stage yield estimation based on shoot count counted from videos is presented.

In general, shoot to bunch ratio remains around 1.1-1.2 for all blocks at the beginning of the season. This ratio generally increased approximate 8% by the end of the season because of the loss of shoots. This ratio is substantially affected by the shoot counts at the end of the season, resulting in a large fluctuation in yield prediction.

The total shoot number generated by Kriging based on the shoot number counted from frames has a better performance than the shoot calculation method proposed in paper [13] since it provides a more smoothed interpolation surface and reasonable average shoot count across a block.

Noted that bunch weight, rachis weight and harvest efficiency have some impact to the yield estimation. But the yield error caused by the rachis weight has the lowest impact given the ratio of rachis is comparatively stable for these two experimental cultivars.

Again, the harvest efficiency is purely reported by the vineyard managers it may cause inaccuracy to the yield forecasting by 5%-10%.

10.3.2 Flowering stage (GoPro + Mobile)

At the flowering stage, inflorescences were counted on 90 marked shoots (three shoots per SSS, 30 marked SSSs per block).

10.3.2.1 Flowering stage: Inflorescences per shoot

The average inflorescences/shoot (I/S) from SSS were calculated and presented in Table 10.9.

Table 10.9 The average ratio between inflorescences and shoot at flowering stage

Year	**FT**	**40A**	**47A**	**B4**	**B12**
2017	3.2	1.467	1.611	1.089	1.144

The distribution of I/S is illustrated in Figure 10.7 for each block. It is clear that many shoots bear no inflorescences.

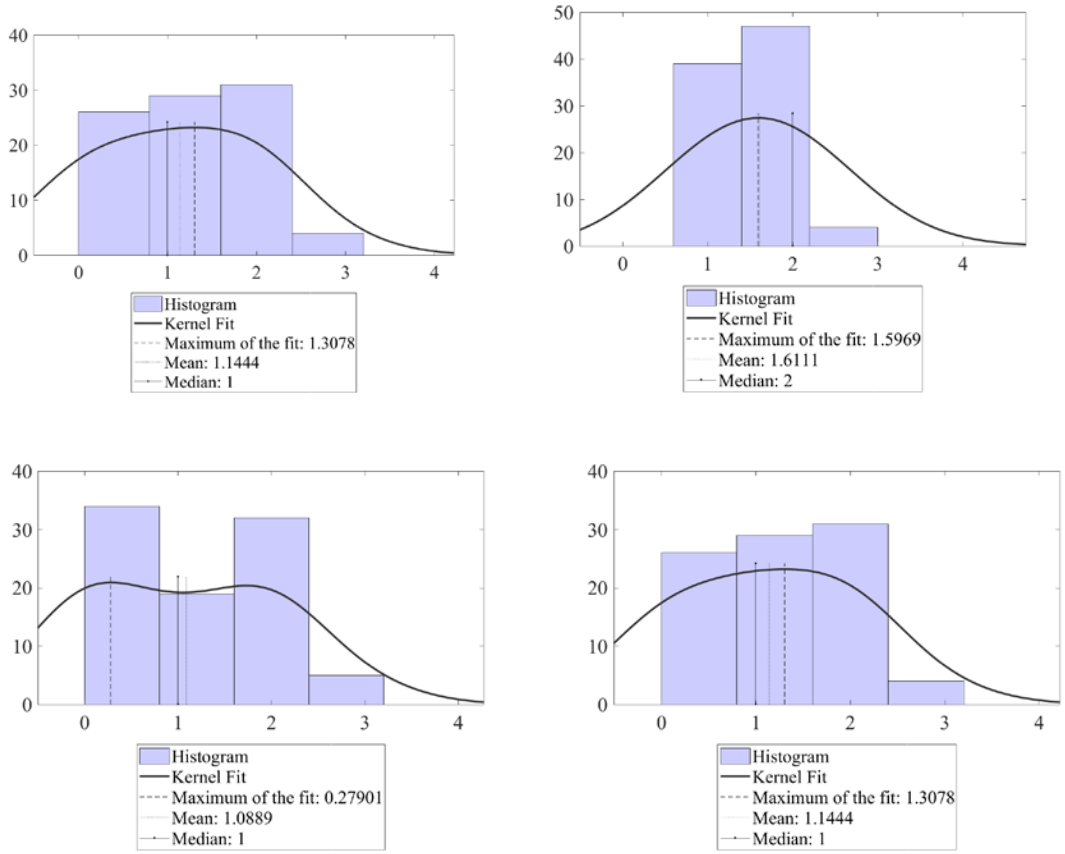


Figure 10.7 The distribution of the average ratio between inflorescences and shoot at flowering stage in Y3. The upper row is 40A and 47A while the bottom row is B4 and B12.

10.3.2.2 Flowering stage: Accuracy of flower counting

In Y3, all photos of inflorescences were taken in-vivo. Hence the relationship between visible flowers and actual flowers needed to be investigated. Data collected in Y2 were used to generate a regression module [15]. In Y2, all sampled inflorescences were photographed under laboratory condition. Follow by this step, each inflorescence was stripped of all flowers and those scattered flowers were placed in a tray. A photo was taken of each tray.

Each sampled inflorescence had two related photos, one is itself and another one is scattered flowers. Two photos are processed for all sampled inflorescences. An example is shown in Figure 10.8. In total, 422 photos were processed.

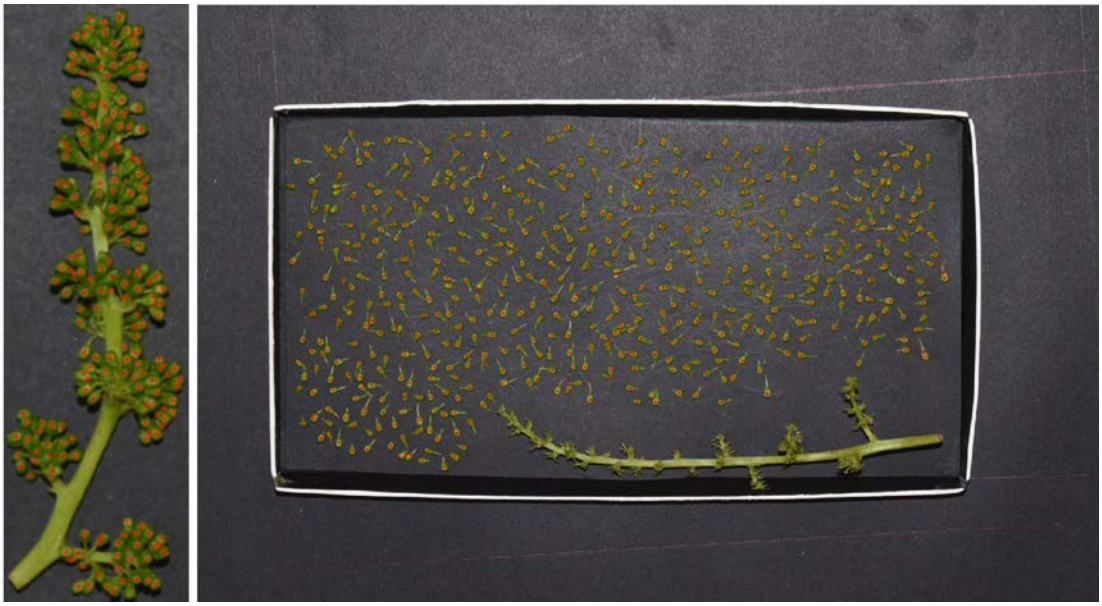


Figure 10.8 A sample of processed inflorescences and related scattered flowers.

To validate the method of flower counting proposed in Paper [15], 13 images were trained with each dataset (there are four datasets) and the generated estimation model was tested on the remaining photos. The average accuracy of flower estimation is demonstrated in Table 10.10.

Table 10.10 The accuracy of flower estimation method proposed method in Paper [15], tested on four datasets collected from four experimental blocks in Y2.

Year	**Accuracy**	**40A**	**47A**	**B4**	**B12**
2016	%	98.059	96.723	97.72	95.764

10.3.2.3 Flowering stage: Flowers per inflorescence

Flower estimation is generated by applying the method proposed in Paper [15]. In total, 467 photos were cropped and processed. The calibration relationship between detected flowers and actual flowers were obtained from the datasets collected from Y2, as described in Section 10.3.2.2.

The average flower/inflorescence ratio (f/I) for each photo was calculated and presented in Table 10.11.

Table 10.11 The average estimated flower number for marked inflorescences at flowering stage by image processing

Year	**FT**	**40A**	**47A**	**B4**	**B12**
2017	3.2	248	239	202	327

The distribution of f/I is illustrated in Figure 10.9 for each block.

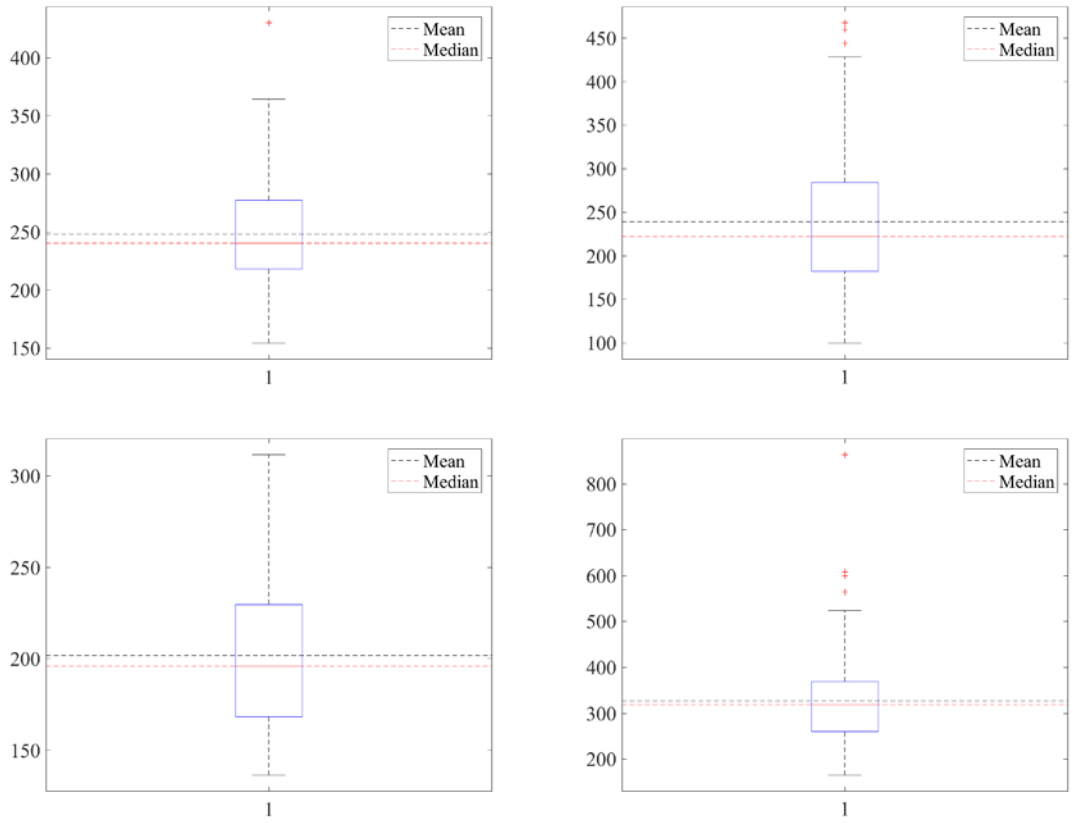


Figure 10.9 The distribution of estimated flower number per inflorescence by image processing. The upper row is 40A and 47A while the bottom row is B4 and B12.

10.3.2.4 Flowering stage: Fruit set ratio

The proposed yield estimation method at flowering stage involves with the ratio of fruit set. By this stage, the available fruit set ratio is generated based on the images collected from Y2. In total, 864 images were processed by the developed automated flower estimation approach [15] and berry counting method (422 photos of sample inflorescences and 442 photos of sample bunches at pea-size stage). The calculated fruit set ratios for four experimental blocks are demonstrated in Table 10.12.

Table 10.12 The fruit set ratio between flower number and berry number at pea-size stage, tested on four datasets collected from four experimental blocks in Y1 and Y2.

Year	**40A**	**47A**	**B4**	**B12**
2015 and 2016 [%]	24.82	28.08	38.96	38.17

Note that all inflorescences and bunches at pea-size stage were destructively sampled, so there is no one-to-one relationship. All numbers are generated based on the average stripped flower counts per inflorescence and average stripped berry number per bunch for each block by image processing.

To investigate the consistency of the fruit set for each block, we collected images of inflorescences and bunches at each marked shoot *in vivo* in Y3. The results are illustrated in Table 10.13.

Table 10.13 The fruit set ratio between flower number and berry number at pea-size stage / harvest stage, tested on four datasets collected from four experimental blocks in Y3.

Year	Fruit Set Ratio	Bunch Stage	Unit	40A	47A	B4	B12
2017	%	Pea-Size	SSS	24.615	25.531	34.722	38.466
		Harvest		24.687	20.331	36.418	43.365
		Pea-Size	Shoot	26.573	29.423	34.304	37.166
		Harvest		26.136	27.421	35.897	42.336
		Pea-Size	Bunch	26.141	31.355	39.096	40.543
		Harvest		26.296	29.199	42.853	45.324

Note that the fruit set ratio decreases when the calculation unit changes from bunch to SSS. This is caused by the death of some bunches at each SSS between flowering stage and harvest stage.

10.3.2.5 Flowering stage: Berry gain loss factor

Berry counts at pea-size stage were processed based on sampled images while berry counts at harvest stage were all counted manually. Except for the berry gain/loss factor in block 40A, which dropped by around 40%, in the remaining blocks there is a slight increase in Y3 compared with the results collected in Y2. The potential reason for decline in berry loss in 40A is that the marked bunches were damaged by human hand since the marked bunches were photographed fortnightly. The detailed results are illustrated in Table 10.14.

Table 10.14 Berry gain/loss factor in Y2 and Y3 by image processing

Year	Unit	40A	47A	B4	B12
2017	SSS	1.033	0.978	1.066	1.151
	Shoot	1.043	0.909	1.082	1.152
	Bunch	1.082	0.902	1.092	1.150
2016	Bunch	0.664	0.973	1.167	1.299

10.3.2.6 Flowering stage: Bunch gain/loss factor

The inflorescence and bunch counts used in this subsection were all counted manually at SS/SSS in Y2 and Y3. The detailed records are demonstrated in Table 10.15.

Table 10.15 Bunch gain/loss factor in Y2 and Y3 counted manually

Year	Unit	40A	47A	B4	B12
2017	SSS	0.988	0.870	1.064	1.114
2016	SS	1.567	1.278	0.735	N/A

According to the data in Table 10.15, there is no consistency in the bunch gain/loss factor over two years for all blocks. This is a key failing of the use of such a small study period without a detailed history of prior measurements.

10.3.2.7 Flowering stage: Flowers per shoot

The flower per shoot ratio was calculated based on all marked bunches at each marked shoot at 30 SSSs. The flower number was estimated by image processing

and the calibration pattern is generated from the data sets collected in Y2. The statistics of flower per shoot are demonstrated in Figure 10.10.

Substantial inflorescences were either dead in marked shoots in block B4 and B12 at flowering stage or it is possible that these shoots never generated bunches.

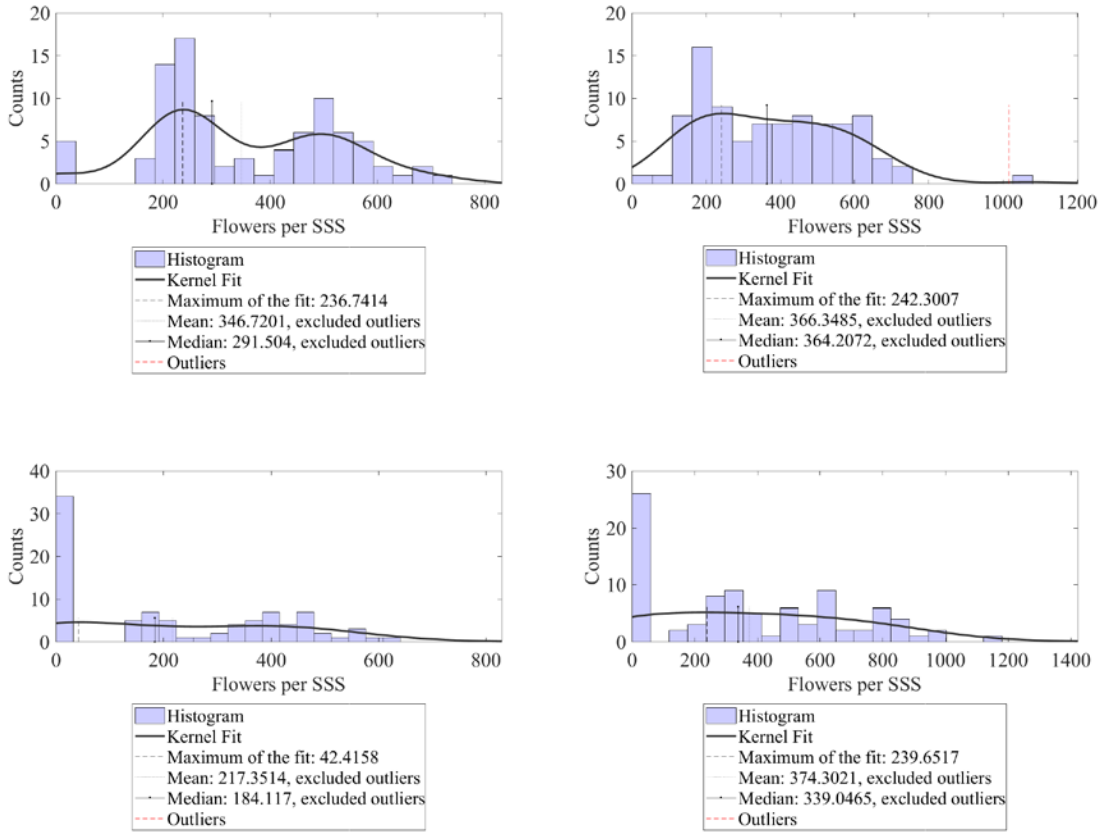


Figure 10.10 The distribution of flowers per shoot in four experimental blocks in Y3. The upper row is 40A and 47A while the bottom row is B4 and B12 respectively.

10.3.2.8 Flowering stage: Predict yield

To estimate the yield by computer vision and mobile solution, we propose the following equation:

$$Y^* = c(S) \times R_{f/s} \times R_{b/f} \times \mu(w(b)_h) \times HE \times S_{gl}$$

where c(S) is the number of shoots estimated from GoPro video of the entire block, $R_{f/s}$ is the average number of flowers per shoot at flowering stage at 30 SSSs. $R_{b/f}$ is the average fruit set ratio calculated as the ratio of flowers at flowering to berries at the harvest stage (Cb_H/CF_F) at 30 SSSs, $\mu(w(b)_h)$ is the average berry weight at

harvest, HE is the harvest efficiency, S_{gl} is the shoot gain / loss factor. The detailed calculation is demonstrated in Table 10.16.

Table 10.16 Yield Estimation at flowering stage by combining related yield components for Y3.

Object	Source	Option	Year	40A	47A	B4	B12
Flower Numbers = c(S) × $R_{f/s_}$	Shoot Count by Kriging*average flower number per shoot	1.1	2017	313330889	723111619	129311477	107314396
	Manual shoot counts (SSSs)*average flower number per shoot	1.2	2017	349826719	439622318	138498575	122645899
$R_{b/f}$ (%)	Flower counts by image processing, Berry counts at harvest (manual counts + image processing) from Y1 and Y2	2.1	2016	24.82	28.08	38.96	38.17
	Flowers counts by image processing, Berry counts at harvest (manual), unit SSS	2.2	2017	26.26	20.33	36.42	44.02
$\mu(w(b)_h)$ (g)	History records	3.1	2015 +2016	0.80	1.10	1.21	1.22
	manual, harvest	3.2	2017	0.80	1.17	1.17	1.13
HE	History records	4.1	2016	0.9069	0.8412	0.9621	0.9572
	Current records	4.2	2017	0.9500	0.9000	0.9621	0.9572
S_{gl}		5	2017	0.6208	0.6587	0.9227	0.9553
AP*		6	2017	0.9982	0.9987	0.9983	0.9969
	Combination						
Yield Estimation (t)	1.1+2.1+3.1+4.1+5+6	P1		35.13	123.27	54.15	45.63
	1.2+2.1+3.1+4.1+5+6	P2		39.23	74.94	58.00	52.15
	1.1+2.2+3.2+4.2+5+6	A1		38.58	101.68	48.70	48.54
	1.2+2.2+3.2+4.2+5+6	A2		43.08	61.82	52.16	55.47
Actual Yield (t)				33.50	106.09	54.25	45.27
Error (%)	P1**			4.88	16.19	-0.19	0.80
	P2			17.09	-29.36	6.90	15.20
	A1**			15.17	-4.16	-10.24	7.22
	A2			28.58	-41.73	-3.87	22.53

*AP is the active percentage (excluding sampled fruit over a season).
** P means yield prediction based on the records only available at the current stage. A means yield estimation by real value in the harvest stage.

Table 10.17 Yield estimation absolute error at flowering stage for four experimental blocks in 2017

Yield Estimation ABS Error (%)	40A	47A	B4	B12	Average
P1	4.88	16.19	0.19	0.80	5.51
P2	17.09	29.36	6.90	15.20	17.14
A1	15.17	4.16	10.24	7.22	9.20
A2	28.58	41.73	3.87	22.53	24.18

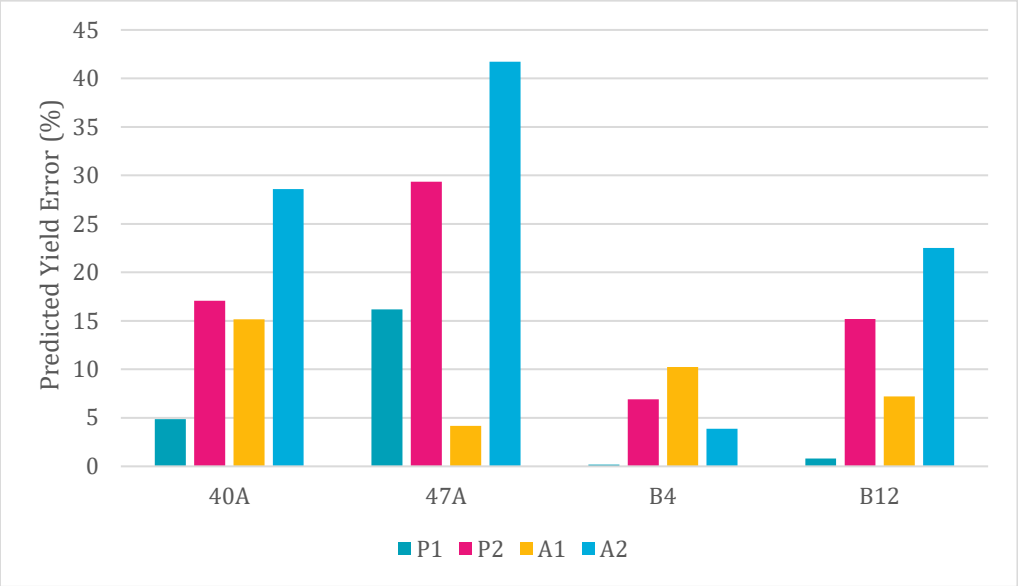


Figure 10.11 The bar chart of Yield estimation absolute error at flowering stage for four experimental blocks in 2017. P1 and A1 are the proposed yield estimation method (GoPro + mobile). P2 and A2 are the manual yield estimation (manual + mobile).

Figure 10.11 shows that the prediction of yield based on the flower numbers calculated by the shoot counts by kriging (P1) has better performance than the yield generated based on the flower numbers calculated by manual calculation of shoot counts (P2) in all four experimental blocks. The average yield estimation absolute error by the proposed system is 5.51%.

Comparing A1 and A2, the overall performance of the proposed yield estimation solution by GoPro and mobile has better performance than manual calculation of shoot counts in terms of final accuracy. By multiplying all yield components, using the real values calculated at harvest stage, the average absolute error for four experimental blocks was 9.20%.

10.3.2.9 Flowering stage: Yield component analysis

For yield components analysis, based on the generated flower numbers across a block, we replace each key yield component by its real value to check the significance of changes it caused.

Table 10.18 Yield estimation error (%) caused by key yield components

Combination		Key Components	Yield Estimation Error (%)				
			40A	47A	B4	B12	ABS Ave Error
P1	1.1+2.1+3.1+4.1+5+6		4.88	16.19	-0.19	0.80	5.51
C2	1.1+2.2+3.1+4.1+5+6	Fruit Set	10.95	-15.88	-6.69	16.23	12.44
C3	1.1+2.1+3.2+4.1+5+6	Berry Weight	3.92	23.73	-3.99	-7.02	9.66
C4	1.1+2.1+3.1+4.2+5+6	Harvest Efficiency	9.86	24.32	-0.19	0.80	8.79
C5	1.1+2.1+3.1+4.1+6	Shoot gain /loss factor	68.95	76.40	8.17	5.52	39.76



Figure 10.12 Yield components analysis at flowering stage in 2017.

Table 10.17 and Figure 10.11 show that the fruit set ratio and shoot gain loss factor has critical influence in terms of yield estimation. By applying the real fruit ratio, the

average absolute error for four blocks is 9.66%, which is close to the real average absolute error of 9.20%.

The shoot gain/loss factor also plays a vital role in the proposed yield estimation. Based on the numbers illustrated in Figure 10.11, the average absolute error increases to 39.76% if the shoot/gain loss factor is not considered (it was 5.51% for P1).

10.3.2.10 Flowering stage: summary

In this section, a solution by GoPro and mobile for forecasting yield at flowering stage is proposed. Based on the shoot count and flowers counts obtained by mobile, the final yield was calculated.

The average absolute yield estimation error is 5.51% for four experimental blocks. The fruit set ratio and the shoot gain/loss factor played a vital role in this yield estimation formula.

The fruit set ratio varies from 23%-45%, which caused uncertainty of yield forecasting. An improvement we made in terms of obtaining this ratio is providing a mobile image processing solution to count the flowers and berries in vivo. The traditional approach to calculate those two numbers is destructive. There is a bias on inflorescences/bunch sampling caused by human intervention. An accurate ratio is more desirable to track the marked inflorescences at the start of the season, by using mobile phone cameras.

10.3.3 Pea-size stage (GoPro + Mobile)

10.3.3.1 Pea-sized stage: Bunches to shoot ratio

The average Bunch/Shoot ratio from manual counts at 30 SSSs is demonstrated in Table 10.19.

Table 10.19 Average Bunch/Shoot ratio from manual counts at 30 SSSs at pea-sized stage in 2017

B/S	40A	47A	B4	B12
Include zeros	1.4667	1.4253	1.0375	1.1444
Exclude zeros	1.5184	1.6728	1.6227	1.6349

10.3.3.2 Pea-sized stage: Berries per bunch

The pea-sized berry counting method presented in Section 7.4 was used in both in-vivo and ex-vivo images to count the number of pea-sized berries in a bunch. The results generated for Y2 were used to develop a linear regression model that was then used to estimate the berry numbers for Y3. The corresponding results are

presented in Table 10.20, where the estimate is from the in-vivo images that were left until harvest and the count is from a separate set of destructively sampled bunches.

Table 10.20 Comparison between the automated pea-sized berry per bunch estimation result and the manual pea-sized berry count for Y3.

Block	40A	47A	B4	B12
Estimated pea-sized berry number per bunch	94	110.07	121.45	198.06
Manually counted pea-sized berry number per bunch	108.7	108.4	104.7	176.6

The counts of berries per bunch was extended to berries per shoot and the detailed numbers are shown in Table 10.21.

Table 10.21 The berry number per shoot at pea-size stage in 2017, processed by image analysis.

Unit	Include 0?	40A	47A	B4	B12
Shoot	N	94.012	110.07	121.51	198.03
SSS*	N	89.833	94.862	76.631	138.66
Shoot	Y	89.833	91.722	71.556	138.62
SSS*	Y	89.833	91.700	71.522	138.66

* Total berry number for all three marked shoots at each SSS / 3.

There are differences when choosing different units for calculating the berry number per shoot. For the purpose of yield estimation by the proposed method, the berry number per shoot calculated from SSS, excluding zeros, is applied in the yield estimation function. The statistics of berry number per shoot are demonstrated in Figure 10.13. It is obviously that in B4 and B12, a large proportion of marked shoots

were missing or did not grow any bunches in the pea-sized stage in 2017.

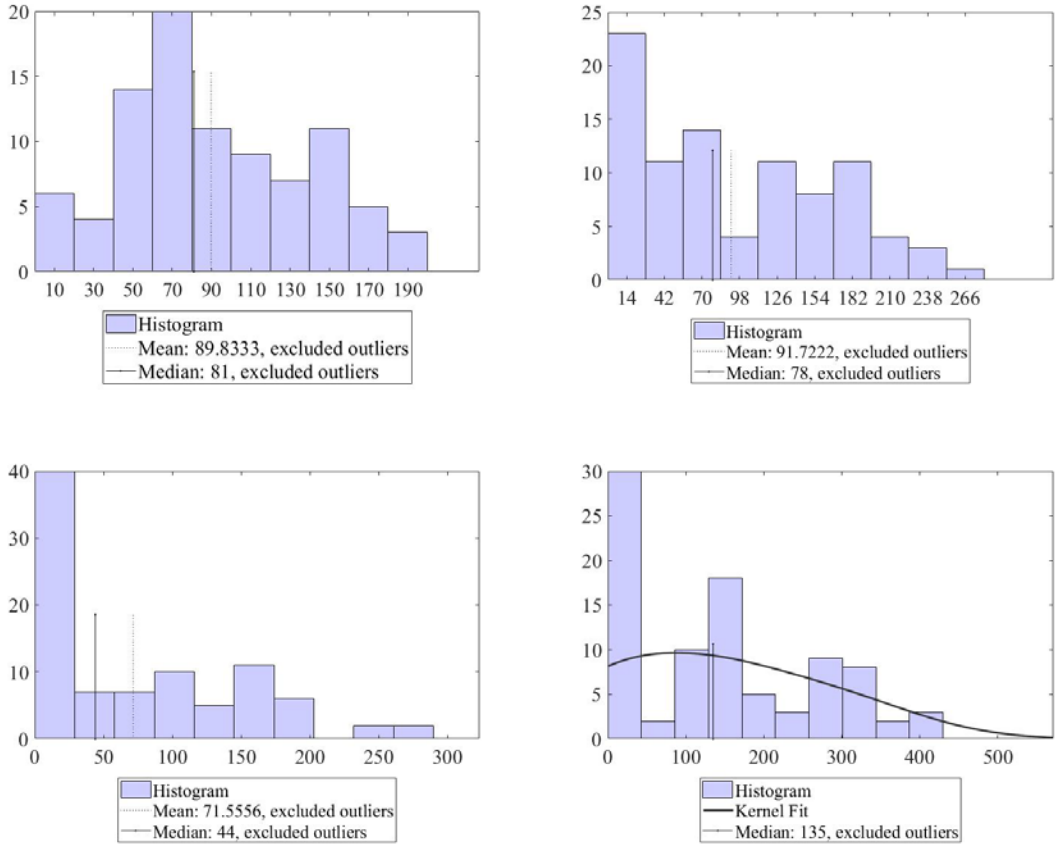


Figure 10.13 The statistics of berry number per shoot. Berry number was counted by processing in-vivo photos. The upper row is 40A and 47A while the bottom row is B4 and B12 respectively.

10.3.3.3 Pea-sized stage: Average berry weight

The average berry weight at harvest by manual measurement is illustrated in Table 10.22.

Table 10.22 The average berry weight from manual measurements in 2015-2017 for four experimental blocks.

Berry Weight (g)	**40A**	**47A**	**B4**	**B12**
2015	1.051	1.489	1.320	1.315
2016	0.557	0.705	1.106	1.129
2015+2016	0.804	1.097	1.213	1.222
2017	0.797	1.168	1.167	1.127

By comparing the historical records of berry weight (the mean of berry weight from 2015 and 2016) with the average berry weight in 2017, there is no dramatic change.

10.3.3.4 Pea-sized stage: Berry gain loss factor

The berry loss/gain factor b_{gl} was calculated from the berry per bunch at pea-size stage against the berry per bunch at harvest stage.

Table 10.23 The berry loss/gain factor between pea-size and harvest stage.

b_{gl}	40A	47A	B4	B12
2016*	0.675	0.960	1.167	1.290
2017**	1.091	0.620	1.050	1.153
2017***	0.804	1.097	1.213	1.222

*per bunch, and there is no to one relationship between bunches since all sampled bunches were collected destructively
** per shoot, unit, SSS
*** per bunch

10.3.3.5 Pea-sized stage: Bunch gain/loss factor

The details about the bunch gain/loss factor B_{gl} between pea-size and harvest stage are presented in Table 10.24.

Table 10.24 The bunch gain/loss factor between pea-size and harvest stages in 2016 and 2017.

B_{gl}	40A	47A	B4	B12
2016	1.083	0.946	0.459	0.477
2017	0.988	0.870	1.064	1.114

The bunch gain/loss factor had no dramatic changes for 40A and 47A in both years. The bunch number decreased by half in B4 and B12 in 2016.

10.3.3.6 Pea-sized stage: Predict yield

To estimate the yield by computer vision and mobile solution, we propose the following equation for yield estimation at pea-size stage:

$$Y^* = c(S) \times R_{B/S} \times b_{gl} \times \mu(w(b)_h) \times HE \times S_{gl}$$

Where c(S) is the number of shoots estimated from GoPro video of the entire block, $R_{B/S}$ is the average number of berries per shoot at pea-sized at 30 SSSs. b_{gl} is the berry gain/loss calculated as the ratio of berries at pea-size stage to berries at the harvest stage (Cb_H/Cb_P) at 30 SSSs, $\mu(w(b)_h)$ is the average berry weight at harvest,

HE is the harvest efficiency, S_{gl} is the shoot gain / loss factor. The detailed calculation is demonstrated in Table 10.25.

Table 10.25 Yield Estimation at pea-size stage by combining related yield components for 2017.

Object	Source	Option	Year	40A	47A	B4	B12
Berry Numbers = $c(S) \times R_{f/s}$	Shoot Count by Kriging*average berry number per shoot	1.1	2017	78476280	183296341	42551600	39753315
	manual shoot counts (SSSs)*average berry number per shoot	1.2	2017	87616959	111436686	45574733	45432684
b_{gl}	Flower counts by image processing, Berry counts at harvest (manual counts + image processing) from Y2 and Y3	2.1	2016	0.67	0.96	1.17	1.29
	Flowers counts by image processing, Berry counts at harvest (manual), unit SSS	2.2	2017	1.09	0.62	1.05	1.15
$\mu(w(b)_h)$ (g)	History records	3.1	2015 +2016	0.80	1.10	1.21	1.22
	manual, harvest	3.2	2017	0.80	1.17	1.17	1.13
HE	History records	4.1	2016	0.9069	0.8412	0.9621	0.9572
	Current records	4.2	2017	0.9500	0.9000	0.9621	0.9572
S_{gl}		5	2017	0.6208	0.6587	0.9227	0.9553
AP*		6	2017	0.9982	0.9987	0.9983	0.9969
	Combination						
Yield Estimation (t)	1.1+2.1+3.1+4.1+5+6	P1		23.93	106.48	53.36	57.14
	1.2+2.1+3.1+4.1+5+6	P2		26.71	64.73	57.16	65.30
	1.1+2.2+3.2+4.2+5+6	A1		40.15	78.60	46.20	47.10
	1.2+2.2+3.2+4.2+5+6	A2		44.83	47.78	49.48	53.83
Actual Yield (t)				33.50	106.09	54.25	45.27
Error (%)	P1**			-28.58	0.36	-1.64	26.22
	P2			-20.26	-38.98	5.35	44.25
	A1**			19.86	-25.92	-14.84	4.04
	A2			33.82	-54.96	-8.79	18.90

*AP is the active percentage (excluding sampled fruit over a season).
** P means yield prediction based on the records only available at the current stage. A means yield estimation by real value in the harvest stage.

Table 10.17 Yield estimation absolute error at pea-size stage for four experimental blocks in 2017

Yield Estimation ABS Error (%)	40A	47A	B4	B12	Average
P1	28.58	0.36	1.64	26.22	14.20
P2	20.26	38.98	5.35	44.25	27.21
A1	19.86	25.92	14.84	4.04	16.16
A2	33.82	54.96	8.79	18.90	29.12

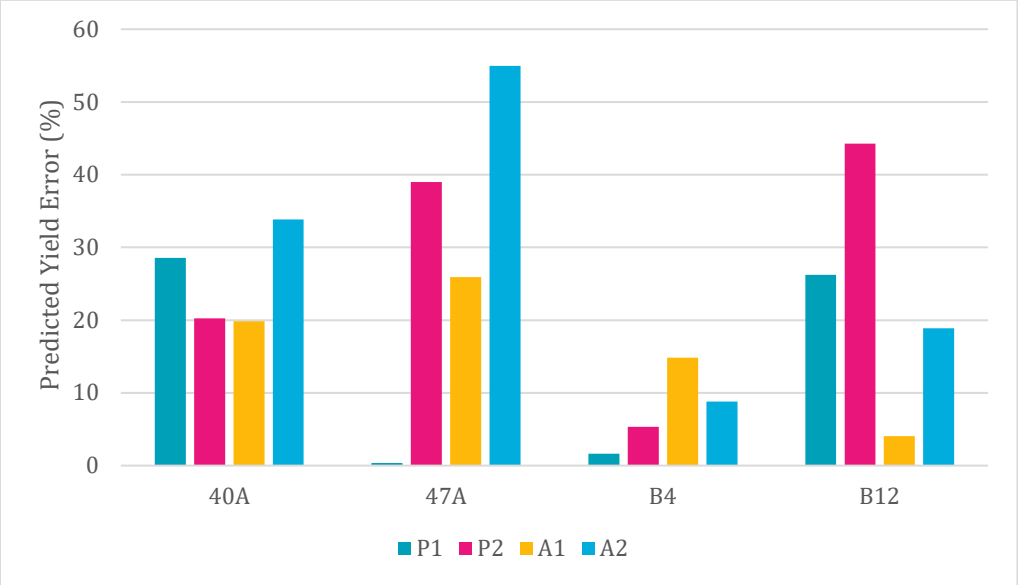


Figure 10.14 The bar chart of Yield estimation absolute error at pea-size stage for four experimental blocks in 2017. P1 and A1 are the proposed yield estimation method (GoPro + mobile). P2 and A2 are the manual yield estimation (manual + mobile).

By observing *AP is the active percentage (excluding sampled fruit over a season).

** P means yield prediction based on the records only available at the current stage. A means yield estimation by real value in the harvest stage.

Table 10.17 and Figure 10.11 show that the prediction of yield based on the berry numbers calculated from the shoot counts by kriging (P1) has better performance than the yield generated based on the berry number by manual calculation of shoot counts (P1) in general, except for block 40. Overall an accuracy of 14.2% was obtained.

Comparing A1 and A2, it also indicates that overall performance of the proposed yield estimation by GoPro and mobile solution has better performance regarding the yield estimation accuracy. By multiplying all yield components, which are the real

values generated at harvest stage, the average absolute error for four experimental blocks was 16.16% (A1).

10.3.3.7 Pea-sized stage: Yield component analysis

As to the yield component analysis, based on the total berry counts generated across a block, we replace each key yield component by its real value to check the significance of changes it caused.

Table 10.26 Yield estimation error (%) caused by key yield components

Combination		Key Components	Yield Estimation Error (%)				
			40A	47A	B4	B12	ABS Ave
P1	1.1+2.1+3.1+ 4.1+5+6		-28.58	0.36	-1.64	26.22	14.20
C2	1.1+2.2+3.1+ 4.1+5+6	Berry Gain/Loss factor	15.47	-34.97	-11.47	12.78	18.67
C3	1.1+2.1+3.2+ 4.1+5+6	Berry Weight	-29.23	6.87	-5.38	16.43	14.48
C4	1.1+2.2+3.1+ 4.2+5+6	Harvest efficiency	-25.19	7.38	-1.64	26.22	15.11
C5	1.1+2.1+3.1+ 4.1+6	Shoot gain /loss factor	15.05	52.37	6.60	32.12	26.54

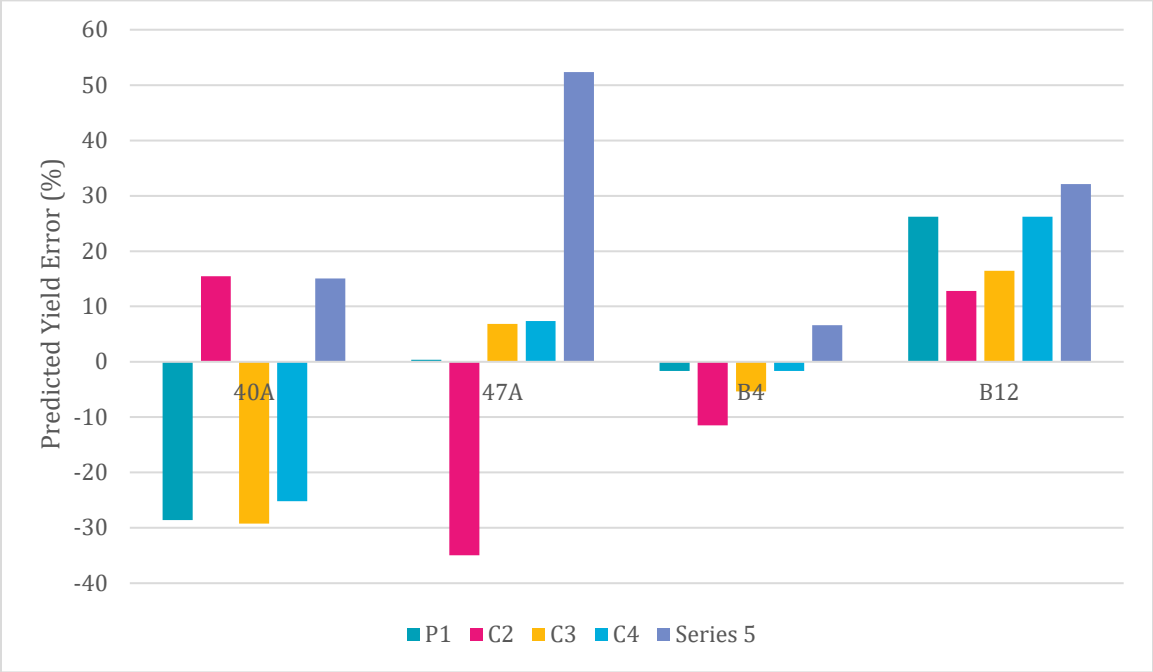


Figure 10.15 Yield component analysis at flowering stage in 2017

From *AP is the active percentage (excluding sampled fruit over a season).

** P means yield prediction based on the records only available at the current stage. A means yield estimation by real value in the harvest stage.

Table 10.17 and Figure 10.11 show that the berry gain/loss factor, average berry weight and harvest efficiency have no critical influence in terms of yield estimation. The average error changes caused by those three components at pea-sized stage are around 1-3% percentage, comparing with P1.

Shoot gain/loss factor has more effect on the proposed yield estimation method. Based on the numbers illustrated in *AP is the active percentage (excluding sampled fruit over a season).

** P means yield prediction based on the records only available at the current stage. A means yield estimation by real value in the harvest stage.

Table 10.17 and Figure 10.11 show that the average absolute error can be decreased to 14.20% when considering the shoot/gain loss factor (it was 26.54% for C1).

10.3.3.8 Pea-sized stage: Summary

In this section, a yield estimation formula is proposed based on the shoot counts generated from GoPro video and the berry number counted by image processing. The average absolute yield estimation error by the proposed method is 14.2%.

At this stage, the berry number per bunch is settled. But as to the final yield, the berry gain/loss factor has an impact on the yield forecast. Although the spatial

distribution of berry number across a block does not show much difference compared with the spatial distribution of flower number at flowering stage and berry number prior to harvest stage, the overall changes in berry number are inevitable. This causes a yield estimation error of around 10%.

The berry weight is another parameter needing attention since it shares the effect of error with the berry gain/loss factor regarding contribution to the final yield. Usually people assume that berry weight is quite stable at the end of the season (about 1g per berry) but this is highly variety-dependent and the data we have show significant variation. Further work would look at applying the automated berry diameter measurement of Section 7.6.

10.3.4 Harvest stage (GoPro + Mobile)

10.3.4.1 Harvest stage: Bunch to shoot ratio

The average bunch to shoot ratio was calculated based on manual counts of shoots and bunches in 30 SSSs at harvest stage. The details are demonstrated in Table 10.27.

Table 10.27 The average bunch to shoot ratio B/S from manual counts at 30 SSSs in Y3

B/S	**40A**	**47A**	**B4**	**B12**
Ratio	1.290	1.649	1.357	1.261

10.3.4.2 Harvest stage: Berries per bunch

The average berry number per bunch at harvest, processed by image processing in 2017, is shown in Table 10.28.

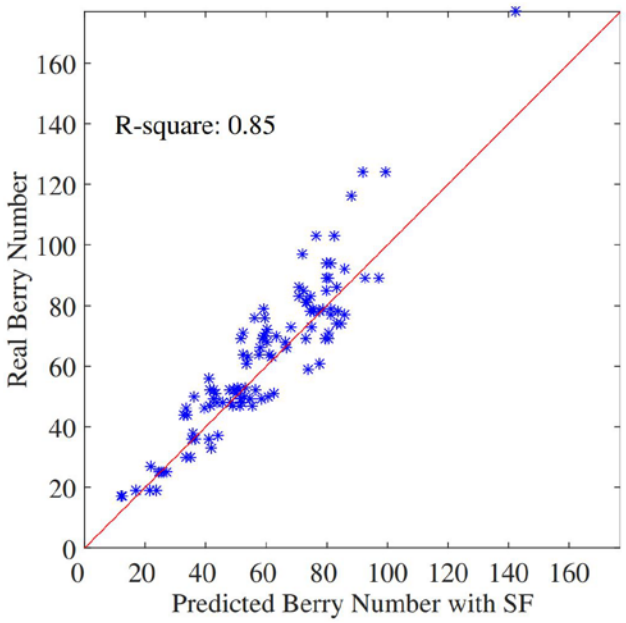


Figure 10.16 *Final berry number estimation by multiplying sparse factor, with average absolute error 12.4%*

Table 10.28 The average berry number per bunch at harvest for three experimental blocks in 2017.

b/B	**40A**	**47A**	**B4**	**B12**
Ratio	61.706	54.755	N/A	140.703

The estimated berry numbers were compared with the actual berry numbers counted manually. The berry number estimation errors are illustrated in Figure 10.17 which shows how they aggregate when using 90-120 bunches per block – a much smaller error on average than 12%. The data collected from B4 was not applicable as an inappropriate background for the bunches was chosen and the error was not identified until after the bunches had been harvested.

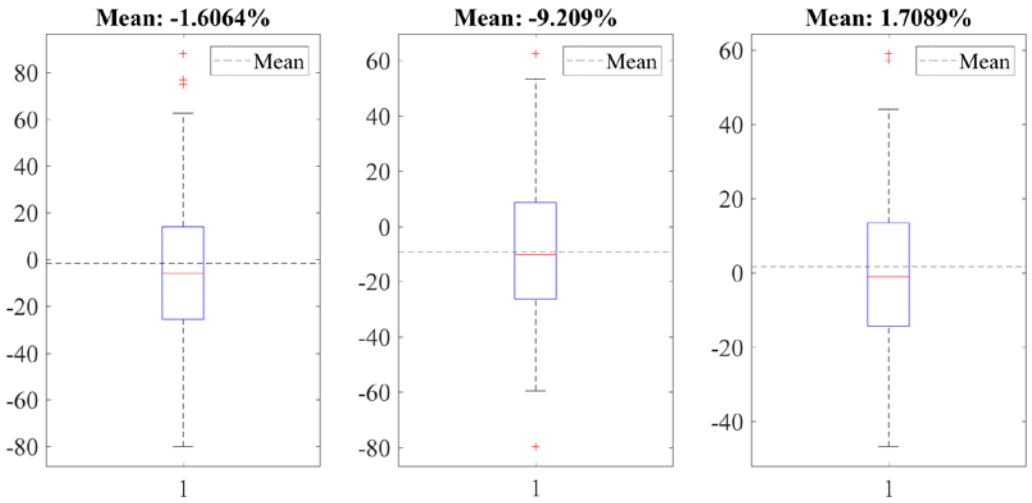


Figure 10.17 The errors of berry estimation per bunch for three experimental blocks, averaged across all 90-120 bunches. From left to right: 40A, 47A, B12.

10.3.4.3 Harvest stage: Berries per shoot

The number of berries per shoot (from image processing) is illustrated in Table 10.29.

Table 10.29 The average berry number per shoot at 30 SSSs in 2017 for four blocks.

Block	**40A**	**47A**	**B4**	**B12**
Berry Number	86	66	82*	158

* berry number was counted manually since the collected photos were not applicable for B4

It is noticeable that the number of berries per shoot is substantially higher in B12 (Chardonnay) than the number collected from 40A (Chardonnay) although these are in different terroirs.

10.3.4.4 Harvest stage: Predict yield

To estimate the yield by computer vision and mobile solution, we propose the following equation for yield estimation at harvest stage:

$$Y^* = c(S) \times R_{B/S} \times \mu(w(b)_h) \times HE \times S_{gl}$$

Where c(S) is the number of shoots estimated from GoPro video of the entire block, $R_{B/S}$ is the average number of bunches per shoot at harvest stage at 30 SSSs. $\mu(w(b)_h)$ is the average berry weight at harvest, HE is the harvest efficiency, S_{gl} is the shoot gain / loss factor. The detailed calculation is demonstrated in Table 10.30.

Table 10.30 Yield Estimation at harvest stage by combining related yield components for 2017.

Object	Source	Option	Year	40A	47A	B4	B12
Berry Numbers = c(S) × $R_{f/s}$	Shoot Count by Kriging*average berry number per shoot	1.1	2017	75515730	128470906	45380933	45270767
	manual shoot counts (SSSs)*average berry number per shoot	1.2	2017	2017	84311572	78105062	48605079
$\mu(w(b)_h)$ (g)	History records	2.1	2015 +2016	0.80	1.10	1.21	1.22
	manual, harvest	2.2	2017	0.80	1.17	1.17	1.13
HE	History records	3.1	2016	0.9069	0.8412	0.9621	0.9572
	Current records	3.2	2017	0.9500	0.9000	0.9621	0.9572
S_{gl}		4	2017	0.6208	0.6587	0.9227	0.9553
AP*		5	2017	0.9982	0.9987	0.9983	0.9969
	Combination						
Yield Estimation (t)	1.1+2.1+3.1+4+5	P1		34.12	77.99	48.78	50.43
	1.2+2.1+3.1+4+5	P2		38.09	47.41	52.25	57.63
	1.1+2.2+3.2+4+5	A1		35.41	88.85	46.93	46.52
	1.2+2.2+3.2+4+5	A2		39.54	54.02	50.26	53.17
Actual Yield (t)				33.50	106.09	54.25	45.27
Error (%)	P1**			1.84	-26.49	-10.08	11.39
	P2			13.71	-55.31	-3.70	27.31
	A1**			5.72	-16.25	-13.51	2.76
	A2			18.03	-49.08	-7.36	17.44

*AP is the active percentage (excluding sampled fruit over a season).
** P means yield prediction based on the records only available at the current stage. A means yield estimation by real value in the harvest stage.

Table 10.31 Yield estimation absolute error at pea-size stage for four experimental blocks in 2017

Yield Estimation ABS Error (%)	40A	47A	B4	B12	Average
P1	1.84	26.49	10.08	11.39	12.45
P2	13.71	55.31	3.70	27.31	25.00
A1	5.72	16.25	13.51	2.76	9.56

A2	18.03	49.08	7.36	17.44	22.98

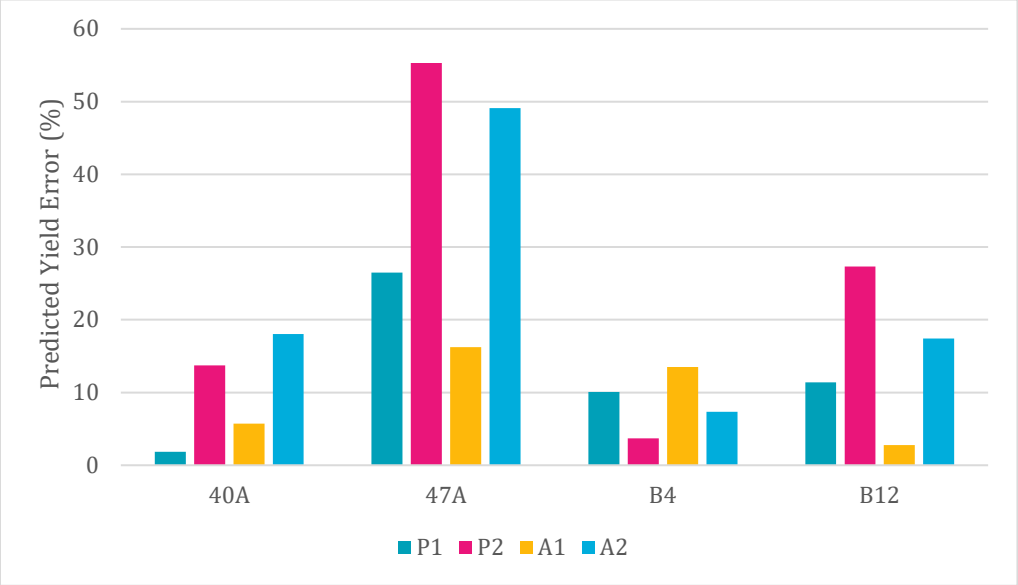


Figure 10.18 The bar chart of yield estimation absolute error at harvest stage for four experimental blocks in 2017. P1 and A1 are the proposed yield estimation method (GoPro + mobile). P2 and A2 are the manual yield estimation (manual + mobile).

By observing Table 10.30 and the Figure 10.18, the prediction of yield based on the berry numbers calculated from the shoot counts by kriging (P1) has better performance than the yield generated based on the berry number by manual calculation of shoot counts (P1) in general, except for block B4.

Comparing A1 and A2, we also see that the overall performance of the proposed yield estimation by GoPro and mobile solution has better performance. By multiplying all yield components, which are the real values calculated at the harvest stage, the average absolute error obtained for four experimental blocks was 9.56% (A1), compared with 22.58% by A2.

10.3.4.5 Harvest stage: Yield component analysis

As to the yield components analysis, based on the berry counts across a block, we replace each key yield component by its real value to check the significance of changes it caused.

Table 10.32 Yield estimation error (%) caused by key yield components

Combination		Key Components	Yield Estimation Error (%)				
			40A	47A	B4	B12	Average
P1	1.1+3.1+4.1+5+6		1.84	-26.49	-10.08	11.39	12.45
C3	1.1+3.2+4.1+5+6	Berry weight	0.92	-21.72	-13.51	2.76	9.73
C4	1.1+3.1+4.2+5+6	Harvest efficiency	6.68	-21.35	-10.08	11.39	12.38
C5	1.1+3.1+4.1+6	Shoot gain /loss factor	64.07	11.61	-2.55	16.61	23.71

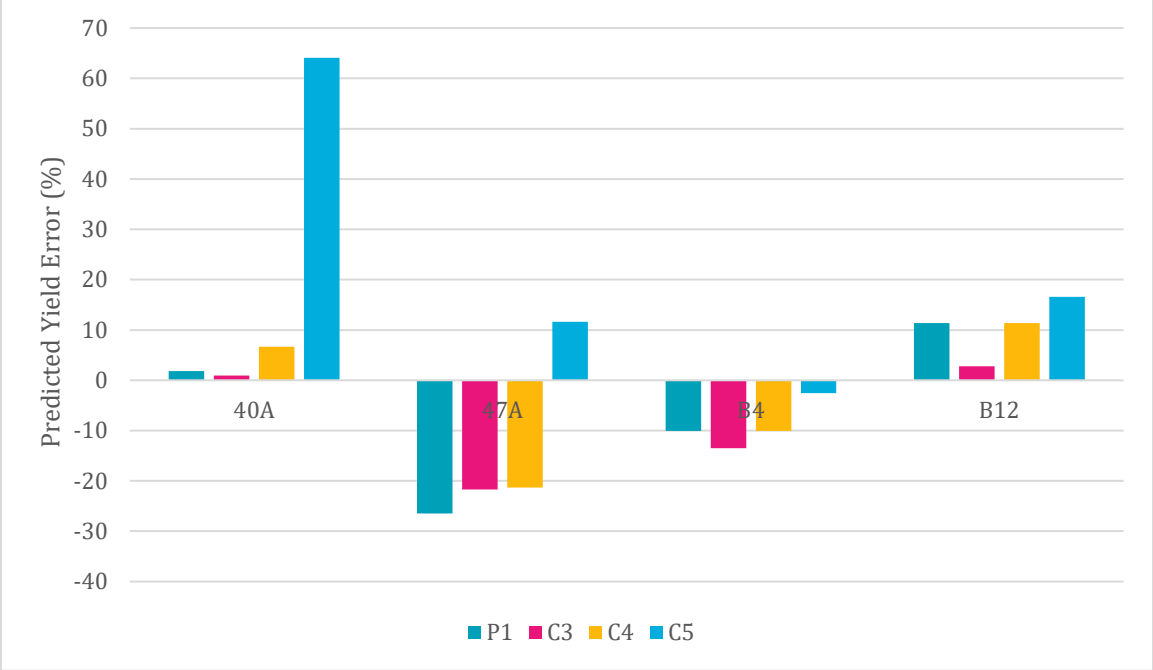


Figure 10.19 Yield components analysis at harvest stage in 2017.

Table 10.32 and Figure 10.19 show that the shoot gain/loss factor (C5) plays an important role in 40A and 47A. But it has no major impact to B4 and B12 regarding yield estimation. The harvest efficiency almost has no impact on yield estimation according to the average error of 12.38% (C4), compared with 12.45% (P1).

Apparently if the berry weight can be accurately estimated, the final yield estimation (C3, 9.73% error) is closer to the real yield estimation (A1, 9.56% error).

10.3.4.6 Harvest stage: Summary

In this section, a yield estimation formula by GoPro and mobile solution has been presented. Based on the shoot counts and the berry number per shoot, an estimated yield was obtained.

At this stage, there are fewer parameters in the yield estimation formula since it is closer to the harvest stage. The main attributes in this formula are the shoot counts generated in shoot stage by filming the whole block, the shoot gain/loss factor and the berry weight. We have made the assumption that the shoot number across a block can be accurately counted from the videos. The number obtained in our experiments is similar to the shoot counts calculated by traditional methods except for block 47A. Given that shoot counts are the basis of this formula, the shoot gain/loss factor is of critical importance in obtaining an accurate yield estimate.

Again, as for the conclusion in section 10.3.3.8, the berry weight needs more attention for yield estimation. This could be improved by combining the technique with that shown in Section 7.6.

10.4 Overall summary of Y3 results

Across the four blocks, the absolute error was compared at each stage for each of three methods – the proposed method, the best practice manual method and the use of the long term average as a proxy for no forecasting at all. These results are shown in Table 10.34.

Table 10.33 Comparison of proposed and manual methods for yield estimation in Y3

Block	Stage	P1 Yield [t]	Manual Method Yield [t]	Actual Yield [t]	P1 Abs Error [%]	Manual Method Abs Error [%]
40A	Shoot	38.99	43.19	33.5	16.38	28.93
	Flowering	35.13	31.07	33.5	4.88	7.26
	Pea-sized	23.93	47.05	33.5	28.58	40.44
	Harvest	34.12	30.04	33.5	1.84	10.34
47A	Shoot	122.04	79.39	106.09	15.04	25.16
	Flowering	123.27	56.33	106.09	16.19	46.9
	Pea-sized	106.48	148.74	106.09	0.36	40.2
	Harvest	77.99	80.17	106.09	26.49	24.43
B4	Shoot	47.05	51.72	54.25	13.27	4.67
	Flowering	54.15	31.15	54.25	0.19	42.58

	Pea-sized	53.36	86.39	54.25	1.64	59.23
	Harvest	48.78	65.15	54.25	10.08	20.08
B12	Shoot	28.61	30.62	45.27	36.81	32.36
	Flowering	45.63	36.21	45.27	0.80	20.02
	Pea-sized	57.14	77.01	45.27	26.22	70.11
	Harvest	50.43	43.97	45.27	11.39	2.88

The proposed method of image based yield estimation has reduced the error on average compared with the best practice manual method and at flowering in particular, it is closer to the grower and winemaker target of 5%. In all cases it is substantially better than using the long term average, i.e. the 'do-nothing' case.

Table 10.34 Comparison of proposed method, best practice manual method and long-term average for yield estimation at each stage averaged over all four blocks in Y3

Stage (Y3)	Proposed Method Abs Error [%]	Manual Method Abs Error [%]	Long Term Average Abs Error [%]
Shoot	20.38	22.78	32.35
Flowering	5.51	29.19	
Pea-sized	14.20	52.50	
Harvest	12.45	14.43	

The fundamental basis on which the proposed method hinges is the shoot count performed five months prior to harvest. This is one reason for the increase in error after the flowering stage, as the shoots were only counted once other than for validation as discussed in Section 10.3.1.2. Further work is recommended to update this method with counts of the shoots at each stage of estimation.

11 Conclusions

11.1 Yield estimation

- **A novel method for yield estimation combining row videos with mobile phone imagery has been introduced and tested in this project**. The accuracy was shown to be substantially better than industry standard manual methods at the flowering and pea-sized stages and slightly better at the shoot and harvest stages.

- **5.5% error is achievable at flowering** using the method proposed in Y3. This is very close to the winemaker target of 5% error which was set as the aim of this project and demonstrates that image processing methods can improve yield estimation without increasing the amount of sampling with respect to manual methods.

- 30 **stratified** samples are sufficient for obtaining an average of a block, rather than using a much larger number of samples at random locations. This was true for the four study blocks which has substantial yield variation and ranged from 3 to 10 ha in area.

- Manual yield estimation by destructive sampling at harvest was inaccurate by 15% on average, showing that **manual methods are futile for achieving the winemaker goal of 5% error earlier in the season**.

- **'Do-nothing' yield estimation results in 35% error** - in 40% (24/60) of cases this was better than manual yield estimation methods. In short, industry standards for manual yield estimation are unprofitable and consideration must be given to automated solutions.

- The **bunch to shoot and bunch to inflorescence ratios** have been shown to contribute the greatest to errors in manual yield estimation at the shoot and flowering stages. Longer term data are needed to understand the variability in these ratios and their impact on yield.

- **Poor prediction of berry weight** at harvest had a large impact on the inaccuracy of manual yield estimation at the pea-sized stage. However, the **count of berries per bunch** contributes even more to the inaccuracy and methods need to be devised to eliminate sampling bias in the selection of bunches for berry counting.

- **Consumer grade GoPro cameras are able to detect and count shoots on spur pruned vines to an accuracy of 88%** based on existing work [13]. This opens the possibility of early stage yield estimation and yield variation mapping using only a simple consumer camera on a standard vineyard tractor pass. However, they are not yet feasible for in-vivo berry and bunch

detection from moving vehicles due to occlusion, blur, motion of the canopy and insufficient dynamic range.

- The use of an expensive machine vision camera (Manta) was not found to be of particular benefit in yield estimation, particularly due to the poor usability of such a system. As commercial products develop, it is likely that more advanced and more controllable cameras with grower-friendly user interfaces will become available and open up more possibilities for image capture.
- A **system for the capture, processing and management of row videos was introduced in this project**. While not automated in its entirety, major components of the system have been automated and potential exists to extend this for generating maps of visible vine parameters throughout the season.

11.2 Project novelty

- Using an existing shoot count mapping from GoPro videos: **E-L 9 / first spray is the best stage for counting shoots by image processing.**
- A novel **flower counting method** suitable for Australian varieties was introduced in this project. It achieved 84% accuracy from a single image and was shown to perform best at E-L16.
- **A novel pea-sized berry counting** method was developed in this project and shown to be over 90% accurate when applied to a single image.
- Using the previous two components, **fruit set ratios** can be efficiently measured non-destructively and on a large scale by image processing.
- **Combining shoot maps with flower counts spatially improves accuracy** as opposed to using average values of shoot counts over the entire block.
- The spatial distribution of berry counts per shoot does not match spatial yield variation perfectly, hence **berry diameter needs to be measured**.
- This project has briefly tested a method for **berry diameter measurement** which is accurate to 95%, in line with existing research. It is more portable than commercial solutions like the Dyostem.
- Counting inflorescences in spur-pruned blocks is not feasible by visual means.

11.3 General learnings

- **Consistency** in data collection, storage and management is critical. While enormous effort was put into achieving this, and Table 5.5 shows the scale of

the problem, many hundreds of manual measurements were invalid and needed to be manually checked and corrected where possible. Removing human error from all steps of the process is recommended.

- Purely data driven approaches **without long term records** are doomed to fail. In several cases, the grower was able to better estimate the final yield by relying on 20 years of observations, inclinations about the weather and a fuller understanding of the interrelationships between all the factors that affect yield. This project was limited to a very small amount of prior information, but shows what can be achieved if this approach was newly applied.
- All manual measurements are subject to **bias**, particularly bunch selection. This was most evident in the selection of bunches for berry counts, where a 30% difference was observed between manually selected bunches and averages across complete destructively sampled sections of vines. Doing **in-vivo counting of anything is exceptionally tedious**, a large source of error and should be minimised.
- The **NBN is valuable** for managing data. Sending Gigabytes of data per field trip on hard drives around the country using Australia Post is impractical and the recent NBN installations on both study sites greatly reduced the time for feedback to the field workers as to the veracity of their processes and results.
- **Harvest efficiency needs to be improved**. This is a simple step which can generate vast savings by not losing fruit which has been tended all season.
- **Training in digital viticulture, experiment design and fieldwork**. This project has trained a number of researchers in digital viticulture, dozens of casual field workers in data collection and several vineyard managers in the need for consistent data. This has the potential to have benefits for the wine industry far beyond the technical results in this particular report. Outcomes have been disseminated to the wine industry through well known forums such as the AWITC and AWRI seminars as well as a number of high quality journal and conference papers.

12 Recommendations

12.1 Development

- **Commercialise** current shoot counting systems to generate early season maps of variability within a block. This has substantial value for the grower in terms of management practices within the same season, where earlier interventions are much cheaper than late stage thinning or canopy management.
- **Fully automate** the early season video data collection. Seamless integration of GPS with video (not just still images) is critical to reduce human input.
- Make a **cloud-based system for yield estimation**, both manual and automated with data validation. This could conceivably integrate with a system such as VinSites, providing an Australia-wide snapshot of the state of the industry. This would have significant commercial benefit for large winemaking companies in terms of logistics and marketing planning, but also reduce the workload on smaller vineyards where resources for yield estimation are scarce.
- The flower counting, pea-sized and existing harvest berry counting algorithms should be developed into a **single app that growers can use to collect data** that will feed into an automated online yield estimation system. Automatic validation of the data will greatly improve the quality of data collected.
- The flower counting and pea-sized berry counting algorithms should be implemented in an **app for growers to rapidly calculate fruit set ratios** specific to Australian cultivars.
- Although this project has introduced methods to reduce the amount of manual counting required for yield estimation, further development of autonomous UAV or ground vehicles to **automate data collection** would minimise the time spent on yield estimation.

12.2 Testing

- **Testing of the proposed system should be extended to cane pruned blocks** where there is exceptionally good potential for shoot counting to provide a solid basis for early season yield estimation. This would most efficiently be done in blocks where prior information about the yield components is available.
- **Extension of field data collection to other cultivars and regions** would further evaluate the robustness of the proposed approach across the Australian wine industry.

12.3 Policy

- Provide incentives for growers to move towards **cane-pruned systems** for better visibility of shoots and bunches.
- **Educate industry and implement improved methods for data management, including defining and disseminating protocols for data collection, validation, storage, transfer, backup, access and usability.** The skills required to do this are available but need to be applied for the direct benefit of growers and indeed across the entire supply chain. Providing an intuitive online tool for validating data and calculating yield estimates would allow the outcomes of this project to be more widely disseminated and improvements made to the Australian wine industry.

13 Bibliography

[1] G. Dunn and S. Martin, "The current status of crop forecasting in the Australian wine industry," in *Proceedings of the ASVO Seminar Series: Grapegrowing at the Edge*, Tanunda, Barossa Valley, South Australia, 2003.

[2] P. Clingeleffer, "Crop development, crop estimation and crop control to secure quality and production of major wine grape varieties: a national approach," Grape and Wine Research and Development Corporation, Adelaide, 2001.

[3] P. Blom and J. Tarara, "Trellis tension monitoring improves yield estimation in vineyards," *HortScience,* vol. 44, no. 3, pp. 678-685, 2009.

[4] J. Baldwin, "The relation between weather and fruitfulness of the Sultana vine," *Australian Journal of Agricultural Research,* vol. 15, no. 6, pp. 920-928, 1964.

[5] A. Hall and M. Wilson, "Object-based analysis of grapevine canopy relationships with winegrape composition and yield in two contrasting vineyards using multitemporal high spatial resolution optical remote sensing," *International journal of remote sensing,* vol. 34, no. 5, pp. 1772-1797, 2013.

[6] D. Font, T. Pallejà, M. Tresanchez, M. Teixidó, D. Martinez, J. Moreno and J. Palacín, "Counting red grapes in vineyards by detecting specular spherical reflection peaks in RGB images obtained at night with artificial illumination," *Computers and electronics in agriculture,* vol. 108, pp. 105-111, 2014.

[7] S. Nuske, S. Achar, T. Bates, S. Narasimhan and S. Singh, "Yield estimation in vineyards by visual grape detection," in *2011 IEEE/RSJ International Conference on Intelligent Robots and Systems (IROS)*, San Francisco, CA, USA, 2011.

[8] G. Dunn and S. Martin, "A functional association in Vitis vinifera L. cv. Cabernet Sauvignon between the extent of primary branching and the number of flowers formed per inflorescence," *Australian Journal of Grape and Wine Research,* vol. 13, no. 2, pp. 95-100, 2007.

[9] P. Dry and B. Coombe, "Grapevine growth stages – The modified E-L system," in *Viticulture I - Resources*, Adelaide, Winetitles, 2004.

[10] R. Bramley and D. Lanyon, "A new approach to vineyard experimentation - where and how?," in *Prceedings of the 12th Australian Wine Industry Technical Conference*, Adelaide, 2005.

[11] S. Liu, "Automated Yield Estimation in Viticulture by Computer Vision," UNSW, Sydney, 2017 PhD Thesis.

[12] S. Liu, J. Tang, S. Cossell and M. Whitty, "Detection of Shoots in Vineyards by Unsupervised Learning with over the Row Computer Vision System," in *Australasian Conference on Robotics and Automation*, 2015.

[13] S. Liu, S. Cossell, J. Tang, G. Dunn and M. Whitty, "A computer vision system for early stage grape yield estimation based on shoot detection," *Computers and Electronics in Agriculture,* vol. 137, pp. 88-101, 2017.

[14] S. Cossell, M. Whitty, S. Liu and J. Tang, "Spatial Map Generation from Low Cost Ground Vehicle Mounted Monocular Camera," in *IFAC-PapersOnLine*, Seattle, 2015.

[15] S. Liu, X. Li, H. Wu, B. Xin, P. R. Petrie and M. Whitty, "A Robust Automated Flower Estimation System for Grape Vines," *Biosystems Engineering,* 2017.

[16] S. Liu, M. Whitty and H. Jayakody, "Grape Berry Counting based on Automated 3D Bunch Reconstruction from a Single Image," in *16th Australian Wine Industry Technical Conference*, Adelaide, 2015.

[17] Z. Liu, "Grape Diameter Detection in Yield Estimation," UNSW Bachelor Thesis, 2016.

[18] A. Kicherer, R. Roscher, K. Herzog, S. Simon, W. Förstner and R. & Töpfer, "BAT (Berry Analysis Tool): A high-throughput image interpretation tool to acquire the number, diameter, and volume of grapevine berries," *Vitis,* vol. 52, no. 3, pp. 129-135, 2013.

[19] S. Cubero, M. P. Diago, J. Blasco, J. Tardáguila, B. Millán and N. Aleixos, "A new method for pedicel/peduncle detection and size assessment of grapevine berries and other fruits by image analysis," *Biosystems Engineering,* vol. 117, pp. 62-72, 2014.

[20] J. Tardaguila, M. P. Diago, J. Blasco, B. Millán, S. Cubero, O. L. García-Navarrete and N. Aleixos, "Automatic estimation of the size and weight of grapevine berries by image analysis," in *International Conference of Agricultural Engineering*, Valencia, 2012.

[21] O. Mirbod, L. Yoder and S. Nuske, "Automated Measurement of Berry Size in Images," *IFAC-PapersOnLine,,* vol. 49, no. 16, pp. 79-84, 2016.

[22] S. Liu, M. Whitty and S. Cossell, "A Lightweight Method for Grape Berry Counting based on Automated 3D Bunch Reconstruction from a Single Image," in *ICRA, International Conference on Robotics and Automation (IEEE), Workshop on Robotics in Agriculture*, 2015.

[23] S. Liu, Y. Lu and M. Whitty, "Progression of Wine Grape Spatial Variation within a season: A Case Study in using Image Processing to understand the Key Components affecting Spatial Variation in a block," *Australian Journal of Grape and Wine Research,* 2017 (submitted).

[24] J. Tang and M. Whitty, "Non-Productive Canopy Detection from Aerial Imagery," in *Australian Wine Industry Technical Conference (poster)*, Adelaide, 2016.

[25] J. Tang, M. Woods, S. Cossell, S. Liu and M. Whitty, "Non-Productive Vine Canopy Estimation through Proximal and Remote Sensing," *IFAC-PapersOnLine,* vol. 49, no. 16, pp. 398-403, 2016.

[26] G. M. Dunn and S. R. Martin, "Yield prediction from digital image analysis: A technique with potential for vineyard assessments prior to harvest," *Australian Journal of Grape and Wine Research,* vol. 10, no. 3, p. 196–198, 2004.

[27] S. Liu and M. Whitty, "Automatic Grape Bunch Detection in Vineyards with an SVM Classifier," p. 11, 2015.

[28] P. Van Kerk Oerle, "Machine Learning for Grape Bunch Detection and Yield Estimation," UNSW Bachelor thesis, 2017.

[29] M. Whitty, "Study tour to support automated yield estimation project," Wine Australia, Adelaide, 2015.

[30] S. Nuske, K. Wilshusen, S. Achar, L. Yoder and S. Singh, "Automated Visual Yield Estimation in Vineyards," *Journal of Field Robotics,* vol. 31, no. 5, pp. 837-860, 2014.

[31] M. Woods, M. Whitty, S. Cossell, S. Liu, J. Tang, G. Dunn, P. Petrie, A. Davidson, C. Wotton and J. J, "An Initial Investigation into Harvest Efficiency," in *Australian Wine Industry Technical Conference (Poster)*, Adelaide, 2016.

[32] S. Martin, R. Dunstone and G. Dunn, "How to Forecast Wine Grape Deliveries using Grape Forecaster Excel Workbook version 7," Department of Primary Industries, Tatura, Victoria, 2003.

[33] D. W. Wong, "The International Encyclopedia of Geography".*Interpolation: Inverse-distance weighting.*

[34] R. Team, "Integrated development environment for r," 2015. [Online]. Available: http://www.rstudio.com/.

[35] Wikipedia, "Inverse distance weighting," [Online]. Available: https://en.wikipedia.org/wiki/Inverse_distance_weighting.

[36] S. Liu and M. Whitty, "Automatic Grape Bunch Detection in Vineyards with an SVM Classifier," *Journal of Applied Logic,* 2014.

[37] M. Whitty, "Next Generation Yield Prediction Technologies," in *Next Generation Yield Precdiction Technologies, Australian Wine Industry Technical Conference*, Adelaide, 2016.

[38] S. Marden and M. Whitty, "GPS-free localisation and navigation of an unmanned ground vehicle for yield forecasting in a vineyard," in *International workshop collocated with the 13th International Conference on Intelligent Autonomous Systems*, 2015.

[39] S. Liu, S. Marden and M. Whitty, "Towards automated yield estimation in viticulture," in *Proceedings of the Australasian Conference on Robotics and Automation*, Sydney, 2013.

[40] G. Awadhwal, "Image Acquisition Techniques for Computer Vision Wine Grape File Detection," UNSW Bachelor Thesis, 2016.

[41] S. Singh, “Automated Image Capture for Grape Vine Inspection,” UNSW Bachelor Thesis, 2016.

[42] D. Wiseham, “Grape Yield Estimation Techniques with Focus on Isolation and the Effect of Sample Size,” UNSW Bachelor Thesis, 2016.

[43] S. Liu, M. Whitty and S. Cossell, “Automatic Grape Bunch Detection in Vineyards for Precise Yield Estimation,” in *AIPR, International Conference on Machine Vision Application*, 2015.

[44] J. Tang, S. Liu, S. Cossell and M. Whitty, “Addressing Big Issues in Agriculture: A Case Study on Rapid and High Fidelity Yield Mapping,” in *14th APRU Doctoral Students Conference*, Hangzhou, China., 2015.

14 Appendices

A. Communication

List of Publications

[1] S. Liu, S. Cossell, J. Tang, G. Dunn, and M. Whitty, ‘A computer vision system for early stage grape yield estimation based on shoot detection,’ *Computers and Electronics in Agriculture,* vol. 137, pp. 88-101, 2017.
[2] S. Liu, M. Whitty, 'Automatic grape bunch detection in vineyards with an SVM classifier', *Journal of Applied Logic*, 2014.
[3] J. Tang, M. Woods, S. Cossell, S. Liu, M. Whitty, 'Non-Productive Vine Canopy Estimation through Proximal and Remote Sensing', in *IFAC-PapersOnLine*, pp. 398 – 403, 2016.
[4] S. Cossell, M. Whitty, S. Liu, J. Tang, 'Spatial Map Generation from Low Cost Ground Vehicle Mounted Monocular Camera', *in IFAC-PapersOnLine*, pp. 231 – 236, 2016.
[5] M. Whitty, 'Next Generation Yield Prediction Technologies', *in Next generation yield prediction technologies, Australian Wine Industry Technical Conference, Adelaide, presented at Australian Wine Industry Technical Conference*, Adelaide, 25 - 28 July 2016.

[6] S. Liu, M. Whitty, H. Jayakody, 'Grape berry counting based on automated 3D bunch reconstruction from a single image', *in 16th AWITC proceedings, 16th Australian Wine Industry Technical Conference, Adelaide, South Australia, presented at 16th Australian Wine Industry Technical Conference, Adelaide,* South Australia, 24 - 28 July, 2016.
[7] S. Liu, J. Tang, S. Cossell, M. Whitty, 'Detection of shoots in vineyards by unsupervised learning with over the row computer vision system', *in Australasian Conference on Robotics and Automation, ACRA*, 2015.
[8] J. Tang, S. Liu, S. Cossell, M. Whitty, 'Addressing Big Issues in Agriculture: A Case Study on Rapid and High Fidelity Yield Mapping', *in Addressing Big Issues in Agriculture: A Case Study on Rapid and High Fidelity Yield Mapping, 14th APRU Doctoral Students Conference, Hangzhou,* China*, presented at 14th APRU Doctoral Students Conference, Hangzhou*, China, 23 - 27 November, 2015.
[9] S. Liu, M. Whitty, S. Cossell, 'Automatic grape bunch detection in vineyards for precise yield estimation', *in Proceedings of the 14th IAPR International Conference on Machine Vision Applications, MVA*, pp. 238 – 241, 2015.
[10] S. Liu, M. Whitty, S. Cossell, 'A Lightweight Method for Grape Berry Counting based on Automated 3D Bunch Reconstruction from a Single Image', *in International Conference on Robotics and Automation (IEEE), Workshop on Robotics in Agriculture, Seattle*, May, 2015.
[11] S. Liu, S. Marden, M. Whitty, 'Towards automated yield estimation in viticulture', *in Australasian Conference on Robotics and Automation, ACRA*, 2013.
[12] S. Liu, 'Automated yield estimation in viticulture by computer vision', UNSW Ph.D Thesis, 2017.
[13] G. Awadhwal, 'Image acquisition techniques for computer vision wine grape field detection', UNSW Bachelor Thesis, 2016.
[14] S. Singh, 'Automated image capture for grape vine inspection', UNSW Bachelor Thesis, 2016.
[15] Z. Liu, 'Grape diameter detection in yield estimation', UNSW Bachelor Thesis, 2016.
[16] D. Wiseham, 'Grape yield estimation techniques with focus on isolation and the effect of sample size', UNSW Bachelor Thesis, 2016.
[17] P. van Kerk Oerle, 'Convolutional neural networks for vineyard yield estimation', UNSW Bachelor Thesis, 2017.

Media Articles

Table 14.1 Related Media Articles published during the research

Date	Article Source	Link
	Bayside Group	https://www.baysidegroup.com.au/blog/how-robotics-technology-is-

26 July 2017		transforming-winemaking-in-australia/
9 June 2017	Wine Australia RD&E News	https://www.wineaustralia.com/news/articles/robotics-lured-scarlett-into-the-world-of-wine
9 March 2017	NAB Agribusiness news	https://business.nab.com.au/new-technology-boosts-grape-yield-forecasting-accuracy-22928/
18 February 2015	Prime TV News	https://au.prime7.yahoo.com/n3/video/-/watch/26337347/grape-counting/
6 February 2015	ABC Rural	http://www.abc.net.au/news/rural/2015-02-06/wine-grape-calculator-world-first/6069552
6 February 2015	UNSW Newsroom	https://newsroom.unsw.edu.au/news/science-tech/robotic-cars-help-wine-growers-predict-future-yield
	Replicated by a number of online sources:	http://www.sciencealert.com/robotic-cars-could-predict-how-much-wine-you-ll-be-drinking-this-vintage http://www.zdnet.com/article/unsw-to-use-robot-technology-to-save-wine-growers-au200m-a-year/ https://vinoenology.com/wine-news/read/9089/

Presentations

In addition to conference presentations made in conjunction with conference papers listed in the list of publications, several presentations have been made to publicise results from this research.

Table 14.2 Presentations publicising this research

Date	Presentation	Audience
23 November 2017	AWRI Webinar	Webinar participants
31 March 2017	Vinelink, Auckland	International viticulture industry and researchers
1 February 2017	Plant and Food Research New Zealand, Auckland	PFR researchers
1 December 2016	Society of Precision Agriculture Australia	Famers and researchers from Murray Region
9 November 2016	Webinar to IEEE Technical Committee on Agricultural Robotics	International robotics researchers
29 July 2016	Reference Group Meeting, Adelaide	Industry reference group members
18 September 2015	Wine Tasmania Field Day	Growers from Tasmania
19-21 August 2015	AWRI Roadshow	Growers from Canberra, Orange and Mudgee regions
15 July 2015	Reference Group Meeting, Sydney	Industry reference group members

B. Intellectual Property

This project has focussed on the development of knowledge for industry rather than commercialisable outcomes. The improved algorithm for flower counting has potential for commercialisation.

The project has proposed a system for yield estimation which combines several published elements, some of which were develop prior to and others in parallel with this project.

C. Staff

The following staff have been engaged on this project;

First name	Surname	Employer	Role type	Employed	Tasks
Gregory	Dunn	NSW DPI	20% In-kind	Y1, Y2, Y3	Project Supervisor
Mark	Whitty	UNSW	25% In-kind	Y1, Y2, Y3	Chief Investigator, fieldwork, analysis and project management
Samsung	Lim	UNSW	5% In-kind	Y1, Y2, Y3	Advice
Stephen	Cossell	UNSW	Full time Postdoctoral Research Associate	Y1, Y2	Fieldwork and analysis
Scarlett	Liu	UNSW	Casual Research Assistant (Y1, Y2), Full time Postdoctoral Research Associate (Y3)	Y1, Y2, Y3	Fieldwork and analysis
Matt	Atallah	UNSW	Casual Research Assistant	Y2	Fieldwork at Orange
William	Carey	UNSW	Casual Research Assistant	Y1	Fieldwork at Orange
Alexander	Carey	UNSW	Casual Research Assistant	Y1	Fieldwork at Orange
Wei Hua	Chen	UNSW	Casual Research Assistant	Y1	Fieldwork
William	Crowe	UNSW	Casual Research Assistant	Y2	Fieldwork
Penglei	Dai	UNSW	Casual Research Assistant	Y1	Fieldwork
Angus	Davidson	TWE	Advice In-kind	Y1, Y2	Fieldwork and advice
Dan	Glasgow	UNSW	Casual Research Assistant	Y2	Fieldwork at Orange
Justin	Jarrett	SeeSaw Wines	Advice In-kind	Y1, Y2, Y3	Vineyard owner (SeeSaw wines)
Pip	Jarrett	SeeSaw Wines	Advice In-kind	Y1, Y2, Y3	Vineyard owner (SeeSaw wines)
Hiranya	Jayakody	UNSW	Casual Research Assistant	Y2, Y3	Fieldwork and analysis
Eliza	Kiel	UNSW	Casual Research Assistant	Y2	Fieldwork at Orange
Xuesong (Ben)	Li	UNSW	Casual Research Assistant	Y3	Analysis
Stephen	Lin	UNSW	Casual Research Assistant	Y1, Y2, Y3	Fieldwork and analysis
Shilong	Liu	UNSW	Casual Research Assistant	Y3	Analysis

Yi (Chris)	Lu	UNSW	Casual Research Assistant	Y3	Analysis
Patrick	Madden	UNSW	Casual Research Assistant	Y1	Fieldwork at Orange
David	McDonald Sparks	UNSW	Casual Research Assistant	Y2	Fieldwork at Orange
Rickie-Lee	McLaurin-Smith	UNSW	Casual Research Assistant	Y2	Fieldwork
Christopher	Mills	UNSW	Casual Research Assistant	Y2	Fieldwork at Orange
Tim	Moreton	Acklands Vineyard Services	Casual Research Assistant	Y2	Fieldwork at Clare
Phillip	Moser	UNSW	Casual Research Assistant	Y1	Fieldwork
Rebecca	Nalder	UNSW	Casual Research Assistant	Y2	Fieldwork at Orange
Ashara	Patterson	UNSW	Casual Research Assistant	Y2	Fieldwork at Orange
Keith	Patterson	UNSW	Casual Research Assistant	Y2	Fieldwork at Orange
Paul	Petrie	AWRI/SARDI	Advice In-kind	Y1, Y2, Y3	Advice
Gihan	Samarasinghe	UNSW	Casual Research Assistant	Y2, Y3	Analysis
Phil	Scarles	Self-employed	Contractor	Y2, Y3	Fieldwork at Clare
Jana	Shepherd	TWE	Advice In-kind	Y2, Y3	Advice
Lingling (Lily)	Shi	UNSW	Casual Research Assistant	Y1, Y2, Y3	Analysis
Sudeep	Singh	UNSW	Casual Research Assistant	Y2	Fieldwork and analysis
Frazer	Slack-Smith	UNSW	Casual Research Assistant	Y2	Fieldwork at Orange
Adam	Smith	UNSW	Casual Research Assistant	Y1	Fieldwork at Orange
Nigel	Squire	SeeSaw Wines	Advice In-kind		Vineyard manager at Orange
Sarah	Squire	UNSW	Casual Research Assistant	Y2	Fieldwork at Orange
Cameron	Stewart	UNSW	Casual Research Assistant	Y2	Analysis
Tina	Stocco	Self-employed	Contractor	Y2, Y3	Fieldwork at Clare
Alan	Stocco	Self-employed	Contractor	Y2, Y3	Fieldwork at Clare
Javad	Taghia	UNSW	Casual Research Assistant	Y2	Fieldwork
Julie	Tang	UNSW	Casual Research Assistant	Y1, Y2, Y3	Fieldwork and analysis

Albert	Taylor	UNSW	Casual Research Assistant	Y1	Fieldwork at Orange
Josh	Walton	UNSW	Casual Research Assistant	Y2	Fieldwork at Orange
Braiden	Whitby	UNSW	Casual Research Assistant	Y2	Fieldwork at Orange
Michael	Woods	NSW DPI	Casual Research Assistant	Y2, Y3	Fieldwork, analysis and logistics
Catherine	Wotton	TWE	Advice In-kind	Y2, Y3	Advice
Gilbert	Wright	UNSW	Casual Research Assistant	Y1	Fieldwork at Orange
Lisa	Ziersch	Self-employed	Contractor	Y2, Y3	Fieldwork at Clare

Contributions have also been kindly made to this project through thesis projects at UNSW:

Gaurav Awadhwal – BE, November 2016, 'Imaging techniques for viticulture assessment'

Scarlett Liu – Ph.D, December 2016, 'Automated yield estimation in viticulture by computer vision'

Zhen (Steven) Liu – BE, November 2016, 'Grape diameter detection in yield estimation'

Sudeep Singh – BE, November 2016, 'Automated image capture for grape vine inspection'

Phillip Van Kerk Oerle – BE, November 2017, 'Machine learning for grape bunch detection and yield estimation'

Drew Wiseham – BE, November 2016, 'Grape yield estimation techniques with focus on isolation and the effect of sample size'

D. Other Materials

Historical Yield Values

Table 0.1 Historical yields and long-term average for the study blocks

Year	40A	47A	B4	B12
2002	16.96	70.9	33.5	
2003	32.38	44.76	8	5.2
2004	33.98	94.86	27.1	18.92
2005	55.91	80.21	40.72	31.69
2006	70.7	102.51	26.884	15.18
2007	43.6	48.58	hail	24.957
2008	52.17	107.58	66.205	44.48
2009	48.84	60.26	74.441	47.371
2010	21.4	83.06	9.86	7.968
2011	100.02	62.54	23.83	28.57
2012	48.52	55	40.122	35.779
2013	34.76	32.54	46.525	56.862
2014	35.14	67.66	46.25	27.96
2015	47.92	36.98	30.702	24.912
2016	67.1	59.32	69.005	61.742
2017	33.5	106.09	54.254	45.272
LTA	46.43	69.55	39.83	31.79

Table 0.2 Management actions (not including chemical application or repairs and maintenance)

Block Name	40A	47A	B4	B12
V2015	22/08/2014 Pruning	08/08/2014 Pruning 12/12/2014 Trimming	18/07/2014 Pruning 16/11/2014 Wire lifting 26/11/2014 Leaf Plucking	24/06/2014 Pruning 12/11/2014 Wire lifting

			15/12/2014 Trimming	
V2016	24/07/2015 Pruning	27/08/2015 Pruning 20/11/2015 Trimming 27/11/2015 Trimming	14/07/2015 Pruning 02/11/2015 Wire lifting 15/11/2015 Trimming 02/12/2015 Leaf plucking 18/12/2015 Trimming 04/01/2016 Trimming	28/06/2015 Pruning 04/11/2015 Wire lifting 23/11/2015 Trimming
V2017	20/01/2017 Trimming 17/02/2017 Trimming	09/12/2016 Trimming 16/12/2016 Trimming 03/02/2017 Trimming	03/08/2016 Pruning 21/11/2016 Wire lifting 30/11/2016 Trimming 14/12/2016 Leaf Plucking 04/01/2017 Trimming	18/06/2016 Pruning 14/11/2016 Wire lifting

E. Budget Reconciliation

A budget reconciliation will be provided under a separate document.